

Baker

Department of Transportation
Research and Special Programs Administration
Office of Pipeline Safety



TTO Number 5

*Integrity Management Program
Delivery Order DTRS56-02-D-70036*

*Low Frequency ERW and
Lap Welded Longitudinal Seam
Evaluation*

FINAL REPORT

*Submitted by:
Michael Baker Jr., Inc.
October 2003*

*In association with:
Kiefner and Associates, Inc.
CorrMet Engineering Services, PC*

This page intentionally left blank

***TTO Number 5
Low Frequency ERW and
Lap Welded Longitudinal Seam Evaluation
Table of Contents***

EXECUTIVE SUMMARY1

1 INTRODUCTION3

2 BACKGROUND5

2.1 LF-ERW, DC-ERW, AND EFW PIPE6

2.2 FURNACE LAP-WELDED PIPE9

 2.2.1 *Historical Performance*11

2.3 REFERENCES12

3 PRESSURE TESTING FORMATS13

3.1 INTRODUCTION13

3.2 HYDROSTATIC TESTING13

3.3 DYNAMIC TESTING13

3.4 SPIKE TESTING13

3.5 TESTING FORMAT COMPARISON13

3.6 REFERENCES14

4 PRESSURE TESTING AND NDT TECHNOLOGIES AND PRACTICES REVIEW15

4.1 SUBTASK 01 – SCOPE15

4.2 INTRODUCTION15

4.3 DETERMINATION OF SUSCEPTIBILITY16

 4.3.1 *Types of Seam-Related Defects and the Possible Implications*19

 4.3.2 *Failure History*20

 4.3.3 *Implications of Toughness*21

 4.3.4 *Predicting Retest Intervals Based on Fatigue Crack Growth*23

 4.3.5 *Relative Aggressiveness of the Pressure Cycles*24

 4.3.6 *Selective Seam Corrosion*28

4.4 USE OF THE SPIKE TEST28

4.5 IMPACT OF INTEGRITY-ASSESSMENT METHOD ON REASSESSMENT INTERVAL29

 4.5.1 *Failure Pressure Versus Defect Size*29

4.6 REFERENCES34

5 CURRENT IN-LINE INSPECTION TECHNOLOGY REVIEW35

5.1 SUBTASK 02 – SCOPE35

5.2 TASK OVERVIEW35

5.3 CODE PROVISIONS RELEVANT TO ILI36

5.4 ILI FOR PRE-1970 PIPE36

5.5 NDT TECHNOLOGY37

 5.5.1 *Introduction*37

 5.5.2 *Metal wall loss*38

 5.5.3 *Crack Detection Tools*39

5.6 INTERVIEWS45

5.7 PERFORMANCE HISTORY45

5.8 EVALUATION OF METHODOLOGIES46

5.9	EVALUATION OF INFORMATION SUPPLIED TO OPERATORS FROM VENDORS.....	48
5.9.1	<i>MFL tools</i>	48
5.9.2	<i>UT Tools</i>	48
5.9.3	<i>EMAT</i>	48
5.10	BASELINE PIPELINE INTEGRITY USING ILI METHODS.....	48
5.10.1	<i>Economic Issues</i>	48
5.10.2	<i>Cost for ILI</i>	49
5.11	ILI VERSUS PRESSURE TESTING.....	49
5.12	REFERENCES.....	49
6	CURRENT INTEGRITY EVALUATION PROCEDURE ASSESSMENT.....	51
6.1	SUBTASK 03 – SCOPE.....	51
6.2	49 CFR 192 AND 195.....	51
6.3	ASME B31.4.....	52
6.4	ASME B31.8 AND B31.8S.....	52
6.5	ASME B31G AND RSTRENG.....	53
6.6	API RP579.....	55
6.7	SUGGESTED LIMITATIONS ON THE EVALUATION OF DEFECTS LOCATED IN ERW OR LAP-WELDED SEAMS.....	58
7	MATERIAL TOUGHNESS EVALUATION.....	59
7.1	SUBTASK 05 – SCOPE.....	59
7.2	FATIGUE MECHANICS.....	59
7.2.1	<i>Initiation</i>	59
7.2.2	<i>Crack-Tip Stress Intensity</i>	61
7.2.3	<i>Propagation</i>	63
7.2.4	<i>Fracture</i>	66
7.3	MATERIAL TESTING AND EXPERIENCE.....	68
7.3.1	<i>Standard Materials Tests</i>	68
7.3.2	<i>Fatigue Properties</i>	71
7.3.3	<i>Lap-Welded Pipe</i>	72
7.4	USING MATERIAL DATA FOR EVALUATING FLAW GROWTH.....	72
7.4.1	<i>Data Needs and Usage</i>	72
7.4.2	<i>Example</i>	73
7.5	REFERENCES.....	76
8	EVALUATION OF PRESSURE TESTING AND ILI COMBINATION.....	77
8.1	SUBTASK 04 – SCOPE.....	77
8.2	OVERVIEW.....	77
8.3	PAST EXPERIENCE USING COMBINED TECHNIQUES.....	78
8.4	FRACTURE MECHANICS IMPLICATIONS FOR HYDROSTATIC TESTING AND IN-LINE INSPECTION.....	78
9	RECOMMENDATIONS AND SUGGESTED GUIDELINES.....	89
9.1	SCREENING EVALUATION.....	89
9.2	ENGINEERING ANALYSIS.....	91
9.3	NDT EVALUATION.....	92

List of Figures

FIGURE 4.1	FRAMEWORK FOR EVALUATION	18
FIGURE 4.2	FRAMEWORK FOR EVALUATION WITH PATH FOR THE SEGMENT ANALYZED HIGHLIGHTED	27
FIGURE 4.3	EFFECTS OF VARIOUS INTEGRITY ASSESSMENT LEVELS ON REASSESSMENT LEVELS (RECTANGULAR FLAWS).....	30
FIGURE 4.4	TIMES TO FAILURE FOR VARIOUS FATIGUE CRACKS (ELLIPTICAL FLAWS)	33
FIGURE 5.1	HOOKE CRACK	37
FIGURE 5.2	ILI INSPECTION TOOL (MFL VECTRA/BJ SERVICES).....	37
FIGURE 5.3	UT TOOL IN A LIQUID BATCH (PIPETRONIX)	39
FIGURE 5.4	ULTRASCAN™ SPECIFICATIONS (PII, GE POWER)	40
FIGURE 5.5	CRACK DETECTION TOOL (PIPETRONIX)	41
FIGURE 5.6	SPECIFICATION FOR ELASTIC WAVE TOOL (PII/GE POWER).....	42
FIGURE 5.7	SCHEMATIC OF TFI SENSOR.....	43
FIGURE 5.8	TRANSCAN (PII, GE POWER).....	43
FIGURE 5.9	SCHEMATIC OF EMAT SENSOR.....	44
FIGURE 5.10	GRAPHICAL COMPARISON OF ILI TECHNOLOGY (PII, GE POWER)	47
FIGURE 6.1	COMPARISON OF B31G AND RELATED METHODOLOGY.....	54
FIGURE 6.2	APPLICATIONS AREA OF B31G AND RSTRENG (BATTELLE).....	55
FIGURE 6.3	FLAW LENGTH VERSUS MATERIAL TOUGHNESS RELATIONSHIP.....	57
FIGURE 7.1	A REPRESENTATIVE S-N CURVE (ASME)	60
FIGURE 7.2	SIMPLIFIED CRACK TYPES (BARSOM AND ROLFE)	62
FIGURE 7.3	EXAMPLE CRACK GROWTH IN SERVICE	64
FIGURE 7.4	AVERAGE CRACK GROWTH RATE FOR CARBON STEEL (BARSOM AND ROLFE).....	65
FIGURE 7.5	EXAMPLE RELATIONSHIP BETWEEN FAILURE STRESS AND FLAW SIZE	68
FIGURE 7.6	SCHEMATIC CVN TEST RESULTS.....	70
FIGURE 7.7	SCHEMATIC OF STRAIN RATE EFFECT ON FRACTURE TOUGHNESS TRANSITION.....	71
FIGURE 7.8	EXAMPLE OF THE EFFECT OF OPERATING PRESSURE SPECTRUM.....	74
FIGURE 7.9	ILLUSTRATION OF THE EFFECT OF VARIATIONS IN C	75
FIGURE 7.10	ILLUSTRATION OF THE EFFECT OF VARIATIONS IN n	75
FIGURE 8.1	STRENGTH-DEPENDENT RELATIONSHIP BETWEEN FAILURE PRESSURE AND FLAW SIZE FOR BLUNT METAL LOSS IN DUCTILE PIPE.....	83
FIGURE 8.2	TOUGHNESS-DEPENDENT RELATIONSHIP BETWEEN FAILURE PRESSURE AND FLAW SIZE FOR CRACKS IN PIPE HAVING NORMAL TOUGHNESS LEVELS (25 FT-LB).....	84
FIGURE 8.3	RELATIONSHIP BETWEEN FAILURE PRESSURE AND FLAW SIZE FOR NEAR-BONDLINE ERW DEFECTS (10 FT-LB)	85
FIGURE 8.4	RELATIONSHIP BETWEEN FAILURE PRESSURE AND FLAW SIZE IN LOW TOUGHNESS SEAMS (2 FT-LB)	86
FIGURE 8.5	RELATIONSHIP BETWEEN FAILURE PRESSURE AND FLAW SIZE IN BRITTLE SEAMS (0.2 FT-LB)	87
FIGURE 9.1	EVALUATION PROCESS (FLOW CHART 1).....	89
FIGURE 9.2	SCREENING EVALUATION (FLOW CHART 2)	90
FIGURE 9.3	ENGINEERING ANALYSIS (FLOW CHART 3)	92
FIGURE 9.4	NDT EVALUATION (FLOW CHART 4).....	93

List of Tables

TABLE 2.1	SMYS FOR LAP-WELDED PIPE.....	11
TABLE 2.2	FAILURE INCIDENT RATE FOR PIPE	12
TABLE 4.1	BENCHMARK CYCLE COUNTS—ANNUAL.....	25
TABLE 4.2	REMAINING LIFE BASED ON CATEGORIZED AGGRESSIVENESS	25
TABLE 4.3	TIME TO FAILURE BASED ON TEST SCENARIOS OF 1.25 X MOP AND 1.39 X MOP	26
TABLE 4.4	COMPARISON OF HYDROSTATIC TESTING VERSUS IN-LINE INSPECTION.....	31
TABLE 4.5	TIMES TO FAILURE AND RETEST INTERVALS FOR VARIOUS HYDROSTATIC TEST STRESS LEVELS	33

TABLE 5.1	NDT METHODOLOGY AND THREATS TO THE INTEGRITY OF PIPELINES (PII, AND NACE 2000).....	46
TABLE 6.1	MATERIAL PROPERTIES & CONDITIONS	56

List of Acronyms

AC	Alternating Current
AGA	American Gas Association
API	American Petroleum Institute
ASME	American Society of Mechanical Engineers
ASTM	American Society of Testing and Materials
CFR	Code of Federal Regulations
CTOD	Crack Tip Opening Displacement
C-UT	Circumferential Ultrasonic Testing
CVN	Charpy V-Notch
DC	Direct Current
DC-ERW	Direct Current Electric Resistance Welded
DSAW	Double Submerged Arc Weld
EFW	Electric Flash Welded
EMAT	Electro Magnetic Acoustic Transducer
ERW	Electric Resistance Welded
ET	Eddy Current Testing
EW	Elastic Wave
FATT	Fracture Appearance Transition Temperature
FSS	Fitness-For-Service
HAZ	Heat Affected Zone
HCA	High Consequence Area
HF-ERW	High-frequency Electric Resistance Welded
ID	Inside Diameter
ILI	In-line Inspection
LF-ERW	Low-frequency Electric Resistance Welded
MFL	Magnetic Flux Leakage
MOP	Maximum Operating Pressure
NACE	National Association of Corrosion Engineers
NDT	Non-destructive Testing
OPS	United States Department of Transportation, Office of Pipeline Safety
PII	GE Power, PII Pipeline Solutions
SATT	Shear Appearance Transition Temperature
SAW	Submerged Arc Weld
SCC	Stress Corrosion Cracking
SMYS	Specified Minimum Yield Strength
TFI	Transverse Field Inspection
UT	Ultrasonic Testing

Executive Summary

This report documents a review focused on evaluation of longitudinal seams on LF-ERW pipe and lap-welded pipe, particularly that manufactured before 1970, as well as DC-ERW pipe and EFW pipe. As part of the integrity management requirements for pipelines in high consequence areas, 49 CFR 195.452 (j) (6) states “for low frequency electric resistance welded pipe or lap-welded pipe susceptible to longitudinal seam failure, an operator must select integrity assessment methods capable of assessing seam integrity and of detecting corrosion and deformation anomalies”.

The likely causes of seam failures that could necessitate a seam-integrity assessment are pressure-cycle-induced fatigue and selective (grooving) corrosion of the bondline region of the seam. Four factors govern the possible growth of seam defects by pressure-cycle-induced fatigue:

- the pressure cycles,
- the presence of a family of initial flaws,
- an environmentally affected crack-growth rate, and
- the toughness of the pipe.

Selective seam corrosion is affected primarily by the degree of exposure to corrosive conditions (i.e., poor or absent coating and ineffective cathodic protection) and by the nature of non-metallic inclusions in the bondline region. Because most of older ERW materials have the types of inclusions that make the material susceptible, the susceptibility by this model in the absence of a history of selective seam corrosion failure is judged solely on the basis of the coating condition and the quality of the cathodic protection. If experience shows that selective seam corrosion is a real threat, the operator will also need to consider the effective corrosion rate on the pipeline and the augmented corrosion rate in the vicinity of the seam.

Since experience shows that in the absence of an indentation in the pipe, pressure-cycle-induced fatigue failures initiate only at relatively large initial defects and since the typical sources of fatigue cracks in LF-ERW or DC-ERW materials have been hook cracks and mismatched skelp edges, one does not need to focus on the bondlines of low-frequency or dc-welded materials when the issue is fatigue; the main concern will be defects near but not in the bondlines. On the other hand, when the issue is selective seam corrosion, the focus should be on the bondline.

Experience indicates that the number of time-dependent failures of lap-welded seams, if any, seems to be small. This review found only two types of seam breaks in lap-welded pipe; poorly fused seams and burned-metal defects. Where such defects have caused failures overpressurization was a known or suspected cause. The implication of the apparent lack of evidence of the occurrence of time-dependent failures associated with lap-welded pipe is that very few if any of these pipelines would be found susceptible to seam failure.

The threat of time-dependent defect growth in pipelines implies that periodic reassessment of pipeline integrity is necessary. The challenges are (1) to be able to determine the appropriate reassessment interval, and (2) to optimize the effectiveness of the reassessment technique such that

the reassessment interval can be as long as possible without exceeding the time of failure of the worst-case growing defect.

While many different ILI tools are available for assessing pipeline integrity, to date only three types are capable of detecting cracks and crack-like features, which are the main defects of interest when discussing longitudinal seam issues on LF-ERW and lap-welded pipe. These tools are TFI, EMAT, and variously, shear wave UT, elastic wave, or C-UT. EMAT has only recently been developed and there is little to no actual performance data available. Another type of tool, ET, is being considered for use as a pipeline ILI technology. Of the two technologies that have seen significant use, TFI and UT, UT typically produces the best results with regard to longitudinal seam issues.

Verifying the serviceability of an ERW, EFW, or lap-welded pipeline from the standpoint of seam integrity often involves hydrostatic tests of the affected segments. Maximizing the difference between the hydrostatic test pressure and the maximum operating pressure allows for a longer interval between tests. This does not mean that the alternative of using a suitable ILI device could or should not be considered. Provided that the ILI device utilized can reliably identify and characterize defects that could affect seam integrity, the proper use of such a device likely would be a more effective way than hydrostatic testing to assess the integrity of the seams. What becomes clear when one gives careful consideration to the process of seam-integrity assessment is that the effectiveness of the assessment is highly a function of the sizes of defects that will remain after the assessment and of the ability of the operator to deal with the possibly remaining defects. In this respect, two things cannot be overemphasized: (1) the higher the test-pressure-to-operating-pressure ratio, the smaller the remaining defects will be and the longer the interval between assessments can be; and (2) ILI, if proven reliable in any given situation, is likely to be far more cost effective than hydrostatic testing.

The use of proven ILI techniques likely provides a higher degree of integrity assurance than hydrostatic testing (at least to practical limits imposed by the quality of older line-pipe materials) for the most important integrity threats (i.e., corrosion-caused metal loss and crack-propagation phenomena in materials with reasonable toughness levels). In these cases, hydrostatic testing provides no added value and clearly is inferior to reliable ILI (with appropriate and timely response) used by itself. In those cases where a low or very low-toughness material is involved, however, the reverse is true. In those cases, it appears with today's tool-inspection thresholds that hydrostatic testing would give superior assurance. Also, it is noted that in these cases, a one-time test would probably suffice, and that one-time test could be either the initial pre-service test or the manufacturer's hydrostatic test if that test was conducted to a sufficiently high level. It would seem then that the only reason for employing both ILI and hydrostatic test would be cases where the confidence in the ILI technology needs to be established.

In most cases, regardless of whether ILI or hydrostatic testing, or even direct assessment, is used, an engineering analysis will also need to be conducted. This analysis should at a minimum determine the reassessment interval based on appropriate techniques.

A series of flow charts have been developed, and are presented in Section 0, in an attempt to provide a standardized, systematic approach to evaluation of longitudinal seam integrity

1 Introduction

This report has been developed in accordance with the Statement of Work and proposal submitted in response to RFP for Technical Task Order Number 5 (TTO 5) entitled “Low Frequency ERW and Lap Welded Longitudinal Seam Evaluation”.

This scope included review of issues related to NDT methods and ILI technologies, traditional hydrostatic testing and spike tests with special emphasis on duration of testing, integrity assessment procedures, and engineering criticality analysis applied to LF-ERW pipe and lap welded pipe longitudinal seams. Suggested guidelines that OPS can use to create policy for applicability of longitudinal seam testing used by operators and to enforce operator compliance with 49 CFR 195.452 (j) (6)¹ have also been developed.

¹ 49 CFR 195.452 (j) (6) states "However, for low frequency electric resistance welded pipe or lap welded pipe susceptible to longitudinal seam failures, an operator must select integrity assessment methods capable of assessing seam integrity and detecting corrosion and deformation anomalies."

This page intentionally left blank

2 Background

Occasional longitudinal seam failures on pre-1970 LF-ERW, DC-ERW, furnace lap-welded and EFW pipe due to defects generic to the seam-welding process have raised concerns related to determining operational integrity of pipelines containing pipe of these types. With the continuing operation of an aging infrastructure containing such pipe materials, the propensity for the time-dependent growth of defects to critical sizes and subsequent failure requires reliable periodic nondestructive inspection and integrity evaluation. The nondestructive inspections must be able to provide a reliable indication of the presence of defects within a very narrow weld zone. The defects generic to these pipe materials are fatigue cracks, lack of fusion, burned metal defects, stitched welds, cold welds, cracks in hard HAZ, surface breaking hook cracks near the weld, and selective seam (grooving) corrosion.

Modern pipelines are typically hydrostatically tested to a minimum 1.25 times the maximum allowable operating pressure. The testing must be completed in accordance with 49 CFR 192 Subpart J for natural gas lines and 49 CFR 195 Subpart E for liquid pipelines. However, exceptions are allowed for a number of reasons; especially for older pipelines, Class 1 natural gas pipelines not converted under 49 CFR 192.14, and liquids pipelines not converted under 49 CFR 195.5. Specific requirements are prescribed in 49 CFR 195.303 for liquid pipelines that were never subjected to hydrostatic testing. For pre-1970 ERW and lap-welded pipe, 49 CFR 195.303 (c), (d) and (f) require an engineering analysis to determine the susceptibility to longitudinal failure and require a plan to meet certain test deadline dates for hydrostatic testing.

As part of the integrity management requirements for pipelines in high consequence areas, 49 CFR 195.452 (j) (6) states “for low frequency electric resistance welded pipe or lap-welded pipe susceptible to longitudinal seam failure, an operator must select integrity assessment methods capable of assessing seam integrity and of detecting corrosion and deformation anomalies”. It is generally accepted that hydrostatic testing completed in accordance with 49 CFR 195 Subpart E provides reasonable assurance that all critical and near-critical defects will have failed at the test pressure and the remaining defects will have an adequate margin safety. It is recognized that this margin of safety will be degraded if defects that were too small to fail during the test become enlarged with the passage of time and that eventually the safety margins will have to be revalidated by another hydrostatic test. When hydrostatic tests are not practical, an alternate method such as ILI ostensibly can be used to locate defects for repair or removal.

Occasionally seam failures have occurred even after hydrostatic tests. Some of these may have been the result of flaw growth during the test while others may represent cases in which the time to failure established by the test was overestimated. Likely it is possible to minimize these types of occurrences by utilizing test-pressure-to-operating-pressure ratios higher than the 1.25-times-MOP level embodied in 49 CFR 195 Subpart E. A so-called “spike” test in which the test pressure is briefly raised to a level significantly above the 1.25-times-MOP level in many cases would provide a feasible means of assuring a larger margin of safety. Many operators are proposing spike tests to confirm the integrity of their long seams.

In implementing testing and evaluation programs to comply with the regulations, operators must adopt reliable NDT and integrity assessment methods. When the need for seam-integrity assessment

arises in conjunction with the required metal-loss and geometry assessments, a combination of pressure testing and the use of high-resolution metal-loss-detection and geometry-measuring tools can provide an effective integrity management plan for particular pipeline segments. Alternatively, it may be possible to substitute the use of TFI, UT, or EW ILI tools for hydrostatic testing. Though these inspection methods are used routinely, some are relatively untested for reliability and consistent results. Current experience clearly indicates a need to review the situation and develop consistent acceptance guidelines related to LF-ERW and lap-welded pipe for longitudinal seams, integrity assessments.

Over the past several years, pipeline operators have used different ILI tools to enable them to detect and size cracks and crack-like features along or close to the longitudinal seam. By using ILI tools to evaluate the condition of the seam, pipeline operators could avoid hydrostatically testing those pipeline segments with suspect seams, thus eliminating a whole host of problems associated with hydrostatic testing. However, the probability of detecting seam problems varied among the types of ILI tools used, and seam failures during subsequent hydrostatic tests resulted in a lack of confidence in these types of tools.

In contrast to the pipeline operators' perspective, ILI vendors painted a different picture. According to the vendors, there are numerous ILI tools available to confidently evaluate the condition of longitudinal seams. Though the physics and the mathematical algorithms differ for the various types of tools, the vendors claim these tools can detect and size cracks and crack-like features with a depth of 0.04 inches (1 mm) or larger, width of 0.004 inches or wider, and length of 1.2 inches or longer. Some trade associations support the vendors' outlook. For example, the API claims that a UT tool is capable of detection, discrimination, and sizing to provide a level of safety superior to that which can be achieved by hydrostatic testing.

However, the OPS believes that nearly all currently available crack detection tools that claim to be able to determine and size cracks and crack-like defects have inherent difficulties because of the direction and intensity of magnetization of the shear wave pulse. Inspection results for a TFI tool from two operators — one hazardous liquid and one natural gas pipeline — produced diametrically opposite results. The inspection was considered a success in the hazardous liquid pipeline, but a failure in the natural gas pipeline. Because of these conflicting reports from pipeline operators and ILI vendors, the OPS desires an independent evaluation of crack detection tools to ensure that the information gleaned from these tools is sufficiently reliable to assure pipeline integrity.

This report evaluates the acceptability of using ILI technology to evaluate the integrity of LF-ERW and lap-welded pipe seams in lieu of a hydrostatic test as currently required. The use of spike tests, alone and in conjunction with ILI or other hydrostatic testing, is also evaluated. Guidelines are presented for evaluating the acceptability of ILI and spike tests, or combination of the two, for assessing the integrity of longitudinal seams on LF-ERW and lap-welded pipe.

2.1 LF-ERW, DC-ERW, and EFW Pipe

ERW line-pipe materials and a similar material called EFW pipe first appeared in the 1920s. Both processes involved making line pipe by cold forming previously hot-rolled plates or strips into circular sections and joining the longitudinal edges by a combination of localized electrical resistance heating and mechanical pressure. (The ERW pipe is formed into pipe sections and welded

as a continuous process from rolled strip, whereas the EFW pipe is formed into “cans” a single pipe joint at a time.) The heat-softened longitudinal edges were forced together extruding excess material to the outside and inside of the newly formed pipe. The excess material was immediately trimmed away leaving smooth surfaces or at most a small protrusion along the bondline. Both types of processes resulted in a narrow bondline and an associated local heat-affected zone. In many instances in the past and in all cases with modern ERW materials, the bondline/heat-affected-zone region was also subjected to a post-weld heat treatment, the purpose of which is to eliminate zones of excessive hardness from the initial welding process as such zones could be susceptible to various forms of environmental cracking. While EFW pipe is no longer made, ERW pipe is still manufactured currently, albeit by improved methods and with improved materials. Currently made ERW materials represent high-quality line pipe and offer one of the best choices of materials for pipeline construction. The concern relevant to seam-integrity assessment arises because this was not necessarily the case prior to about 1980. One must consider these older materials on a case-by-case basis, because the quality of some lots of older ERW pipe is better than the quality of others. The quality or lack thereof is not a function of the manufacturer. Both good and poor-quality lots have been made by most of the manufacturers in the time period of interest (roughly 1930 through 1980). Moreover, manufacturers began to change from low-frequency seam welding processes to high-frequency seam welding processes as early as 1960.

Prior to 1960, all ERW materials and EFW pipe were made by means of DC or low-frequency AC (up to 360 cycles) using low-carbon steels made in open hearth or electric-arc furnaces and cast into ingots. The DC or low-frequency AC used for resistance heating required intimate contact between the rolling electrodes and the “skelp” (i.e., the plate or strip used to form the cans). Dirt, grease, scale, or other oxide films on the skelp could and often did cause enough interference to prevent adequate heating at the bondline interface. Momentary reductions or loss of current could and often did result in isolated or repeated areas of non-bonding called “cold welds”. Cold welds could be partly through the wall thickness or all of the way through. Even if a through-wall cold weld was formed, it might not result in a leak, because typically such areas were completely filled with a scale that formed from the surfaces being exposed to oxygen while at a high temperature. A significant number of cold welds in close proximity could sufficiently reduce the strength of the bondline such that a rupture would occur when the pipe was subjected to pressurization. In these cases, a hydrostatic test to a sufficiently high pressure if performed by the manufacturer at the pipe mill or the user prior to putting the pipeline into service would usually eliminate the most injurious areas. An adequate test in this respect would be one carried out at 90 percent of the SMYS for a pipeline to be operated at 72 percent of SMYS. Prior to 1960, many sizes and grades of ERW pipe were tested by the manufacturer to levels of only about 75 percent of SMYS, and prior to 1970, it was typical for liquid pipelines to be tested to no more than 1.1 times their MOP.

Other phenomena that would result in poorly or weakly bonded ERW materials included electric power fluctuations during welding, poorly trimmed skelp, cambered or twisted skelp, and inadequate or excessive mechanical pressure at the instant of bonding. Running skelp too fast through an a.c. welder, for example, could cause the heat to fluctuate with the current cycle resulting in a periodic variation in properties along the seam. When broken along the bondline, these variations are made visible in terms of the fracture surface characteristics. The resulting pattern is referred to as

“stitching”. A stitched weld does not necessarily create a pipeline-integrity problem because a defect of some kind other than the stitching itself must be present to start a fracture in a stitched bondline. However, a stitched bondline is generally characterized by low toughness, and only a relatively small defect may be required to start a fracture. Poorly trimmed skelp may contain edge defects that end up on the bondline. Cambered or twisted skelp can result in offset edges at the bondline. The offset can be significant, reducing the net thickness by 30 to 40 percent in extreme cases. Unfortunately, offset edges were seldom caught by visual inspection because the outside surface trim tool removed the excess material from one side leaving the visible mismatch at the ID surface where it was hard to detect by visual inspection.

Starting in 1960, manufacturers began to convert ERW mills from low-frequency-welding equipment to high-frequency equipment (450,000 cycles). After 1978, it is believed that few if any low-frequency welders were still being used. With the use of high-frequency current, the problem of contact resistance is virtually nonexistent. As a result, high-frequency-welded pipe tends to be relatively free of the bondline defects that were common in the low-frequency and DC-welded material.

The performance of ERW materials has improved steadily with time. The number of test failures per mile decreased from levels as high as 6.5 per mile in the 1940s to a level of 0.01 per mile in 1970 for pipelines tested to levels of 90 percent of SMYS or more. Not only has the ERW process itself improved, but cleaner, tougher steels have been developed as the result of the conversion throughout the 1970s and 1980s to basic oxygen steel making, continuous casting, microalloying, and thermomechanical processing. These trends have virtually eliminated three other potential problems associated with ERW seams, low-heat-affected-zone toughness, hook cracks, and grooving corrosion. These potential problems are not welding problems per se, but they have occurred in conjunction with ERW seams in the past. It is safe to say that all low-frequency² and DC-welded materials possess bondline regions that are prone to low toughness and brittle-fracture behavior. This is because there was no way to prevent grain coarsening in the heat-affected zones. The enlarged grains invariably made the weld zones less tough and more prone to brittle fracture than the parent material. To some extent, this tendency was reduced with the use of high-frequency welding because a smaller volume of material is heated than in the case of a low-frequency or DC process. In addition, by the 1970s most manufacturers were using microalloyed, thermomechanically treated skelp. These steps prevented or eliminated grain coarsening and thereby resulted in bondline regions of ERW pipe that are as tough as the parent metal.

The use of cleaner steels (i.e., with greatly reduced sulfur contents) has virtually eliminated the risks of hook cracks and grooving corrosion. The precursors for hook cracks are non-metallic inclusions, primarily manganese sulfide “stringers”. These flattened, non-metallic inclusions are formed during hot rolling of plate or skelp. In general, they reduce the ductile toughness of the steel even in their normal position (i.e., layers interspersed between the rolling-elongated grain structure of the steel). In this position, they can cause poor through-thickness properties that inherently reduce ductile-

² Note that low frequency as used herein refers to the range of 360 Hz or less, typically used with “Yoder” mills prior to 1980. It is recognized that modern high-quality ERW pipe can be made with a variety of frequencies, though usually these are much higher than 360 Hz (e.g., 150 to 450 KHz).

fracture tearing resistance but not necessarily the yield or tensile strength of the material. Near an ERW bondline, however, these weak layers become reoriented such that they are subjected to tensile hoop stress when the pipe is pressurized. The layers may be of sufficient extent or so closely associated that the resulting planes of weakness separate, forming J-shaped (i.e., hook) cracks that curve from being parallel to the plate surfaces near mid-wall to being nearly parallel to the ERW bondline at the OD or ID surface. These cracks can be up to 50 percent of the wall thickness in depth and up to several inches in length. They are in effect a pipe defect, not a weld defect, and their behavior is governed more by parent pipe toughness than bondline toughness. They tend to be much larger than bondline defects in the older materials because the low toughness of the bondline regions assures that no large defects can exist after a hydrostatic test to a reasonably high-pressure level.

Grooving corrosion is also a phenomenon that results from the sulfide-inclusion problem. The sulfide layers appear to make the material immediately adjacent to the bondline more susceptible to corrosion than the surrounding material. As a result, when corrosion (external or internal) occurs in an area that includes the bondline, the corrosion rate will be higher in the bondline region than in the parent material. The frequent result of such corrosion is the creation of a long, sharp V-notch along and centered on the bondline. In no case should such corrosion be treated or evaluated as one would treat or evaluate pitting corrosion in the parent pipe. The resulting anomaly is equivalent to a sharp crack in a relatively brittle material with a depth of penetration that is difficult if not impossible to accurately measure. It is worth noting that HF-ERW pipe may be susceptible to hook cracks or grooving corrosion or both. However, with the advent of the use of materials with even lower sulfur contents from the 1980s onward, one can expect that these problems will be less extensive than is likely in the case of the older low frequency and DC-welded materials.

2.2 Furnace Lap-Welded Pipe

Furnace lap-welded pipe was manufactured for use in oil and gas pipelines from the late 19th century until about the mid 20th century. It was made by bending 22 to 44-foot-long, hot-rolled plates called “skelp” into circular “cans”. The edges of the cans that would be joined to form a longitudinal seam were scarfed prior to can formation such that each was tapered. The skelp was heated to about 1,400°F in a “bending” furnace after which it was formed into a can by means of “pyramid” rolls. The tapered edges were overlapped and either spot welded or mechanically locked together at each end of the can. The can was then placed in a “welding” furnace where it was heated to a temperature above 2,450°F. It was withdrawn from the welding furnace upon reaching the appropriate temperature, whereupon it was forced through a pair of rolls forming the external circular shape of the pipe and over a stationary “welding ball”, which formed the internal circular shape of the pipe. In the process, the tapered edges of the can, having been formed such that upon overlapping they were slightly thicker than the can itself, were brought together with great force. If the temperature of the can was within the appropriate range, about 2,450°F to 2,650°F, the resulting bond between the tapered surfaces was likely to be complete. In such cases, a high-integrity seam was the result, and the user of the pipe could expect it to have an ultimate strength equal to that of the base metal.

Given the fact that lap-welded pipe was made during the period prior to the advent of modern pipe-mill instrumentation and equipment and prior to the advent of quality-control procedures such as nondestructive inspection, completely bonded lap-welded seams were not always achieved. If the

temperature at welding was too low, significantly below 2,450°F, iron-oxide compounds would have a tendency to solidify, and hence, not be squeezed out of the joint upon welding. In such cases, portions of the joint would contain weak, brittle lenses of oxide. If the welding temperature was too high, above 2,650°F for example, non-metallic compounds such as manganese sulfide would have a tendency to liquefy and migrate to grain boundaries where upon cooling the material would essentially contain an internal crack. The latter were referred to as “burned-metal” defects. The existence of significant amounts of either oxide lenses or burned-metal defects could greatly reduce the integrity of the resulting seam, leaving it a region with lower ultimate stress-carrying capacity than the base metal.

One manufacturer conducted 70 burst tests of samples of lap-welded pipe to assess its average reliability. The results of the burst tests showed that, on average, one could expect to achieve 92 percent of the burst pressure of a sound pipe (i.e., one that would fail at the ultimate strength of the base metal at a location other than the lap-welded seam). In 57 of the samples, the failures initiated in the seams. Data of this type are believed to have led to the use of a joint factor of 0.8 for lap-welded pipe in piping design codes such as ASME B31.4 and ASME B31.8. As part of the manufacturing process, each piece of lap-welded pipe, of course, was subjected by the mill to an internal pressure test for at least 5 seconds to prove its integrity up to a specific pressure level. In most cases, however, the hoop stress level imposed by such a test was on the order of 60 percent of the specified minimum yield strength (SMYS) of the pipe.

Lap-welded pipe was made from one of four types of material: wrought iron, open-hearth iron, Bessemer steel, or open-hearth steel. Prior to the advent of the API Specification 5L for the manufacture of line pipe, one of the main manufactures of lap-welded pipe guaranteed a minimum yield strength of 36,000 psi for Bessemer steel pipe and 33,000 psi for open-hearth steel pipe. Specified minimum yield strengths for lap-welded pipe manufactured according to the API Specification 5L (1st Edition, January 1928) are presented in Table 2.1.

Table 2.1 SMYS for Lap-welded Pipe

Bessemer steel	30,000 psi
Open-hearth steel	
Class I	25,000 psi
Class II	28,000 psi
Wrought iron	24,000 psi
Open-hearth iron	24,000 psi

2.2.1 Historical Performance

The California Department of Forestry and Fire Protection, Office of the State Fire Marshal commissioned a risk analysis of the regulated hazardous liquid pipelines within the state that culminated in a report titled “*Hazardous Liquid Pipeline Risk Assessment*” being published in early 1993. This report states: “The data indicated that lap weld pipe had a very high leak incident rate; nearly 50 incidents per 1,000 mile years. However, it was also the oldest pipe, with a mean year of construction of 1933.” Of particular interest was that the incident rate caused by weld failure was also the highest (1.83 incidents per 1,000 mile years).

As shown in Table 2.2 (Table 4-14 from “*Hazardous Liquid Pipeline Risk Assessment*”), the incident rate for lap-welded pipe is essentially an order of magnitude higher than that for other pipe types.

Table 2.2 Failure Incident Rate for Pipe

Cause of Incident	SAW¹	SMLS²	ERW³	LW⁴	Other
External Corrosion	8.35	3.66	1.47	31.59	0.00
Internal Corrosion	2.09	0.22	0.02	1.83	0.00
3 rd Party – Construction	0.00	0.86	0.45	6.41	0.00
3 rd Party – Farm Equipment	0.00	0.22	0.02	1.83	0.00
3 rd Party – Train Derailment	0.00	0.00	0.02	0.00	0.00
3 rd Party – External Corrosion	0.00	0.00	0.09	0.00	0.00
3 rd Party – Other	0.00	0.00	0.12	0.46	0.00
Human Operating Error	0.00	0.11	0.05	1.37	0.00
Design Flaw	0.00	0.00	0.00	0.46	0.00
Equipment Malfunction	0.00	0.54	0.17	1.37	0.00
Maintenance	0.00	0.11	0.00	0.46	0.00
Weld Failure	0.00	0.00	0.12	1.83	0.00
Other	0.00	0.43	0.14	2.29	0.00
Total	10.44	6.14	2.68	49.90	0.00
Number of Mile Years	479	9,280	42,112	2,184	1,106
Mean Year Pipe Constructed	1978	1951	1963	1933	1952
Mean Operating Temperature (F)	120.28	83.59	98.02	86.87	85.58
Average Spill Size (barrels)	5	83	285	87	0
Average Damage (\$US 1983)	18,830	195,426	405,013	68,656	0
¹ Submerged Arc Weld ² Seamless ³ Electric Resistance Weld ⁴ Lap Weld					

2.3 References

- California State Fire Marshal, “*Hazardous Liquid Pipeline Risk Assessment*”, March 1993.

3 Pressure Testing Formats

3.1 Introduction

49 CFR 192 and 195 require pressure testing of newly constructed pipelines and replaced segments of existing pipeline facilities. This pressure testing, known as a hydrostatic testing, is normally accomplished by filling the line with water and pressurizing to a level at least 1.25 times the MAOP. This pressure is then held for a minimum of 8 hours. The use of other test mediums, both liquid and gaseous, is allowed provided certain conditions are met. The length of the test may also vary.

In addition to hydrostatic testing, there are at least two other types of pressure testing: dynamic testing and “spike” testing. Dynamic testing is used to qualify the pressure containment capability of an existing in-service system to its original operating stress level, i.e., not to address proposed increases in operating stress level. Spike tests have been recommended for use as integrity tests (Kiefner, 2000) for revalidating pipeline serviceability and are conducted when lines are not in-service.

3.2 Hydrostatic Testing

API, *Recommended Practice for the Pressure Testing of Liquid Petroleum Pipelines, RP1110* (API RP1110) defines hydrostatic testing as “the application of internal pressure above the normal or maximum operating pressure to a segment of pipeline, under no-flow conditions, fixed a fixed period of time, utilizing a liquid medium.” Hydrostatic testing is usually conducted at a minimum of 125 percent of the MAOP of the line and a minimum duration of 8 hours.

3.3 Dynamic Testing

Dynamic testing is defined in API RP1110 as “the application of pressure to a segment of an operating pipeline above normal operating pressure under flowing conditions for a fixed period of time, utilizing a liquid normally handled through the line.” Dynamic testing is usually limited to 110 percent of the MOP of the line and a minimum duration of 2 hours.

3.4 Spike Testing

Spike testing is similar to hydrostatic testing in that it would normally be conducted using water as the test medium under no-flow conditions. It has been recommended that spike tests be conducted at the highest possible pressure, frequently 139 percent of the MAOP of the line based on the ratio of 100 percent of SMYS to 72 percent SMYS (maximum hoop stress), with a very short duration, usually not more than ½ hour (Kiefner, 2000).

3.5 Testing Format Comparison

Pipeline defects, other than very deep cracks, are not typically within the creep regime (i.e., will not grow over time when subjected to a constant load), and thus the test pressure, and not the hold time, is the main parameter that affects the margin of safety. Thus the higher the test pressure the higher the margin of safety.

Dynamic testing, as defined by API RP1110, results in the lowest factor of safety of the three testing formats. However, dynamic testing does offer one advantage in that it does not require line shut

down. On the other hand, this maybe offset by the added risks (environmental, safety, etc.) associated with any failures that result from the test.

Conversely, a successful spike test would result in the highest factor of safety, but has the downside (mainly economical) that it requires the line to be shut down. The line must then be evacuated, cleaned and re-filled with the test medium. Once the test has been completed, the line must once again be evacuated and, in some, if not most cases, cleaned before it is re-inventoried. The test medium must then be disposed of which can be a significant challenge.

While the environmental risk of a failure during testing is normally considered lower if using water as the test medium, in some sensitive environments the opinion is that the test medium actually maybe more harmful.

3.6 References

1. API, *Recommended Practice for the Pressure Testing of Liquid Petroleum Pipelines, RP 1110*, December 1981.
2. Kiefner, John F., Willard A. Maxey “*The Benefits and Limitations of Hydrostatic Testing*”, 2000.

4 Pressure Testing and NDT Technologies and Practices Review

4.1 Subtask 01 – Scope

This chapter addresses Subtask 01 of the Work Scope which states:

Review current pressure testing and NDT (in-line inspections) technologies and practices employed by pipeline operators for pre-1970 ERW and lap welded pipe seam integrity assessment.

Activities:

- a) Research and collate information concerning pre-1970 ERW and lap-welded pipe.
- b) Research areas of concern and failure mechanisms for this pipe.
- c) Research current pressure testing and NDT technologies and practices.
- d) Research applicable past operator experience with testing/inspection. Interview operators as available.

Deliverables:

- a) Narrative, with sketches as applicable, of pre-1970 ERW and lap welded pipe seams
- b) Narrative summarizing areas of concern and failure mechanisms
- c) Narrative detailing current pressure testing, requirements and references
- d) Narrative of current available NDT technology with summary of operator interviews.

4.2 Introduction

Verifying the serviceability of an ERW, EFW, or lap-welded pipeline from the standpoint of seam integrity often involves hydrostatic tests of the affected segments. Hydrostatic testing of the line either removes any defects that have grown beyond critical size at the test pressure since the last test, or it proves that no defects of critical size exist. After the hydrostatic test, the “clock” on these types of defects restarts. Maximizing the difference between the hydrostatic test pressure and the maximum operating pressure allows for a longer interval between tests. This does not mean that the alternative of using a suitable ILI device could or should not be considered. Provided that the ILI device utilized can reliably identify and characterize defects that could affect seam integrity, the proper use of such a device likely would be a more effective way than hydrostatic testing to assess the integrity of the seams. However, if an operator decides to use ILI, the responsible party should choose a proven ILI technology. As discussed elsewhere herein, such tools exist for some but not all situations at this time. What becomes clear when one gives careful consideration to the process of seam-integrity assessment is that the effectiveness of the assessment is highly a function of the sizes of defects that will remain after the assessment and of the ability of the operator to deal with the possibly remaining defects. In this respect, two things cannot be overemphasized: (1) the higher the test-pressure-to-operating-pressure ratio, the smaller the remaining defects will be and the longer the interval between assessments can be; and (2) ILI, if proven reliable in any given situation, is likely to be far more cost effective than hydrostatic testing. The reasons are:

- (1) The threshold detection sizes for the proven tool technologies are so much smaller than those that could survive even a very high-pressure hydrostatic test that the time interval between reassessments with a reliable tool will be much longer than that assured by the test,
- (2) ILI does not involve taking the pipeline out of service whereas hydrostatic testing does,
- (3) ILI eliminates water acquisition and disposal problems,
- (4) The location and sizing of defects by means of the tool allows the operator to respond immediately to potentially highly injurious defects while conducting scheduled responses to the less-threatening defects, and
- (5) Defects discovered through ILI can be repaired without taking the pipeline out of service.

49 CFR 195.452 requires an operator to conduct seam-integrity assessments as part of the operator's integrity-management plan for those segments comprised of LF-ERW pipe, DC-ERW pipe, or lap-welded pipe where a release could affect an HCA, and the seams of the segment are susceptible to failure. It appears that the regulator intended the rule also to apply to EFW pipe and that such seam-integrity assessments would consist of a baseline assessment followed by reassessments at intervals established by the operator based on risk and other factors specified in 49 CFR 195.452. The reassessment interval is generally not to exceed 5 years, however, there are provisions for variance in limited situations for operators who can demonstrate an engineering basis for a longer reassessment interval. In any case, it appears that no clear-cut definition of "susceptible" exists within 49 CFR 195.452. One thing that ought to be considered, whether or not it was the intent of the regulator, is that an initial seam-integrity assessment may reveal that a particular segment is not susceptible to seam-related failures. Presented in Section 4.3 is a description of how some operators are deciding what "susceptible" means, and a discussion of one way in which a reassessment interval is determined. Section 4.4 contains a brief discussion of the concept of a "spike" test and Section 4.5 presents a demonstration of why ILI will allow much longer reassessment intervals than hydrostatic testing.

4.3 Determination of Susceptibility

The means of determining whether or not the seam of a particular pipeline is susceptible to failure are illustrated in Figure 4.1. Some of this material was presented and discussed in *Dealing with Low-Frequency-Welded ERW Pipe and Flash-Welded Pipe with Respect to HCA-Related Integrity Assessments* (Kiefner, 2002), but the process has evolved over time. Figure 4.1 represents a decision tree that allows one, by supplying appropriate data on a given segment, to determine if a seam-integrity assessment is required based on the federal pipeline integrity management regulations. Data that may be needed by the operator of the pipeline to determine its susceptibility include the grade of the material, the diameter and wall thickness of the pipe, the type of seam, the manufacturer of the pipe, the age of the pipe, the history of seam failures, the causes of the failures, the operating stress level, the hydrostatic test history, the causes of test failures, the inherent fracture toughness of the material, the fatigue crack-growth-rate characteristics of the material in its environment, the type and condition of the coating, the quality of cathodic protection on the pipeline, the likely range of corrosion rates on the pipeline, and the nature of operational pressure cycles on the pipeline. In cases where insufficient data are provided, conservative assumptions may suffice.

It is assumed that the causes of seam failures that could necessitate a seam-integrity assessment are pressure-cycle-induced fatigue and selective (grooving) corrosion of the bondline region of the seam. The four factors that govern the possible growth of seam defects by pressure-cycle-induced fatigue are the pressure cycles, the presence of a family of initial flaws, an environmentally affected crack-growth rate, and the toughness of the pipe. These factors are evaluated to determine the likelihood that the pipeline is susceptible to failures from this cause. Selective seam corrosion is affected primarily by the degree of exposure to corrosive conditions (i.e., poor or absent coating and ineffective cathodic protection) and by the nature of non-metallic inclusions in the bondline region. Because most of older ERW materials have the types of inclusions that make the material susceptible, the susceptibility by this model in the absence of a history of selective seam corrosion failure is judged solely on the basis of the coating condition and the quality of the cathodic protection. If experience shows that selective seam corrosion is a real threat, the operator will also need to consider the effective corrosion rate on the pipeline and the augmented corrosion rate in the vicinity of the seam.

The examiner uses the data to “walk through” the tree to arrive at one of four possible outcomes: (1) the segment is not covered by the seam-failure susceptibility requirement, (2) the segment is not susceptible to seam failures, (3) a baseline assessment is needed because susceptibility or non-susceptibility has not been satisfactorily demonstrated by the information available at this time³, or (4) the segment is susceptible to seam failures.

It is noted that a given pipeline segment may contain seamless pipe and/or HF-ERW pipe as well as LF-ERW pipe. The analysis typically is directed solely at the LF-ERW pipe and usually does not address the status of the seamless pipe or the HF-ERW pipe.

³ A baseline assessment in the form of a hydrostatic test will demonstrate a level of serviceability consistent with the test-pressure-to-operating-pressure ratio the operator selects. Additional information may be derived from the examination of test leaks or breaks if any occur. Remaining life after the test can be assessed from the standpoint of pressure-cycle-induced fatigue. The results of the test are expected to provide sufficient information for the operator to decide whether or not the pipeline is susceptible to seam failure in the context of federal regulations pertaining to pipeline integrity management (49 CFR 195.452)

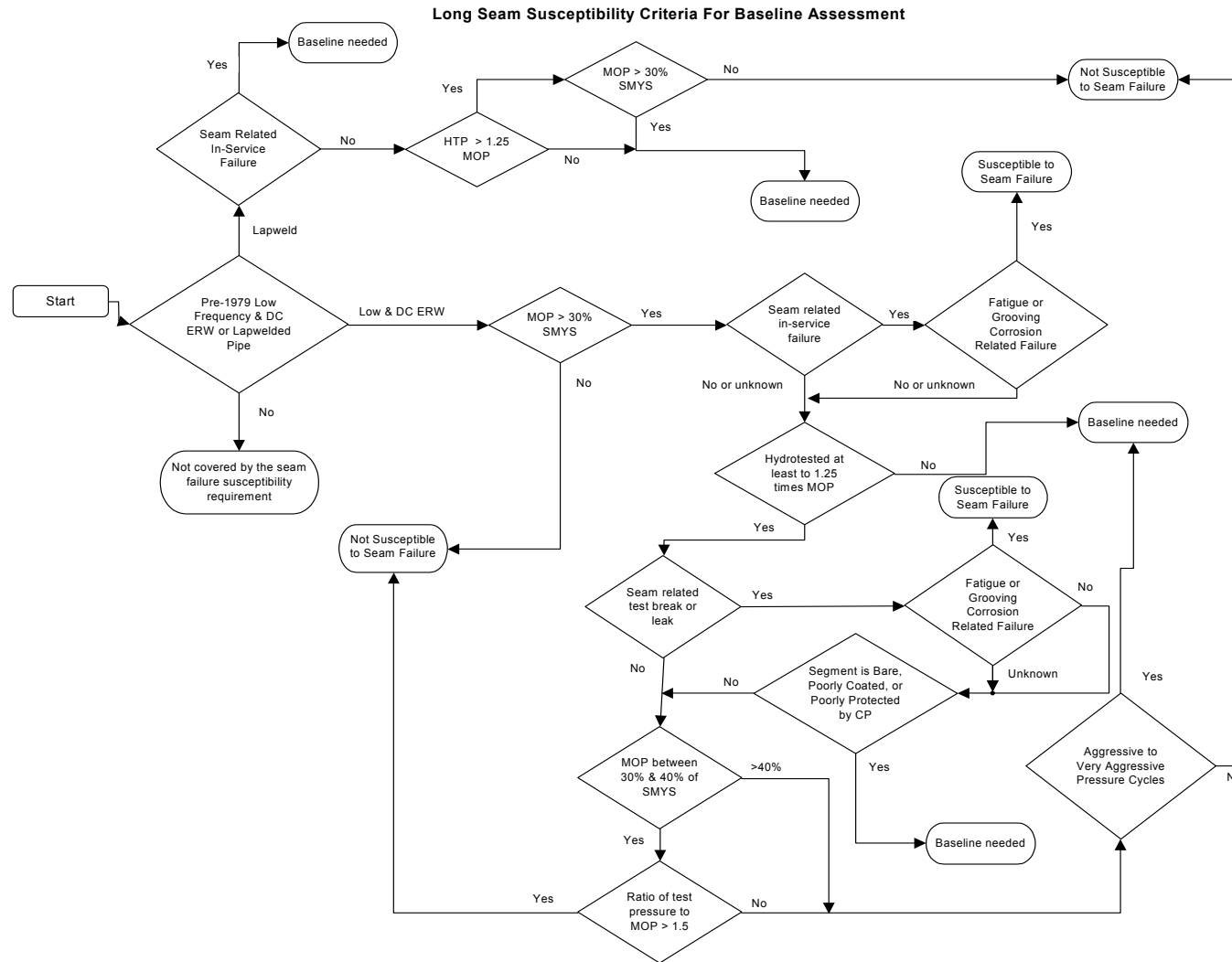


Figure 4.1 Framework for Evaluation

4.3.1 *Types of Seam-Related Defects and the Possible Implications*

4.3.1.1 Lap-Welded Pipe

As stated previously, experience indicates that the number of time-dependent failures of lap-welded seams, if any, seems to be small. The author⁴ has observed only two types of seam breaks in lap-welded pipe, poorly fused seams and burned-metal defects. Where such defects have caused failures, to the author's knowledge, overpressurization was a known or suspected cause. Moreover, among the numerous hydrostatic test failures examined by the author, not one has exhibited evidence of time-dependent growth. One probable reason is the relatively low operating stress levels associated with lap-welded pipe (because of the joint factor). This certainly limits the range of pressure cycles that such pipelines could experience to a level below that one might expect in pipelines operated at or near the maximum permitted level of 72 percent of SMYS. Another reason is that the factors that contribute to selective seam corrosion in ERW and flash-welded materials (microstructural characteristics in the vicinity of the bondline) are not present in lap-welded pipe. Hence, it is not surprising that no such failures have been encountered in the numerous lap-welded seam breaks observed by the author.

The implication of the apparent lack of evidence of the occurrence of time-dependent failures associated with lap-welded pipe is that very few if any of these pipelines would be found susceptible to seam failure. As indicated in Figure 4.1, the threshold for susceptibility for lap-welded pipe is high, so high in fact that it seems likely that few, if any, operators will consider their lap-welded segments in need of seam-integrity assessment.

4.3.1.2 ERW and EFW Pipe

Experience shows that in the absence of an indentation in the pipe, pressure-cycle-induced fatigue failures initiate only at relatively large initial defects. The minimum length initial defect that has been observed by the author is on the order of the square root of the product of diameter times wall thickness (\sqrt{Dt}). Even for a small pipe such as 8.625-inch-OD, 0.188-inch-wall-thickness, this would correspond to a 1.27-inch-long defect. For a 16-inch-OD, 0.250-inch-wall-material, this would correspond to a 2-inch-long defect. Also, it has been observed that the initial depths of defects that were observed to grow by fatigue were at least 10 percent of the wall thickness. Probably for this reason, no fatigue failures are known by the author to have initiated at bondline cold welds in LF-ERW or DC-ERW materials. The typical sources of fatigue cracks in these materials have been hook cracks and mismatched skelp edges. These kinds of defects can be relatively large and still survive a hydrostatic test to 90 percent of SMYS because unlike typical bondline toughnesses for these materials, the toughnesses of the zones where hook cracks and mismatched skelp edges exist are usually about the same as those of the base metal. In contrast, where bondline toughness is relatively high (e.g., the bondline of a modern high-frequency-welded seam), it would appear that

⁴ Comments relative to the author's experience that certain kinds of failures have been observed while others have not are not intended to represent that only certain kinds of failures can occur while others cannot. These comments should be understood in the context that if one does not see a particular outcome among many opportunities, then it is reasonable to assume that the unobserved outcome is a low-probability event.

fatigue could develop at a large bondline flaw. The point is that one does not need to focus on the bondlines of low-frequency or dc-welded materials when the issue is fatigue; the main concern will be defects near but not in the bondlines.

When the issue is selective seam corrosion, the focus should be on the bondline. The crevice-like corrosion that forms, centers on the bondline, creating a relatively sharp defect in a low-toughness material. Typical cases of selective seam corrosion failures suggest that if no initial bondline defect exists, the apparent toughness exhibited by the bondline material will be less than half that of the base metal. Failure pressures of such defects generally are less than half the failure pressure of the same-size defect in the base material. When selective seam corrosion starts at a location where the bondline already contains a weakness such as a cold weld, indications are that the size of defect needed to cause failure at a given pressure level will be considerably smaller than that needed to cause a failure where the bondline is initially sound.

The point of these discussions is to show that operators must consider the implications of material toughness and the threshold sizes of defects that must be detected in a seam-integrity assessment.

4.3.2 Failure History

If a seam-related in-service or hydrostatic test failure has occurred on the segment, the segment is considered susceptible, and if time-dependent growth is shown to be a factor in the occurrence of the failure, reassessment becomes necessary.

Although a single failure does not prove the existence of other similar defects, it is reasonable to assume that defects do exist in the seam. Whether or not these hypothetical defects are susceptible to time-dependent growth is not certain. One must assume that with seams containing populations of defects residing in a pipeline subjected to significant numbers of large pressure cycles, the seams could be susceptible to fatigue failures at some time in the future. Similarly, from the standpoint of selective seam corrosion, if the standard anti-corrosion measures of coating and cathodic protection are absent or deficient, it is assumed that a seam-integrity-assessment program will be needed to assure the absence of failures from selective seam corrosion.

4.3.2.1 Age, Manufacturer, Seam Type

Seam type is an essential parameter. If the seams of the pipe were fabricated by means of LF-ERW, DC-ERW, EFW or furnace lap-welded process, and if the seams are susceptible to failure, a seam-integrity assessment is required as part of the operator's baseline assessment plan.

If the operator knows that the seam type is LF-ERW, DC-ERW, EFW or furnace lap-welded, it is not necessary to know the age of the pipe or its manufacturer. On the other hand, knowing the age and the manufacturer, the operator may be able to determine the seam type if the seam type is not listed in the data on the segment. Information presented in the ASME Research Report, *History of Line Pipe Manufacturing in North America* (Kiefner 1996), may be of help in identifying the seam type based on the age of the pipe and the manufacturer.

As indicated in Section 2, pipelines comprised of LF-ERW pipe, DC-ERW pipe, and EFW pipe have experienced failures from two time-dependent seam-degradation phenomena. One of these phenomena involves the enlargement of seam-related manufacturing defects by pressure-cycle-

induced fatigue, and the other involves selective seam (grooving) corrosion. It is important to note that furnace lap-welded pipe should be considered separately from ERW or EFW pipe for two reasons. First, there is little evidence that lap-welded seams present a significant risk from the standpoint of the typical time-dependent seam-degradation processes that are known to affect ERW pipe and EFW pipe. Second, the maximum operating stress level in a lap-welded pipeline cannot exceed 57.6 percent of SMYS because of the joint factor of 0.8 the operator must use in calculating the required wall thickness under ASME B31.4 and 49 CFR 195. The latter limitation tends to reduce the propensity for a lap-welded pipeline being subjected to aggressive pressure cycles.

4.3.2.2 Maximum Operating Stress Level

The maximum operating stress level (in relation to SMYS) is important because of its relationship with the critical flaw size required to cause a hoop-stress-driven failure, and because of its influence on the sizes of pressure cycles that a pipeline experiences.

4.3.3 Implications of Toughness

The toughness of the pipe material determines the sizes of cracks that can survive a given level of hydrostatic test pressure and the sizes of cracks that will cause the pipe to fail at the MOP⁵. The “starting” sizes established by the test pressure and the toughness have a very significant effect on fatigue life whereas the final crack sizes established by the MOP and the toughness do not. This is the result of the fact that the crack growth per cycle of pressure is a function of both pressure cycle size and crack size. A small starting size, therefore, results in a slowly growing crack and a large starting size results in a more rapidly growing crack. By the same rationale, when the crack is near failure, the steps of growth per cycle become so large that the level of maximum pressure is not that important. That is, the failure pressure will be reached within a few cycles even if the actual maximum level is well below the MOP. In most cases analyzed to date, a toughness of 25 ft-lb was assumed. This value is considered representative of the base material (not the bondline) of ERW pipe manufactured prior to about 1970. A value as high as 40 ft-lb would be at the technologically achievable limit for the time, and it would not result in a significantly shorter predicted fatigue life because 25 ft-lb is close to the level needed to assure the largest possible starting crack size for this size of pipe.

4.3.3.1 Fatigue Crack Growth

In the model used by a number of operators to determine susceptibility to seam failure, a “Paris-law” approach (Paris, unknown) is used to predict the rate of fatigue crack growth. This type of model involves the assumption that the natural logarithm of the rate of crack growth is proportional to the natural logarithm of the range of stress-intensity factor at the crack front during each cycle of pressure. The range of the stress-intensity factor is proportional to the change in pressure that

⁵ A failure pressure level for a given size defect is calculated via the “log-secant” equation developed by W. A. Maxey (Kiefner, 1973) the toughness of the material in terms of ft-lb of Charpy energy and the dimensions (length and depth) are entered to calculate the failure pressure. Conversely, for a fixed level of pressure (such as a hydrostatic test), a range of critical flaw sizes (lengths and depths) can be calculated.

constitutes a particular cycle⁶ but it is also proportional to the square root of the crack depth (degree of penetration through the wall thickness). The latter point is important in two respects. First, the length of the defect is considered but its effect on the stress-intensity factor for fatigue cracks growth is minimal. (Length remains a critical factor in the calculation of failure pressure.) Experience verifies that the focus on depth rather than length is appropriate because by far most of the growth is through the wall thickness. Second, the stress-intensity factor increases as the crack becomes deeper even if the pressure cycles remain constant. The result is that a highly nonlinear growth is predicted in which late in the life of the defect, it grows very rapidly. This circumstance means that reassessment intervals are highly dependent on the sizes of defects that will be revealed during a particular seam-integrity assessment.

The Paris-law equation described above has the following form:

$$\frac{da}{dN} = C(\Delta K)^n \left(\text{or } \log \frac{da}{dN} = \log C + n \log \Delta K \right)$$

$$\Delta K = C_o \Delta P \sqrt{\pi \frac{a}{Q}}$$

where

$\frac{da}{dN}$ is the increase in crack depth per cycle

ΔK is the stress-intensity factor

ΔP is the size (pressure range) of the pressure cycle

a is the instantaneous crack depth

C_o and Q are constants that depend on pipe geometry and defect length, respectively.

The stress-intensity factor is calculated using the technique of Raju and Newman (Raju, unknown).

C and n are constants derived either on the basis of particular fatigue-failure occurrences or from laboratory tests.

The constants C and n are critical to the ability to accurately forecast an appropriate retest interval. However, as will be explained, cycle aggressiveness, one key to determining susceptibility, can be evaluated using any reasonable set of constants. This is because the set of constants chosen “washes out”.

⁶ Pressure-versus-time relationships are available from the operator’s SCADA system. These are “rainflow” counted (ASTM E1049-85) to arrive at a “spectrum” of pressure cycles.

4.3.3.2 Pressure Cycles and Points for Analysis

To evaluate the effects of pressure cycles on the system, pressure cycles recorded for one or more representative periods of time are considered. Sets of pressure-versus-time relationships for relevant locations are reviewed. Points that are analyzed almost always include pump station discharges. These locations tend to coincide with the high-pressure points on the hydraulic gradients. It is logical to expect these locations to experience the largest ranges of pressure cycles. The largest cycles can be expected to have the most detrimental effects on fatigue life. Another consideration for the fatigue-life analysis is the starting defect size. This is influenced both by the toughness of the material and the test-pressure-to-operating-pressure ratio. Thus, when a high-elevation point is located near a pump station discharge, it could conceivably experience the worst combination of large pressure cycles and large starting defect sizes. Such points are examined on the basis that the terrain could result in the shortest time to failure occurring at points other than the pump station discharges. In any case, the choice of multiple points based on these two considerations tends to assure that the locations with the shortest fatigue lives will be discovered through the analyses.

For the analysis of pressure cycles at a station discharge, one can utilize the discharge pressures. For locations that lie between stations, however, one should calculate the pressures from those at the upstream discharge and downstream suction by means of the following equation.

$$P_x = (P_1 + K \cdot h_1 - P_2 - K \cdot h_2) \left(\frac{L_2 - L_x}{L_2 - L_1} \right) - K(h_x - h_2) + P_2$$

where

P_1 = Discharge pressure at the upstream station, psig

P_2 = Suction pressure at the downstream station, psig

K = Pressure per foot of head for the product, psi/ft

L_1 = Milepost of upstream discharge station, miles

L_2 = Mile post of downstream suction station, miles

L_x = Mile post of point of analysis, miles

h_1 = Elevation of upstream discharge station, feet

h_2 = Elevation of downstream suction station, feet

h_x = Elevation of point of analysis, feet.

Either a hydrostatic test or an in-line inspection can be used to establish starting defect sizes for calculation of times to failure. Potential defects that could have barely survived the last hydrostatic test or the largest defect that can escape detection by the last-used in-line inspection tool are postulated to grow for a period of time as the pipeline as the pipeline is subjected to the pressure cycles and/or a specific selective seam corrosion rate. It should be noted that the predicted number of years until failure is based on the assumption that defects of a given size exists. If no such defects exist, the time to failure will be longer.

4.3.4 Predicting Retest Intervals Based on Fatigue Crack Growth

If service or test failures related to fatigue crack growth have occurred or if after a baseline assessment, the operator still considers that fatigue crack growth is a risk, it is important to consider the likely times to failure possibly associated with this phenomenon. Such information is essential to establish appropriate reassessment intervals. To do this, one selects appropriate analysis locations as noted previously that would likely experience the most aggressive pressure cycling. The parameters for these analysis cases include diameter, wall thickness, grade, toughness, an assumed “worst-case” crack-growth rate as defined by appropriate choices of “C” and “n” values, and a set of initial flaw sizes. If the initial defect size is established by an ILI tool, the tool’s threshold detectable depth and an arbitrary length of $2\sqrt{Dt}$ should probably be used to predict the time to failure. The characteristic lengths of fatigue cracks seem to lie between \sqrt{Dt} and $2\sqrt{Dt}$ in most cases. Choosing the longer limit results in a shorter time to failure for a defect with a depth fixed by the tool threshold. If the initial defect size is established by a hydrostatic test, an infinite number of length/depth combinations of starting sizes exists because longer, shallower defects can have the same failure pressure as shorter, deeper defects. The deeper defects, even though shorter, up to a point can be expected to grow the fastest by fatigue. This situation can be handled by analyzing nine length/depth combinations where the depths vary in 10-percent increments from 10 percent to 90 percent of the wall thickness. Each will have an associated length that will cause it to fail at the test pressure. The shortest lives are generally found to be associated with the 60 to 90 percent through-wall defects.

4.3.5 Relative Aggressiveness of the Pressure Cycles

An important element in determining susceptibility to seam failure is the relative aggressiveness of the pressure cycles on the segment. One may evaluate relative aggressiveness by comparing the fatigue lives associated with the spectra provided by the operator to those associated with the pressure cycles listed on a benchmarking scale given in *Dealing with Low-Frequency-Welded ERW Pipe and Flash-Welded Pipe with Respect to HCA-Related Integrity Assessments* (Kiefner, 2002). The benchmarking list is shown in Table 4.1. It is based on actual pressure patterns observed for pipelines in which fatigue failures have occurred. These four spectra are used with other parameters of the actual segment of interest (i.e., its diameter, wall thickness, grade, toughness, etc.) to calculate times to failure. One assumes that the pipeline has been tested to 100 percent of SMYS⁷ and that it is operated at a MOP corresponding to 72 percent of SMYS⁸. These assumptions establish initial and final flaw sizes and key the ranges of pressure cycles to the segment being analyzed. Note that the aggressiveness comparisons are independent of the crack-growth-rate constants, because the same constants are used for time-to-failure calculations involving both the actual and the benchmark cycles. A typical set of resulting times to failure is shown in Table 4.2. As seen in Table 4.2, the very aggressive benchmark cycles produce a life less than 2 years and the aggressive cycles produce a minimum time to failure around 7 years. Because the pressure cycles for the actual segment, as

⁷ Whether or not it actually has been tested to this level does not matter. The purpose of the calculation is to assess the aggressiveness of the actual cycles relative to the benchmark cycles.

⁸ The benchmark cycles have a maximum stress range of 72 percent of SMYS, so the benchmark cycles are keyed to a maximum of 72 percent of SMYS for the segment being examined.

shown in Table 4.3, result in minimum predicted times to failure for the deeper defects around 5 years, the actual cycles are considered aggressive for the case in which the starting defect size was established by a hydrostatic test to 1.25 times MOP. The predictions for times to failure based on the flaws that would survive a test to 1.39 times MOP show that the pressure cycles in this case lie in the moderate-to-aggressive range. Clearly, if the segment was previously tested to a level of only 1.25 times MOP, it would require seam-integrity assessment in the context of the federal pipeline integrity management regulation. On the other hand, if it had been subjected to a previous test of 1.39 times MOP or higher, it might not fall in to the “susceptible” category. Even if the segment has had no seam-related failures due to fatigue or selective seam corrosion, the fact that it was previously tested to a level of only 1.25 times MOP means that it gets rated as susceptible because it is subjected to aggressive pressure cycles.

Table 4.1 Benchmark Cycle Counts—Annual

Percent SMYS	Very Aggressive	Aggressive	Moderate	Light
72%	20	4	1	0
65%	40	8	2	0
55%	100	25	10	0
45%	500	125	50	25
35%	1000	250	100	50
25%	2000	500	200	100
Total	3660	912	363	175

Table 4.2 Remaining Life Based on Categorized Aggressiveness

Pressure Cycle Category	Years to Failure for Various Defect Depth-to-Thickness Ratios			
	90%	70%	50%	30%
Very Aggressive	1.88	1.88	2.38	5.38
Aggressive	7.12	7.37	9.62	21.67
Moderate	18.12	19.12	25.12	56.12
Light	55.63	56.89	71.38	144.89

Table 4.3 Time to Failure Based on Test Scenarios of 1.25 x MOP and 1.39 x MOP

Test Stress Level	Years to Failure for Various Defect Depth to Thickness Ratios			
	90%	70%	50%	30%
1.25 x MOP	5.00	5.47	7.52	24.10
1.39 x MOP	10.32*	10.62	13.79	31.08

*Minimum value of 10.06 occurred for 80-percent-through defect.

As the highlighted path through Figure 4.2 based on the analysis shows, a baseline assessment is needed for the segment. The normal practice is to suggest reassessment by the time “half the time to failure” has been reached. If one does not know the actual crack-growth rate one cannot say what that retest interval should be. Usually in such a case, the suggested solution is to perform a hydrostatic test of the segment as part of the operator’s baseline-assessment program. The results of such a test (or an equivalent in-line inspection) can then be used to determine whether or not reassessment is necessary.

Failures that occur during the hydrostatic test should be investigated for evidence of fatigue. If fatigue exists, reassessment will be needed and the analysis of the defects as affected by the pressure-cycle history can result in the calculation of an approximate crack-growth rate for the segment. This would permit an acceptably accurate means of determining the hydrostatic retest (or re-inspection) interval. If no fatigue-related failures exist, it is reasonable to certify that the pipeline is not susceptible to seam failures in the context of the federal integrity management requirements.

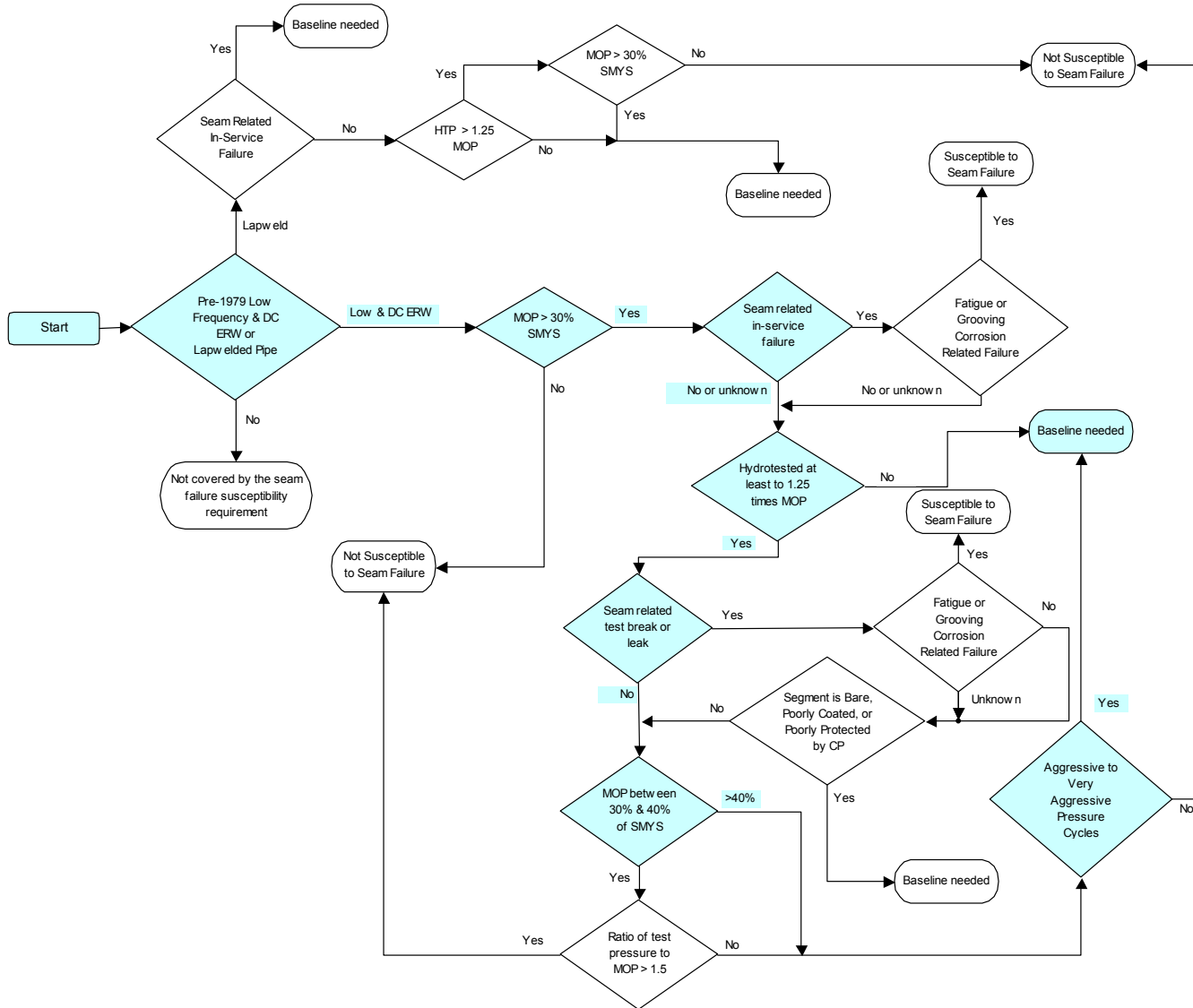


Figure 4.2 Framework for Evaluation with Path for the Segment Analyzed Highlighted

4.3.6 *Selective Seam Corrosion*

Analysis schemes for predicting the times to failure for selective seam corrosion have been put forward in the past and are often considered to forecast reassessment intervals in cases where failures from this phenomenon have occurred. The simplest of these are based on the assumption of a constant corrosion rate. If a base metal rate is known or can be inferred, then the seam corrosion rate will likely be two to four times as great (Groeneveld, 1991). One can then use the log-secant equation (Kiefner, 1973) knowing a representative value of bondline toughness to calculate times to failure for initial defects that could just survive a hydrostatic test to predict the times to failure for representative lengths of defects that will fail at a particular depth at the MOP of the segment. Similar predictions can be made if the initial flaw size is based on the detection threshold depths and lengths associated with particular in-line-inspection tools.

All of the above is relevant to establishing reassessment intervals for segments affected by selective seam corrosion, but it may not be necessary merely to examine susceptibility for the purpose of compliance with 49 CFR 195.452. As Figure 4.1 implies, in the absence of service or test failures from this phenomenon and if a segment is well coated and cathodically protected, an operator could reasonably maintain that the segment is not susceptible and, hence, not a candidate for seam-integrity assessment based on its selective seam corrosion risk. One justification for this approach is that metal-loss inspections will be done in any case, and the results can be used indirectly to monitor for selective seam corrosion. As the operator responds to anomalies in the base metal, it is likely that locations of selective seam corrosion, if any, will become apparent. The operator can revisit the susceptibility question based on what is found.

4.4 *Use of the Spike Test*

Hydrostatic testing constitutes a logical and scientifically valid means of assuring the serviceability of a pipeline. By custom and by federal regulations, a test-pressure-to-operating-pressure ratio of 1.25 is accepted as a satisfactory demonstration of the fitness of a pipeline for service. Empirical evidence of this fact has existed since 1970 (Bergman, 1974). However, it has also been shown that the confidence level in the safety of a pipeline established by a hydrostatic test continues to increase as the test-pressure-to-operating-pressure ratio increases beyond 1.25 (Kiefner, July 2000 and August 2000). One concept of enhancing the assurance level provided by a hydrostatic test is the so-called “spike” test. The spike test consists of raising the hydrostatic test pressure to a level well above 1.25 times MOP for a short period of time (not more than ½ hour). At the end of the spike test, the pressure can be lowered to a level of 1.25 times MOP if necessary to conduct a “Subpart E” test to comply with federal regulations. Because the spike test demonstrates a higher level of integrity than a test to 1.25 times MOP, one can expect to be able to achieve the Subpart E test with little or no risk of failures during the 8-hour hold period. While there is no fixed test-pressure-to-operating-pressure ratio for a spike test, the ratio of 1.39 is frequently used because it is equal to 100/72, the ratio of 100 percent of SMYS to 72 percent of SMYS (the maximum design stress permitted by the regulations).

A downside to the use of spike test is the increased risk of test failures as the pressure is raised beyond a level of 1.25 times MOP. If multiple test failures cannot be tolerated, an operator can set a

target spike test pressure level but settle for a lower level if test failures begin to occur. Of course, it is necessary to achieve a minimum test pressure of at least 1.25 times MOP, so accepting a test pressure below 1.25 times the current MOP means having to lower the MOP. But whatever level the operator is able to achieve in terms of a spike test above 1.25 times MOP becomes the demonstrated level of integrity for the pipeline.

4.5 Impact of Integrity-Assessment Method on Reassessment Interval

The threat of time-dependent defect growth in pipelines implies that periodic reassessment of pipeline integrity is necessary. The challenges are (1) to be able to determine the appropriate reassessment interval, and (2) to optimize the effectiveness of the reassessment technique such that the reassessment interval can be as long as possible without exceeding the time of failure of the worst-case growing defect. In the previous parts of this section, one technique for predicting appropriate reassessment intervals for pipelines affected by pressure-cycle-induced fatigue has been described. In principle, analogous techniques can be used for other modes of time-dependent degradation (i.e., corrosion, stress-corrosion cracking) provided that the rate of degradation can be estimated. This part of the report addresses the second challenge, namely, what determines the effectiveness of a given reassessment technique and allows the operator of a pipeline to apply the technique at timely intervals.

4.5.1 Failure Pressure Versus Defect Size

The relationship of failure pressure versus defect size for a particular pipe material, 22-inch OD, 0.344-inch-wall, API 5L Grade X46 ERW line pipe with toughness corresponding to 17 ft-lb full-size equivalent CVN upper-shelf energy is shown in Figure 4.3. The relationship is based on the log-secant equation (Kiefner 1973). Failure pressure is plotted versus defect axial length for nine different uniform-depth defects with depth-to-thickness ratios ranging from 0.1 to 0.9. Four horizontal lines representing pressure levels of 1,751 psig (theoretical burst pressure of defect-free pipe), 1,439 psig (corresponding to 100 percent of SMYS), 1,295 psig (corresponding to 90 percent of SMYS), and 1,036 psig (corresponding to 62 percent of SMYS) are also shown in Figure 4.3.

This figure is useful for understanding the importance of detectable defect size with respect to integrity assessment. As an example, one can look at the relative sizes of defects that are detectable in a hydrostatic test to a particular pressure level, and from that size one can see how much growth would have to occur for the defect to fail at the maximum operating pressure. If one chooses any particular axial length of defect, say 5.5 inches, the family of 5.5-inch-long defects of various depths all lay on the vertical line at the 5.5-inch mark on the x-axis of Figure 4.3. Only one with zero depth can survive 1,751 psig, but a 5.5-inch-long defect with a depth-to-thickness (d/t) ratio of 0.24 can barely survive at 1,439 psig (100 percent of SMYS). Similarly, a 5.5-inch-long defect with a d/t of 0.37 can barely survive a pressure level of 1,295 psig (90 percent of SMYS). In contrast, it takes a 5.5-inch-long defect with a d/t of 0.56 to cause a failure in service at an MOP of 1,036 psig (72 percent of SMYS).

Next, one can understand the implications of time to failure for a growing defect in the context of Figure 4.3 by assuming a growth rate. For simplicity, consider the case of uniform growth of 0.01 inch per year. When the pipe is new, no defect exists but if a 5.5-inch-long axial strip started to

corrode uniformly over its entire length at a rate of 0.01 inch per year (starting at Point A), it would reach a depth of 0.193 inch in 19.3 years. At that point it would be 56 percent through the 0.344-inch wall thickness, and it would cause a failure at the maximum operating pressure (Point B).

The significance of a particular level of hydrostatic test can also be understood in the context of Figure 4.3. Suppose that the operator suspects that corrosion is occurring and elects to conduct a hydrostatic test after the pipeline has been in service for 10 years. Because the corrosion is progressing at a rate of 0.01 inch per year, the defect will have reached a uniform depth of 0.1 inch (29 percent of the wall thickness) over its 5.5-inch length. Its failure pressure at that time based on the information presented in Figure 4.3 will be 1,385 psig (Point C). If the operator elects to conduct a hydrostatic test to 1,385 psig (96 percent of SMYS), the defect will fail. If the defect should barely survive, it would not grow to failure in less than 9 years, the time it would take to grow from 29 percent of the wall thickness (Point C) to 56 percent of the wall thickness (Point B). But if the operator elects to test to a level below 1,385 psig, not only will the defect not fail, the operator will have no way of knowing that it exists. Ironically, if the operator had waited until 12.7 years after the pipeline was installed and then tested the pipeline to a level of 1,295 psig (90 percent of SMYS), the defect would have grown to a depth of 37 percent of the wall thickness (Point D). At that depth, it would fail at 1,295 psig. However, a just-surviving defect with a depth of 37 percent of the wall thickness would survive only another 6.5 years. So the higher pressure test (1,385 psig) conducted every 9 years is as effective as the lower pressure test (1,295 psig) conducted every 6.5 years.

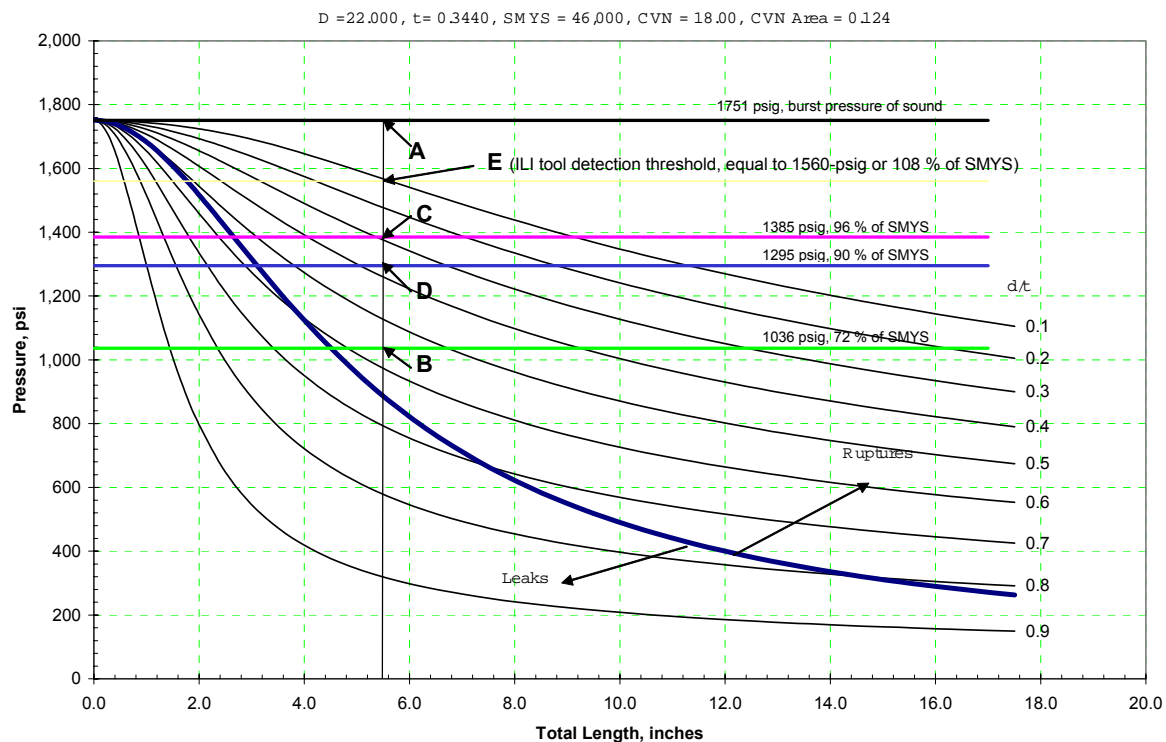


Figure 4.3 Effects of Various Integrity Assessment Levels on Reassessment Levels (Rectangular Flaws)

The above examples illustrate that the higher the test pressure, the smaller will be the defects than can survive the test and the longer will be the required interval between retests conducted at the same pressure level as the initial test to assure continued pipeline integrity. By extension it is clear that an ILI with a tool capable of detecting the defect by the time it reaches a depth of 10 percent of the wall thickness (Point E), would be equivalent to a hydrostatic test to a pressure level of 1,560 psig. Furthermore, the reassessment interval with the tool could be nearly 16 years (Point E to Point B at 0.01 inch per year) on the same basis as the retest intervals discussed previously (i.e., conducting the assessment just before the defect fails without considering a factory of safety).

In the above discussion, no factor of safety was considered. If one adopts a factor of safety of 2, four possible reassessment scenarios can be compared as shown in Table 4.4.

Table 4.4 Comparison of Hydrostatic Testing Versus In-Line Inspection

Scenario	Minimum Time to Failure After Reassessment	Suggested Reassessment Interval Based on Factor of Safety of 2
Hydrostatic test (100 percent SMYS)	11	5.5
Hydrostatic Test (96 percent SMYS)	9	4.5
Hydrostatic Test (90 percent SMYS)	6.5	3.25
In-Line Inspection, minimum detectable depth of 10 percent of wall thickness (equivalent of test to 108 percent SMYS)	16	8.0

The ILI scenario is superior in terms of having the longest reassessment interval. In addition, the operator learns where corrosion is occurring, enabling the prevention of future corrosion and the monitoring of defects that are too small to fail. These advantages accrue without the need to take the pipeline out of service and without the concern of releasing contaminated test water. All that is necessary is that the operator use a tool that can reliably detect the threshold defect size assumed and that the operator responds to the findings in a timely manner. The effectiveness of the tool usually also depends on the operator verifying that the tool is as reliable as claimed. Note that the latter does mean adding an arbitrary “tolerance”; it depends on establishing the statistical confidence level and responding to the findings on that basis. In-line-tool tolerances and reliability are discussed in more detail in Section 5.

The examples provided above are based on a linear rate of degradation. The type and level of reassessment become even more important if the mechanism of degradation is nonlinear in the sense that degradation accelerates with the passage of time. In this respect, pressure-cycle-induced fatigue is a classic example.

Consider the example of fatigue crack depth versus time to failure shown in Figure 4.4. The pipe and defect parameters used to construct Figure 4.4 are almost the same as those used to construct Figure 4.3. The only difference is that Figure 4.4 is based on an elliptically shaped defect whereas Figure 4.3 is based on a rectangularly shaped defect. The difference this makes is that the elliptically shaped

defect must have a greater maximum depth to have the same failure pressure as the equivalent length rectangular (uniform-depth) defect. For example, the 5.5-inch-long rectangular flaw that fails or just survives a pressure level of 1,295 psig has a uniform depth of 0.127 inch (37 percent of the wall thickness) whereas the 5.5-inch-long elliptical flaw that fails or just survives a pressure level of 1,295 psig has a maximum depth of 0.180 inch (52 percent of wall thickness). Because observations of fatigue cracks show that they are actually more elliptical than rectangular in shape, the assumption of elliptical shape for constructing Figure 4.4 seems appropriate.

The crack-depth versus time-to-failure curve in Figure 4.4 was generated using a specific crack-growth rate and a specific set of pressure cycles. However, the principle to be illustrated with this figure would be the same irrespective of the crack-growth rate or the pressure-cycle intensity. What the figure shows is that an initially 0.102-inch-deep, 5.5-inch-long, elliptically shaped defect would be expected to grow in response to the particular crack-growth/pressure-cycle circumstances to a maximum depth of 0.22 inch in 78 years, whereupon it would cause a failure at an operating stress level of 72 percent of SMYS. The horizontal lines on Figure 4.4 labeled 85 percent of SMYS, 90 percent of SMYS, and 100 percent of SMYS represent the maximum depths (on the “crack-depth” axis) that the defect could have reached while barely surviving those test levels. Thus, the defect would have to have a maximum depth no more than 0.18 inch to survive the 85 percent SMYS level, a maximum depth of no more than 0.155 inch to survive the 90 percent of SMYS level, or a maximum depth of no more than 0.11 inch to survive the 100 percent of SMYS level. The crack-depth versus time-to-failure curve shows that it takes 69 years for the crack to reach a depth of 0.18 inch, 57 years to reach a depth of 0.155 inch, and only 17 years to reach a depth of 0.11 inch. What this means is that the elimination of this defect (i.e., the prevention of it failing in service) could be assured by an 85 percent of SMYS test as long as that test is conducted within 9 years before the failure stress level of 72 percent of SMYS is reached, by a 90 percent of SMYS test as long as that test is conducted within 21 years before the failure stress level of 72 percent of SMYS is reached, or by 100 percent of SMYS test as long as that test is conducted within 61 years before the failure stress level of 72 percent of SMYS is reached. These time intervals thus constitute the maximum possible retest intervals (with no factor of safety) for these three hydrostatic test stress levels. These results are summarized in Table 4.5.

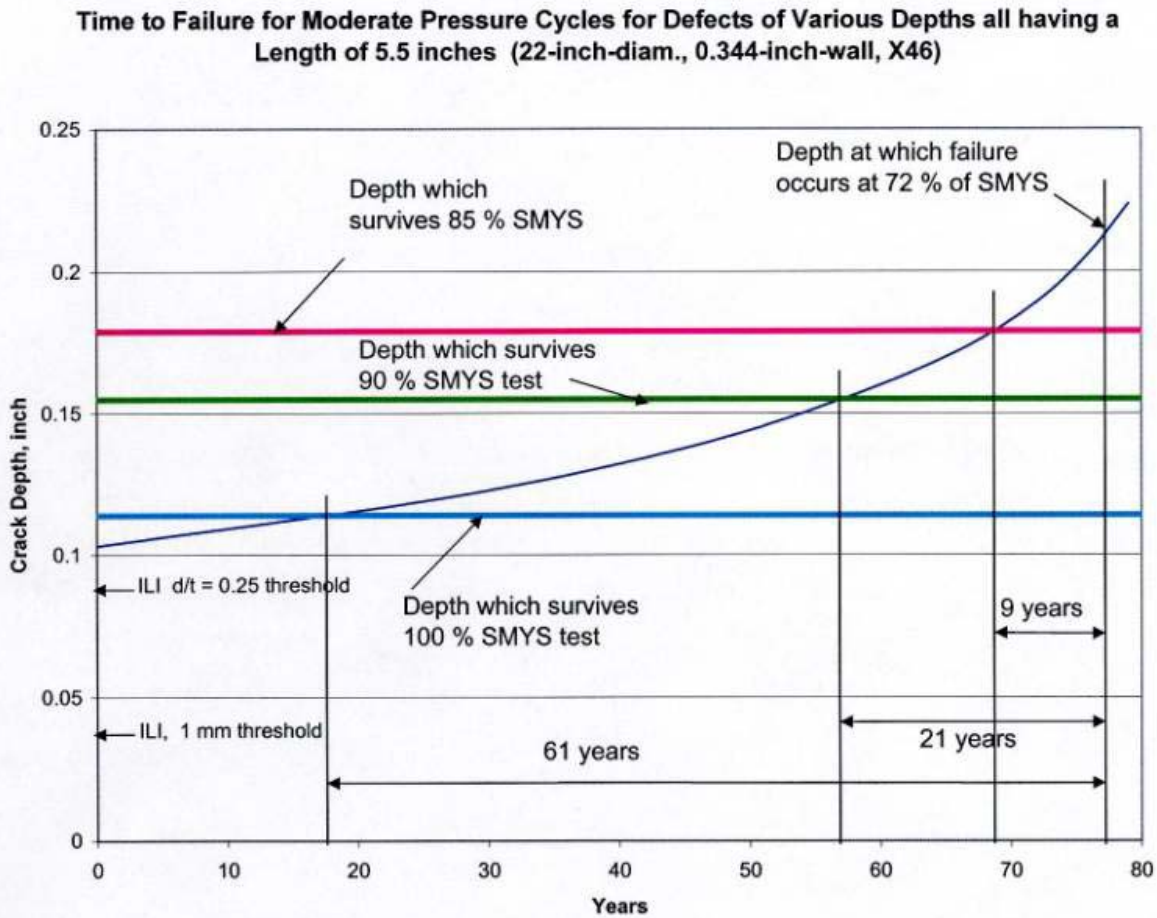


Figure 4.4 Times to Failure for Various Fatigue Cracks (Elliptical Flaws)

Table 4.5 Times to Failure and Retest Intervals for Various Hydrostatic Test Stress Levels

Test Stress Level, percent SMYS	Time to Failure, years	Retest Interval, years (half the time to failure)
85	9	4.5
90	21	10.5
100	61	30.5

Clearly, choosing as high as possible a test-pressure-to-operating-pressure level results in the longest feasible retest interval.

The above comparisons consider only the option of hydrostatic testing. If ILI with a reliable crack-detection tool is considered, the advantages of ILI over hydrostatic testing become obvious. Threshold detection sizes for the known crack-detection ILI tools at this time are (1) a minimum depth-to-thickness ratio of 0.25 for a defect with a length not less than 50 mm (about 2 inches), and (2) a minimum depth of 1 mm for a defect with a length of not less than 50 mm. In terms of the 5.5-inch-long defect portrayed in Figure 4.4 (or for any defect longer than 50 mm), these two threshold depths correspond to 0.09 inch and 0.04 inch. This means that defects smaller than the initial postulated 0.102-inch-deep, 5.5-inch-long defect would have been detected by the tools. It also means that reinspection intervals can be much longer than the 30.5-years inspection interval for the 100 percent of SMYS hydrostatic test.

4.6 References

1. Bergman, S. A., “Why Not Higher Operating Pressures for Lines Tested to 90% SMYS?”, *Pipeline and Gas Journal*, December 1974.
2. Groeneveld, T. P., Davis, G. O., and Williams, D. N., “Evaluations of the Susceptibilities of Electric-Welded Pipe to Selective Seam-Weld Corrosion”, *Eighth Biennial Joint Technical Meeting on Line Pipe Research*, EPRG/NG-18, May 14-17, 1991.
3. Kiefner, J. F., Maxey, W. A., Eiber, R. J., and Duffy, A. R., “Failure Stress Levels of Flaws in Pressurized Cylinders”, *Progress in Flaw Growth and Toughness Testing*, ASTM STP 536, American Society for Testing and Materials, pp461-481, 1973.
4. Kiefner, J. F. and Clark, E. B., *History of Line Pipe Manufacturing in North America*, ASME Research Report CRTD-Vol. 43, Book Number 100396, 292 pages, 1996.
5. Kiefner, J. F. and Maxey, W. A., “Hydrostatic Testing—1, Pressure Ratios Key to Effectiveness”, *Oil and Gas Journal*, pp 54-61, July 31, 2000.
6. Kiefner, J. F. and Maxey, W. A., “Hydrostatic Testing—Conclusion, Model Helps Prevent Failures”, *Oil and Gas Journal*, pp 54-58. August 7, 2000.
7. Kiefner, J. F., “Dealing with Low-Frequency-Welded ERW Pipe and Flash-Welded Pipe with Respect to HCA-Related Integrity Assessments”, *Proceedings of Engineering Technology Conference on Energy*, Houston, Texas, February 2002.
8. Paris, P. C. and Erdogan, F., “A Critical Analysis of Crack Propagation Laws”, *Transactions of the ASME Journal of Basic Engineering*, Series D, Vol. 85, No. 5, pp 405-409, Unknown.
9. Raju, I. S. and Newman, J. C., Jr., “Stress-Intensity Factors for Internal and External Surface Cracks in Cylindrical Vessels”, *ASME Journal of Pressure Vessel Technology*, Unknown.

5 Current In-line Inspection Technology Review

5.1 Subtask 02 – Scope

This chapter addresses Subtask 02 of the Work Scope which states:

“Develop practicable data evaluation procedure for current in-line inspection technologies capable of detecting and characterizing various types of defects generic to pre-1970 ERW and lap welded pipe seams. The purpose is to provide an acceptable degree of confidence in results.

Activities:

- a) Research current NDT technology and develop matrix of applicability (e.g. tool type vs. gas/liquid/both, accuracy range, types of defects).
- b) Interview and collect information regarding data collection, evaluation methodology, and report preparation from no less than two ILI tool vendors.
- c) Compare evaluation methodologies, by tool/defect as appropriate.
- d) Research summary presentations of ILI vendors – statement of accuracy, flaw assessment (size, orientation).
- e) Baseline ILI inspection methods:
 - ≡ relative to each other.
 - ≡ relative to “ultimate” inspection (i.e., hydrotest, spike test, or combination of either with ILI).
 - ≡ relative to economic value of:
 - a) loss of service.
 - b) cost of “ultimate” inspection (cost/benefit).

Deliverables:

- a) Narrative of applicable NDT technology, including summary of vendor interviews
- b) Performance history of vendor tools applied to this situation
- c) Narrative of evaluation methodologies and comparison of techniques
- d) Evaluation of reports/information supplied to operators from vendors”

5.2 Task Overview

The focus of this task is to research available ILI technologies to develop a data evaluation procedure for current methods capable of detecting and characterizing various types of defects generic to pre-1970 ERW and lap welded pipe seams that will provide an acceptable level of confidence in the test results.

ILI is an important investigation tool for determining the condition of a pipeline and is a significant part of a pipeline integrity management program recognized by codified provisions that promotes safe, efficient, and cost effective pipeline operation (NACE, 2000). However, all ILI tools are not equally effective for all types of defects. Rather, the selection of the tool, along with its resolution and accuracy requirements, must be targeted to the type of failure mechanism of concern.

5.3 Code Provisions Relevant to ILI

In the proposed rule making for 49 CFR 192, the operator can assess the integrity of a gas pipeline by one of the following methods:

1. Internal inspection (also known as ILI)
2. Pressure testing
3. Direct assessment
4. Any other method that provides an equivalent understanding of the condition of the line pipe

49 CFR 195.452 allows the operator of a liquid pipeline to assess the integrity of the line pipe by the following methods:

1. Internal inspection
2. Pressure testing (in accordance with 49 CFR 195 Subpart E)
3. Any other method that provides an equivalent understanding of the condition of the line pipe of which direct assessment is normally considered an alternative method.

5.4 ILI for Pre-1970 Pipe

49 CFR 195.452 (j) (6) states: "...for low frequency electric resistance welded pipe and lap welded pipe *susceptible to longitudinal seam failures*, an operator must select integrity assessment methods capable of assessing seam integrity and detecting corrosion...". The reality is that pre-1970 LF-ERW, EFW, and lap welded pipe do present a higher risk of longitudinal seam failure as evidenced by their performance records (Kiefner, 2002).

The most common defects in ERW and EFW pipe are stitched welds or longitudinal lack of fusion (welds that are intermittently fused), longitudinal anomalies, selective corrosion of the longitudinal HAZ, and hook cracking (Kiefner, 2002). Hook cracks are manufacturing defects in the longitudinal weld of the pipe, caused by inclusions at the plate edge that are turned out of the plane of the steel during the welding process. It is the turning out of the metal at the weld that gives the characteristic "hook" or "J" shape to the crack (see Figure 5.1). These cracks may pass the manufacturer's initial hydrostatic test, but fail later due to metal fatigue.

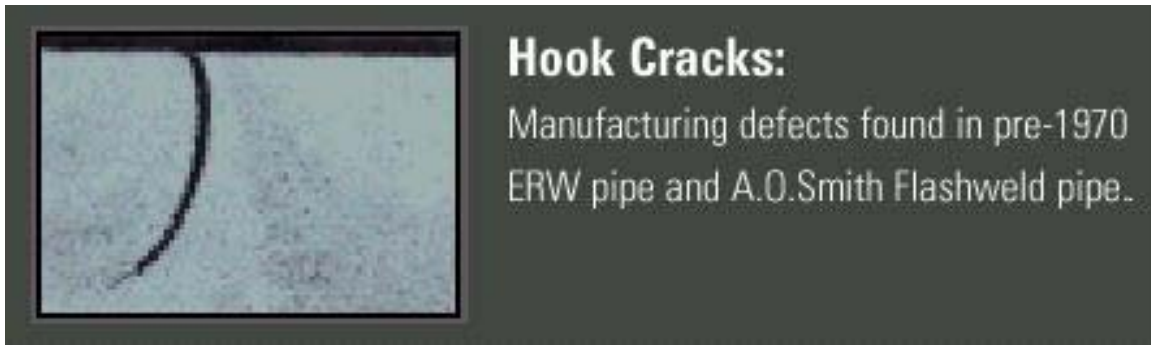


Figure 5.1 Hook crack

Both gas and liquid pipelines can use ILI and pressure testing to assess pipeline integrity. The method the operator selects to assess LF-ERW pipe or lap welded pipe susceptible to longitudinal seam failure must be capable of assessing longitudinal cracking and hook cracking, lack of fusion, as well as detecting selective corrosion of the longitudinal HAZ. In response, operators of pipelines containing these types of line pipe have used or proposed ILI to validate the integrity of these lines, sometimes but not always in conjunction with hydrostatic or spike testing.

5.5 NDT Technology

5.5.1 Introduction

Many different ILI tools are available for assessing the integrity of a pipeline, but must be selected with care for the particular type of defect and level of accuracy required. Figure 5.2 shows an example of an ILI tool (MFL Vectra by BJ Services).



Figure 5.2 ILI Inspection Tool (MFL Vectra/BJ Services)

For detection of internal and external metal loss, MFL and UT tools are commonly used. Both UT and MFL technology have been used to detect corrosion of longitudinal welds. Further explanation and comparison of these techniques is given in Section 5.5.2.

Section 5.5.3 presents a discussion of applicable technology for crack detection. For cracks and longitudinal anomalies, the most common method of detection is shear wave UT. Liquid coupled tools are the most accurate and most common tools used for crack detection. Due to the need for a liquid couplant, these type tools are most commonly used in liquid pipelines. Gas pipelines require the introduction of a liquid slug to provide the needed liquid couplant. Recently introduced wheel coupled tools do not need a couplant and can therefore be used in both gas and liquid pipelines.

Section 5.5.3 also discusses TFI, a relatively recent development in ILI technology. These tools introduce a circumferential magnetic field and can be used to detect cracks, lack of fusion in the longitudinal weld seam, and SCC. However, TFI tools are not able to discriminate between internal and external anomalies and have difficulty in sizing defects.

Various other new ILI technologies are also introduced for completeness, although confidence can only be obtained from practical applications.

5.5.2 *Metal wall loss*

There are two principal methods for detection of metal loss in pipe wall: the MFL method and the UT method. Both UT and MFL technology have been used to detect corrosion of longitudinal welds, but, because longitudinal corrosion can be narrow, both methods have had limited success.

5.5.2.1 **MFL for Metal Loss**

MFL was the first method fully developed for pipeline ILI and has been the most widely used. (Bickerstaff, and NACE, 2000). The MFL tool induces an axial magnetic flux into the pipe wall between two poles of a magnet. A uniform homogeneous steel pipe without defects creates a uniform distribution of magnetic flux. Metal loss causes a disturbance in the magnetic flux, which, in a magnetically saturated pipe wall, “leaks” out. Sensors detect this leakage caused by the metal loss. Because the measurement of metal loss is indirect, only limited quantification using complex interpretation techniques is possible. MFL can be used to measure metal loss in both gas and liquid pipelines. Based on the testing needs, varying levels of sensitivity can be used. These levels are:

- Standard, or low-resolution
- High-resolution
- Extra high-resolution (high number of sensors)

Low-resolution tools can size anomalies to a minimum of 20% wall loss with 15-20% accuracy. High-resolution tool can size anomalies to within 10% of wall loss with 10-15% accuracy. Extra high-resolution tools can detect lower levels of corrosion to less than 10% (Bickerstaff).

5.5.2.2 **UT for Metal Loss**

UT tools directly measure the remaining wall thickness as the tool travels through the pipeline. UT tools have transducers that generate ultrasonic signals perpendicular to the pipe wall. An echo is received from both the inside and outside surface of the pipe. By timing these return signals the tool measures the distance from the pipe wall and the pipe wall thickness. Because the transducers require a liquid couplant to transmit the sound wave, UT tools work best in liquid pipelines.

UT tools can be used in gas pipelines but usually present an increased level of difficulty. To use a UT tool in a gas pipeline requires a liquid slug be introduced into the pipeline to act as a couplant (see Figure 5.3). This procedure usually requires several pigs in front of the UT tool to hold back the liquid and several pigs behind the ILI tool to help remove the liquid when the tool run is complete. This may require modification to existing pig launchers and receivers in order to accommodate staged launching of the pigs. And, since the couplant is usually water, which is a prime contributor to internal corrosion in gas pipelines, the liquid must be removed when the run is complete. Disposal of the liquid used as the couplant also can present a problem.

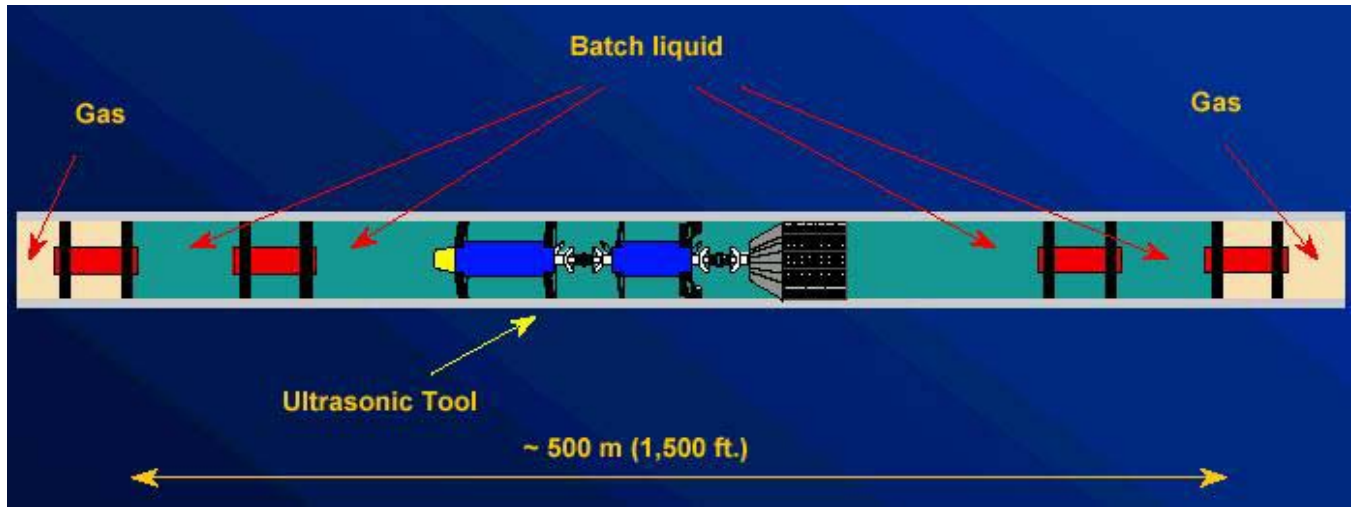


Figure 5.3 UT tool in a liquid batch (Pipetronix)

Several pipeline operators have demonstrated that the rate of metal loss can be estimated by comparison of subsequent ILI UT surveys (Brown, 2003 and Desjardins, 2002). Extrapolating this information leads one to the conclusion that growth rates for other types of anomalies, such as cracks, may also be determined through multiple surveys. A probabilistic approach is necessary to account for accuracy of the UT data. For example, if the level of accuracy is ± 0.0005 mm, and the first run yielded a crack length of 0.01, and a subsequent run recorded the length for the same crack as 0.0105, then it must somehow be determined whether the difference is actually growth or whether the readings are really the same and only vary by the level of accuracy.

5.5.3 Crack Detection Tools

Crack detection is very important to the pipeline industry because of the occurrences of crack-like defects such as SCC, fatigue cracking, hook cracks, lack of fusion, seam weld defects, narrow axial corrosion, dents and gouges associated with cracks, and preferential seam weld corrosion.

C-UT provides ILI with the most reliable results when looking for crack like defects. Most crack like defects (SCC, fatigue, ERW defects, etc.) develop perpendicular to the principal stress in the pipe (hoop stress); therefore, an ultrasonic pulse that is injected into the pipe in the circumferential direction will obtain maximum acoustic response (maximum level of detection) for longitudinal crack-like anomalies.

TFI is a relatively recent development in ILI technology. These tools work similarly to an MFL tool except the magnets introduce a circumferential magnetic field and the transducers detect changes in this field. TFI tools can be used to detect cracks, lack of fusion in the longitudinal weld seam, and SCC. However, TFI tools have difficulty discriminating between internal and external anomalies and in sizing defects.

EMAT is even a newer NDT technology used for ILI tools. EMAT is only recently out of the development phase with few actual runs having been made in pipelines. In fact, several vendors still list EMAT as in development. EMAT does not require a couplant and can be used in either gas or liquid pipelines.

5.5.3.1 C-UT Liquid Coupled tools

Liquid coupled C-UT tools utilize shear waves introduced into the pipe wall through a liquid coupling medium using a propagation angle of 45°. Generally, these tools provide full coverage of the pipe and are sensitive to a larger number of features than MFL as well as being capable of discriminating size of anomaly, defect type and location (internal, external).

C-UT tools have been used on ERW pipe that suffered from hook cracks, lack of fusion, and seam corrosion. Hook cracks and lack of fusion are typically found at the weld centerline and are easily detected by C-UT tools. Weld seam corrosion occurs in the HAZ of the longitudinal weld and can also be detected by C-UT. However, due to the nature of the defect the reliability of the results is not as good.

Figure 5.4 gives the specifications for UltraScan™, the PII UT tool employing shear waves for crack detection, while Figure 5.5 gives the specifications for the Pipetronix tool. The specifications are very similar.

Nominal Tool Diameter	22 to 56 inches
Number of Sensors	up to 1,024, depending on tool size
Wall Coverage	100 percent (longitudinal weld and base material)
Active Range (varies with tool size)	Up to 155 miles / 250 km
Minimum Length of Defect	1.1 inches / 30 mm at 1 m/s 2.2 inches / 60 mm at 2 m/s
Minimum Depth of Defect	1 mm
Location Accuracy - Axial - Circumferential	± 7.8 inches / ± 20 cm ± 5°
Markering System	Time based marker system

Figure 5.4 UltraScan™ Specifications (PII, GE Power)

NACE International	
Table C5: Typical Specifications for Liquid-Coupled Crack-Detection Tools	
Axial sampling distance: 3.0 mm (0.12 in.)	
Circumferential sensor spacing: 10 mm (0.4 in.)	
Detection limitations:	
Detectable defects:	Minimum length: 30 mm (1.2 in.) Minimum depth: 1 mm (0.04 in.)
Defect alignment:	± 15° of the pipe axis
Defect location:	Internal mid-wall, external, base material, longitudinal weld
Inspection speed: Up to 1.0 m/s (2.3 mph) (to achieve maximum axial resolution; axial resolution deteriorates linearly at speeds higher than 1.0 m/s [2.3 mph])	
Available sizes: 56 to 142 cm (22 to 56 in.) (smaller sizes will be available in 2001)	
Sizing accuracy:	
Length:	± 10% WT (for features > 100 mm [4 in.]) ± 10 mm (for features < 100 mm [4 in.])
Width (for crack fields):	± 50 mm (2 in.)
Depth: classification in categories:	< 12.5 % WT 12.5 to 25 % WT 25 to 40 % WT > 40 % WT
Location accuracy:	
Axial (relative to the closest girth weld):	0.1 m (4 in.)
Circumferential:	± 5°
Confidence level: 80 % > 90%	

Figure 5.5 Crack Detection Tool (Pipetronix)

5.5.3.2 C-UT Wheel Coupled Tools

Wheeled coupled C-UT tools utilize shear waves introduced into the pipe wall at an angle of 65° using liquid filled wheels to couple the transducers and the pipe wall. Because wheel coupled tools do not require additional couplant these tools can be used in either gas or liquid. However, these tools have difficulty discriminating between internal and external anomalies and have limited sizing capability.

Figure 5.6 presents the specifications for the Elastic Wave™ tool of PII. A comparison with the specifications for the liquid coupled tools shows that the minimum depth of defect has changed from 1mm to 20-25% of the thickness and the minimum length of defect has more than doubled.

Nominal Tool Diameter	20 to 48 inches / 50 to 122 cm
Features Reported	SCC colonies, fatigue cracks and other defects in the long weld, and axial crack-like anomalies in the body of the pipe
Ultrasonic Frequency	2 MHz
Pulse Repetition Frequency	Up to 600 Hz
Active Range (varies with tool size)	Up to 100 miles / 150 km
Tool Speed	Up to 6.7 mph / 3 m/s in liquid Up to 17.8 mph / 8 m/s with gas bypass
Operating Temperature	30 to 100 °F / 0 to 40 °C
Smallest Bend Radius	Standard: R=3xD Optional: R=1.5xD for 24"
Minimum Length of Defect	3 inches / 75 mm
Minimum Depth of Defect	0.2t - 0.25t
Location Accuracy - Axial - Circumferential	± 8 inches / 0.2 m from reference weld ± 5°
Maximum Pressure	1,000 psi / 70 bar

Figure 5.6 Specification for Elastic Wave Tool (PII/GE Power)

5.5.3.3 TFI Tools

TFI tools are relatively new but have been used on pipelines for detection of “hook” cracking. These tools operate equally well in liquid and gas pipelines, and since the magnetic field is introduced in the circumferential direction, TFI is more sensitive to longitudinal anomalies than standard or high resolution MFL. However, because the tool does not discriminate well between defects, often other tools, such as UT (shear wave), are used to supplement the data gathered. The tool also has difficulty in sizing defects.

A schematic of the operation of the tool is shown in Figure 5.7. Very tight cracks do not alter the propagation of the flux sufficiently to ensure reliable detection. If the cracking is sufficiently large so as to increase the stress concentration, the magnetic flux will be altered increasing the probability of detection. These tools have been used to detect cracks, lack of fusion in the longitudinal weld seam, and SCC.

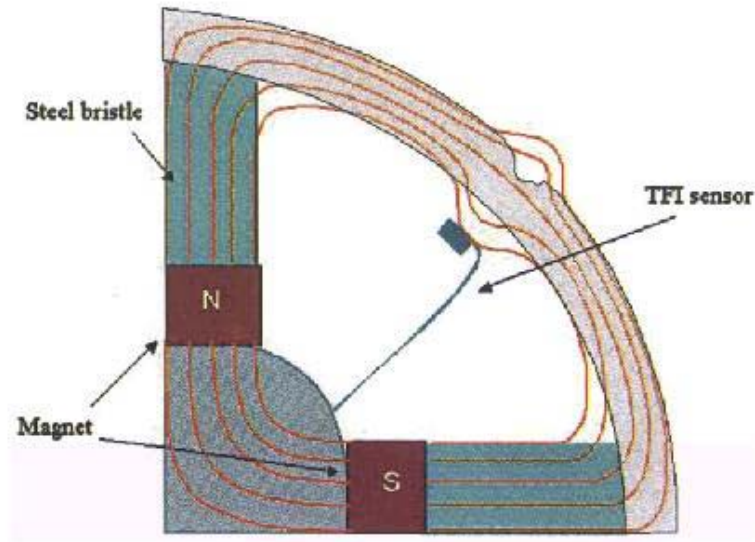


Figure 5.7 Schematic of TFI Sensor

Figure 5.8 gives the specifications for TransScan™, the PII TFI tool.

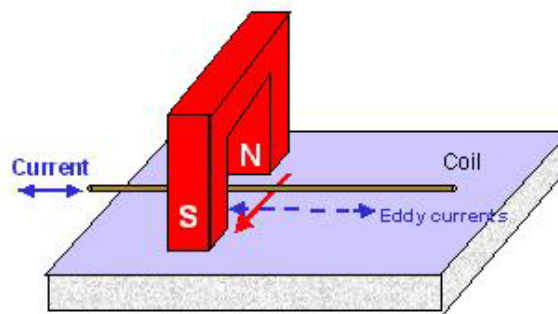
Operating Specifications	TranScan	
Media	Liquid and Gas	
Maximum Pressure	220 bar	
Max. Speed	4.0 m/s	
Min. Speed	0.2 m/s	
Min./Max. Temperature	0 - 60°C	
Min. Bend Radius	3D	
Min./Max. Wall Thickness	5 mm to 15 mm	
Inspection specifications	Pitting	General
Depth Sizing Accuracy	+/- 15%	
Length Sizing Accuracy	+/- 10 mm	+/- 20 mm
Width Sizing Accuracy	+/- 25 mm	
Min. Det. Depth (Gen Corrosion SW/ERW)	20%	
Min. Det. Depth (Pitting SW/ERW)	40%	
Min. Det. Pitting Depth (Seamless)	50%	
Min. Det. Pitting Diameter	5 mm	
Min. Sizable Pitting Diameter	5 mm	

Figure 5.8 TransScan (PII, GE Power)

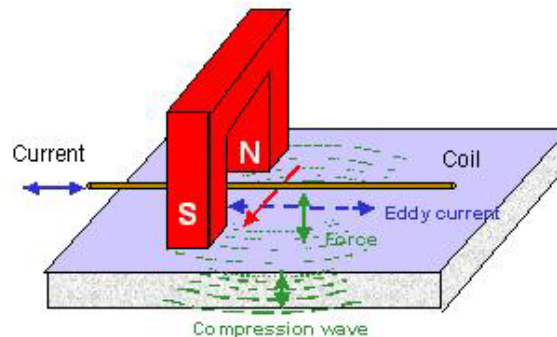
5.5.3.4 EMAT Tools

EMAT has recently been developed for the detection of cracks. The basic principle of EMAT is the generation of an ultrasound compression wave using a magnetic field at the internal surface of the pipe wall. Alternating current placed through the coil induces a current in the pipe wall, causing Lorentz forces (Bickerstaff). After the compression wave has been generated, it travels through the pipe wall and reflects from the surfaces. The returning echo produces a pulse in the transducer. As with traditional UT, the time between firing pulses and the echoes determines the remaining pipe wall thickness. Figure 5.9 shows a schematic of the EMAT operation.

Like wheel coupled ILI tools, EMAT tools do not need a couplant and can, therefore, be used in both liquid and gas pipelines.



- Establish a magnetic field in the pipewall
- A coil carries AC current at a 90° angle to the magnetic field
- 'Mirror' eddy currents start to flow in the pipewall



- A force normal to the pipewall is exerted on the eddy currents
- This force generates ultrasound travelling through the pipewall

Figure 5.9 Schematic of EMAT Sensor

5.5.3.5 ET Tools

ET is an emerging electromagnetic NDT technique similar to EMAT that can only be used on conductive materials. ET is used for crack detection and sorting of materials, and is commonly used in the aerospace, automotive, marine, and manufacturing industries.

Relative to gas pipelines, ET is typically an external inspection technique, but some specialized techniques hold promise for internal inspection (Bickerstaff).

5.6 Interviews

Most pipeline operators use ILI as part of their integrity management program. Only where the pipeline is not capable of using an ILI tool, or where the stress induced by the ILI tool on the pipeline limit its use, do pipeline operators rely on other methods for assessing pipeline integrity, such as direct assessment, which is gaining favor over hydrostatic testing.

While TFI tools are relatively new, TFI has been used on pipelines containing pre-1970 ERW line pipe looking for “hook” cracking, longitudinal weld defects, and selective corrosion in the weld HAZ. As stated earlier, TFI tools do not discriminate well between defect types and also have difficulty in sizing defects, therefore other methods such as UT (shear wave) tools are often used to supplement the data gathered.

UT tools, in general, have difficulties with waxes or solids build up. Several operators indicated that waxes that build up during operation had to be removed prior to running an UT tool. If waxes or other solids can precipitate out of the liquid stream, these solids can coat the UT transducer causing the sound beam to attenuate. Waxes on the pipe wall also can interfere with the UT signal transmission through the pipe wall and result in poor data. Several ILI users indicated problems with waxing that resulting in only partial data being attained during a pig run.

UT tools have been used on ERW pipeline where the pipeline suffered from seam corrosion. The areas of corrosion were very selective, occurring mostly at bends where the coating had become disbonded during bending. The UT tool detected several areas of suspected corrosion associated with longitudinal weld seams, and upon field examination, 50-60% of the areas indicated did have seam corrosion.

EMAT is only recently out of the development stage, and therefore very few pipelines have actually used this technique for ILI.

5.7 Performance History

MFL is the most common ILI tool used to detect metal loss, though UT has also seen significant usage. The use of ILI to detect crack-like anomalies using these type tools has recently been developed.

TFI was developed as a natural out growth of MFL, and builds on standard MFL technology. TFI is intended to evaluate longitudinal cracking. While TFI can successfully identify longitudinal anomalies, the process has difficulty in discriminating between types of anomalies and size of anomaly.

C-UT tools have been used on ERW pipe suffering from hook cracks, lack of fusion, and seam corrosion. Hook cracks and lack of fusion are typically found at the weld centerline and are easily detected by C-UT tools. Weld seam corrosion occurs in the HAZ of the longitudinal weld and can also be detected by C-UT. However, due to the nature of the defect the reliability of the results is not as good. Several ILI users have indicated that this type of corrosion is very selective, occurring mostly at bends where the coating had been damaged during pipeline construction.

EMAT is very new NDT technology. In 1997, Pipetronix proposed the EmatScan™ CD tool concept for gas pipelines, with the first commercial use scheduled in 2003. Very few tools using EMAT technology are available. Few runs in pipelines, and then only recently, have been completed.

5.8 Evaluation of Methodologies

Table 5.1 lists several ILI methods and the types of threats that can be evaluated using each method.

**Table 5.1 NDT Methodology and Threats to the Integrity of Pipelines
(PII, and NACE 2000)**

ILI NDT Technology	Media	Minimum Crack Width	Crack Length	Crack Depth	Threat to Pipeline Integrity
MFL	Gas and Liquid	—	—	—	External and internal metal loss Mechanical damage
UT Compression Wave	Gas and Liquid ^a	—	—	—	External and internal metal loss Dents and gouges
TFI (TranScan)	Gas and Liquid	0.1 mm	Short: 25-50 mm Long: ≥50 mm	Short: 50% Long: 25%	Hook cracks, lack of fusion, seam weld defects, narrow axial corrosion, dents and gouges associated with cracks, preferential seam weld corrosion, axial laps
EW (UltraScan CD)	Gas and Liquid ^{a,b}	0.0 mm	≥30 mm	1 mm	Hook cracks, lack of fusion, seam weld defects, narrow axial corrosion, dents and gouges associated with cracks, preferential seam weld corrosion, axial laps
EMAT	Gas and Liquid	0.0 mm	≥30 mm	1 mm	SCC Colonies, sub-critical SCC, longitudinal fatigue cracks, toe cracks, hook cracks, cracks in or along the seam, lack of fusion cracks

^a— Special provisions for coupling to the wall are necessary for gas.
^b—Fluid filled wheels are available..

Methods like MFL and UT are well established NDT methods and well understood technologies. Confidence in the results using these technologies is high. TFI is understood but has several drawbacks, such as sizing and location. EMAT is just emerging from the development stage. Confidence in this technology is likely to improve with time.

Figure 5.10 from PII/GE Power website depicts the PII recommendations for crack detection for a number of specific flaws. The caption from the website reads:

“Ultrascan CD™

- The most accurate and reliable technology for all types of longitudinal cracks, including SCC

- Cracks as shallow as 1 mm in depth and 30 mm in length can be detected
- Individual cracks less than 0.1 mm wide can be reliably detected

Elastic Wave™

- Appropriate technology for nearly all types of longitudinal cracking in liquid and gas pipelines
- Cracks deeper than 25 percent of wall thickness and 50 mm in length can be detected
- Individual cracks less than 0.1 mm wide can be detected

TranScan™

- Appropriate technology to detect seam weld cracking and/or combinations of mechanical damage and cracking in liquid and gas pipelines
- Cracks deeper than 25 percent of wall thickness and 50 mm in length can be detected
- Individual cracks wider than 0.1 mm can be detected”

Type of Flaw	Tools				
	UltraScan CD	Elastic Wave Vehicle	TranScan	MagneScan	UltraScan WM
Small SCC	***	**			
Large SCC	***	***	**		
Longitudinal Fatigue Cracks, Toe Cracks	***	***	*		
Hook Cracks	***	***	***		
Long Weld Shrinkage Cracks	***	***	*		
Lack of Fusion Cracks	***	***	***		
Axial Laps	**	**	**		***
Dents with Cracking and/or Metal Loss	*		***	*	
Axial Gouging and Cracking	**	**	**		
Narrow Axial Corrosion	*		***	*	**
Hydrogen Induced Cracking					**
Circumferential Cracks	**			*	
Girth Weld Cracks	**			***	

Figure 5.10 Graphical Comparison of ILI Technology (PII, GE Power)**5.9 Evaluation of Information Supplied to Operators from Vendors**

Vendor information was obtained using the Internet. Information was obtained from GE Power Systems (PII), Tuboscope a Varco Company, and BJ Pipeline Inspection Services.

All three vendors offer inspection software for data reporting and fit-for-service evaluation. All three vendors offer pipeline inspection databases.

5.9.1 MFL tools

MFL tools are well established drawing on over 30 years of experience. Most vendors have high-resolution inspection tools. Tuboscope indicated that future options for the Combo Tool would be crack detection and grading improvement modules, though currently the axial magnetizer only has the ability to detect mature cracks or crack-like defects. BJ Pipeline Inspection Services uses a high-resolution MFL pipeline tool that uses tri-axial sensor configuration, which is claimed to give higher resolution of anomalies, especially in the circumferential direction and accurate sizing of long narrow axial corrosion features.

For crack detection, GE Power Systems (PII) has TranScan a TFI tool and claims cracks as narrow as 0.1 mm can be detected. Tuboscope plans the addition of circumferential MFL modules to the Combo Tool.

5.9.2 UT Tools

For crack and crack like anomalies GE Power Systems (PII) has several UT tools including UltraScan CD, a liquid coupled 45° angle circumferential shear wave inspection tool, and Elastic Wave, which uses a fluid filled wheel and injects ultrasound into the pipe wall at a 65° angle. These tools are presented as being able to find very tight, short cracks.

5.9.3 EMAT

GE Power Systems, PII Pipeline Solutions has the EmatScan CD tool that claims to be capable of locating and measuring longitudinal seam cracking including fatigue cracking, SCC, lack of fusion, toe cracks, hook cracks and shrinkage cracks. Tuboscope plans the addition of EMAT modules to the Combo Tool.

5.10 Baseline Pipeline Integrity using ILI Methods

Both the intended gas line rule for 49 CFR 192 and the current liquid rule in 49 CFR 195 allows the use of ILI for establishing a baseline for assessing pipeline integrity. The NDT inspection method used for ILI is based upon the pipeline operator and the anticipated defects.

5.10.1 Economic Issues

An operator must consider the cost of preparation for the ILI inspection run, throughput during the ILI run, and any costs for returning the pipeline back to service. The direct cost for an ILI run is the

ILI tool fee, which usually includes the cost to run the tool, the “first pass” at anomaly identification and sizing, and the “first pass” at fit-for-service. The tool provider will also supply the data for the pipeline database. The operator will also incur the cost of personnel time for launching and receiving the tool, and review of the data. If questionable anomalies are found there is also a cost for investigation and repairs, if needed.

5.10.2 Cost for ILI

The easiest cost to define is the cost for the ILI contractor and data interpretation by the ILI contractor. Competitive bidding is normally used to attain these costs. The cost for operating personnel to launch and receive the ILI tool can be evaluated from the ILI tool bidders data. The following cost estimating “rule-of-thumb” is given for an ILI run:

- Low resolution tool - \$600 per mile
- Medium resolution tool - \$3,000 to \$6,000 per mile
- High resolution tool - \$5,000 to \$10,000 per mile

These costs do not include the operator’s evaluation of the ILI tool data, the internal prioritization and scheduling cost for post-run investigations such as digs to verify the ILI data, nor, as appropriate, the cost for repair to anomalies. In a separate conversation, Neb Uzelac of Pipetronix generally validated these values noting that the “ballpark” cost for the crack detection tool offered by Pipetronix, a shear wave ultrasonic tool, would be about \$6,000 per mile.

For the investigation of cracks and crack-like anomalies, high-resolution tools will be required. Thus, the ILI contractor cost will be at the high end of the given cost range.

5.11 ILI versus Pressure Testing

ILI may be considered the preferred method for evaluating pipeline integrity if it can be demonstrated that the ILI method used accurately identifies any critical defects within the pipe and the cost is equal to or less than that for pressure testing. Obviously, if ILI does not provide reliable results or is more expensive, than it may be considered less desirable than a pressure test.

There maybe, however, occasions where ILI is preferred even though more expensive to perform (e.g., determining defect growth rates, when additional data collection maybe desired, etc.) than pressure testing and vice versa.

In some cases, due to diameter or other system constraints, ILI cannot be performed at all, in which case pressure testing maybe the only real option.

5.12 References

1. Bickerstaff, Robert, et al, “*Review Of Sensor Technology For In-Line Inspection Of Natural Gas Pipelines*”, Sandia National Laboratories.
2. Brown, William H., Wilson Rivera, “*ILI Data Integratrion: Pipeline Integrity Analysis Using Multiple Inspection Technologies*”, 2003.

3. Desjardins, Guy J., et al, “*Analysis Of Corrosion Rates On A Gas Transmission Pipeline*”, NACE Corrosion 2002.
4. Kiefner, John F., Willard A. Maxey, “*Periodic Hydrostatic Testing Or In-Line Inspection To Prevent Failures From Pressure-Cycle-Induced Fatigue*”, 2000
5. Kiefner, John F., “*Dealing with Low-Frequency-Welded ERW Pipe and Flash-Welded Pipe with Respect to HCA-Related Integrity Assessments*”, ASME Engineering Technology Conference on Energy, February 2002.
6. NACE Technical Committee Report, “*In-Line Nondestructive Inspection Of Pipelines*” Publication 35100, December 2000

6 Current Integrity Evaluation Procedure Assessment

6.1 Subtask 03 – Scope

This chapter addresses Subtask 03 of the Work Scope which states:

“Evaluate applicability of current integrity evaluation procedures, such as API 579, ASME B31.4, RSTRENG and other pipeline defect evaluation methods for the ERW and lap welded pipe seam defects. Suggest further improvement and research needs.

Activities:

- a) Research current evaluation technology for seam defects, given information supplied from ILI evaluation. Develop reference list for technology noting critical testing programs as appropriate.
- b) Compare and contrast evaluation procedures, especially noting common problems, errors, misunderstandings. Prioritize data items input to the procedure as to their effect on the summary evaluation.
- c) Research ongoing and/or planned industry efforts. Discuss alternative techniques that have not been subject to group development (e.g. project specific experiences in contrast to code/guide requirements).
- d) Develop matrix of techniques vs. areas of applicability
- e) Develop list of suggested improvements, noting data and or testing requirements as appropriate.

Deliverables:

- a) Narrative detailing available evaluation procedures, noting range of applicability, available”

6.2 49 CFR 192 and 195

49 CFR 192 and 195 are the governing regulations for transportation of gas and hazardous liquids by pipeline and present the minimum federal safety standards that must be met in design and operations of pipeline systems within the United States.

49 CFR 192 requires testing of all new pipeline segments prior to operation or segments that have been relocated or replaced prior to return to service. However, no requirements are given for pipelines already in operation that may not have been tested until changes in Location Classification occur or the operator intends to uprate the operating pressure.

49 CFR 195 has similar requirements for pressure testing of pipelines, including older pipelines currently in operation. 49 CFR 195 does, however, provide a “risk-based alternative to pressure testing” for these pipelines. This alternative requires the establishment of a program for testing a pipeline on risk-based criteria and further states that the program “shall provide for pressure testing for a segment constructed of electric resistance-welded (ERW) pipe and lapwelded pipe manufactured prior to 1970 susceptible to longitudinal seam failures...”. It further states “All pre-

1970 ERW pipe and lapwelded pipe is deemed susceptible to longitudinal seam failure unless engineering analysis shows otherwise.” Guidance for such an engineering evaluation is given in 49 CFR 195.303 (d): “In conducting an engineering analysis an operator must consider the seam-related leak history of the pipe and pipe manufacturing information as available...” Pipe manufacturing information specifically mentioned include:

- Mechanical properties of the steel, including fracture toughness.
- Whether the ERW process was high-frequency or low-frequency.
- Whether the seam was heat treated.
- Whether the seam was inspected.
- Test pressure and duration of mill hydrotest.
- Quality control of the steel-making process.

6.3 ASME B31.4

The ASME Code for Pressure Piping B31.4, *Pipeline Transportation Systems for Liquid Hydrocarbons and Other Liquids* is currently the industry standard for design and operations of liquid pipelines and is used to supplement 49 CFR 195. As with 49 CFR 195, B31.4 details requirements for monitoring and surveillance, as well as corrosion evaluation, however, it too is essentially silent on evaluating seam defects. Basically B31.4 requires that such defects must be repaired when found and does not allow evaluation as a means to avoid a repair. B31.4 does, however, acknowledge a difference between longitudinal welds and the main body of the pipe at least where evaluation of corrosion is concerned as stated in §451.6.2 Item (7), “This method shall not be used to evaluate corrosion concentrated in electric resistance welded seams (ERW), electric induction welded seams or electric flash-welded seams...”.

6.4 ASME B31.8 and B31.8S

The ASME Code for Pressure Piping B31.8, *Gas Transmission and Distribution Piping Systems*, and B31.8S, *Managing System Integrity of Gas Pipelines*, are currently the industry standard for design and operations of gas pipelines and is used to supplement 49 CFR 192. As with 49 CFR 192, B31.8 details requirements for monitoring and surveillance, and is also essentially silent on evaluating seam defects. It is basically similar to B31.4 in requiring repair of certain seam defects rather than permitting an evaluation to avoid a repair.

B31.8S does, however, go into some detail on gathering, reviewing and integrating data for use in risk assessments and presents a somewhat cursory discussion of the use of ILI for defect detection and evaluation. Section 2.2, *Integrity Threat Classification* of B31.8S, lists defective pipe seam as a stable, manufacturing related defect. Section 6.2, *Pipeline In-Line Inspection*, specifically addresses internal and external corrosion, stress corrosion cracking, and third party and mechanical damage, but goes on to state that ILI “is typically not the appropriate inspection method to use in all other threats listed in section 2.” Regardless, B31.8S does not provide actual guidance on evaluating the results of ILI.

6.5 ASME B31G and RSTRENG

ASME B31G, *Manual for Determining the Remaining Strength of Corroded Pipelines*, is based on research completed by Battelle Memorial Institute in 1971. This work examined the fracture initiation behavior of metal-loss defects caused by corrosion in line pipe to better understand failure mechanisms associated with these defects.

Subsequent to these initial efforts, the AGA Pipeline Research Committee assumed responsibility for further research and began developing procedures for predicting the pressure strength of line pipe containing various sizes and shapes of corrosion defects.

The main goal of the research was to “examine the fracture initiation behavior of various sizes of corrosion defects by determining the relationship between the size of a defect and the level of internal pressure that would cause a leak or rupture.”

ASME B31G is limited to corrosion in the body of the line pipe, which have relatively smooth contours and cause low stress concentration. The procedure is based on a total of 47 full-scale tests on pipe containing actual corrosion defects and was further validated in tests conducted by British Gas.

ASME B31G was later modified to reduce perceived conservatism in the model. A total of 86 burst tests on pipe containing corrosion defects were conducted to validate the Modified B31G method. RSTRENG (Remaining Strength of Corroded Pipe) was developed from the Modified B31G method to allow assessment of a river bottom profile of the corroded area to provide more accurate predictions of remaining strength.

Figure 6.1 presents a comparison of how the three methods determine the area of metal loss associated with a corrosion defect. ASME B31G assumes a parabolic shape for short corrosion ($B \leq 4.0$, where B is determined using a formula that is based primarily on the ratio of the depth of the defect to the wall thickness of the pipe) and a rectangular profile for long corrosion. The Modified B31G method assumes a rectangular profile with a depth of 0.85 of the maximum. RSTRENG uses the actual river bottom profile of the defect.

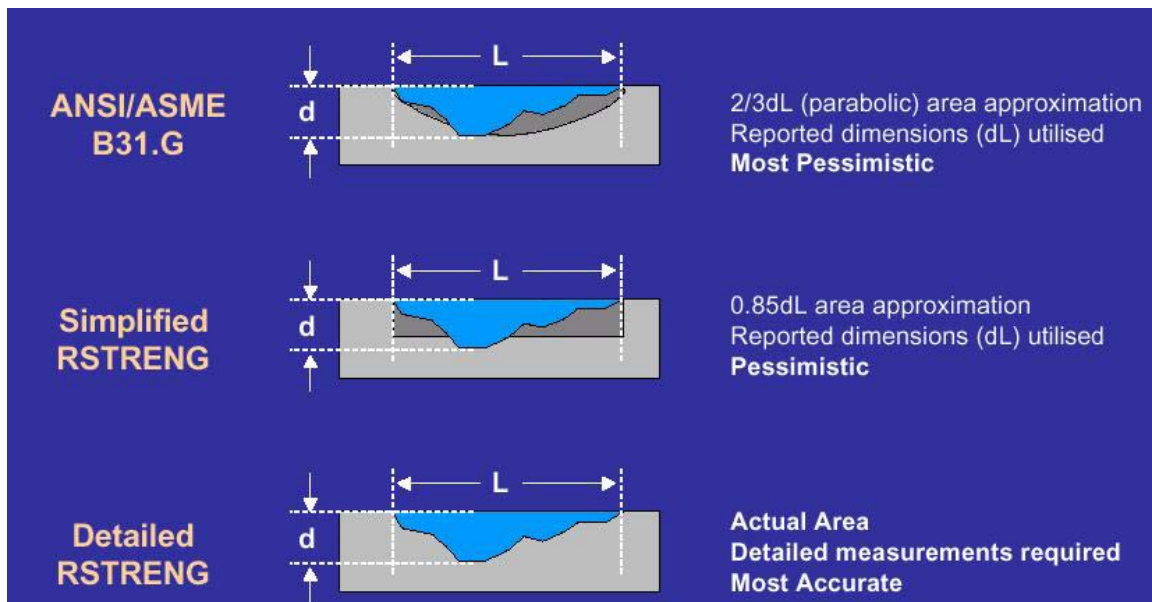


Figure 6.1 Comparison of B31G and Related Methodology

All three methods allow a maximum defect depth of 80 percent of nominal wall thickness and predict failure stress based on an assumed flow stress (1.1 SMYS for B31G and SMYS plus 10 ksi for Modified B31G) and the ratio of area of metal loss to original area with an applied geometry correction factor (Folias Bulging Factor). A defect is considered acceptable if the predicted failure stress level is greater than or equal to SMYS.

Figure 6.2 presents a general description of the acceptable application of these methods. As shown, ASME B31G and its variations are valid for evaluation of general and areal corrosion, pitting and wall thinning, and NOT cracks or grooves including stress corrosion cracking and seam corrosion. Thus, these methods are not applicable for the evaluation of longitudinal welds on LF-ERW and lap-welded pipe.⁹

⁹ The program KAPA allows one to evaluate the failure pressure levels of crack-like defects in the same manner as one evaluates failure pressure levels for corrosion-caused metal loss using RSTRENG and can be downloaded, free of charge (see www.kiefner.com). KAPA calculations are based on the log-secant equation (NG-18 surface flaw equation) described in Section 7.2.4 herein. However, for reasons indicated in Section 6.7 herein, the general use of any direct evaluation procedure for a particular defect in an ERW or lap welded seam that has been exposed for examination is not recommended.

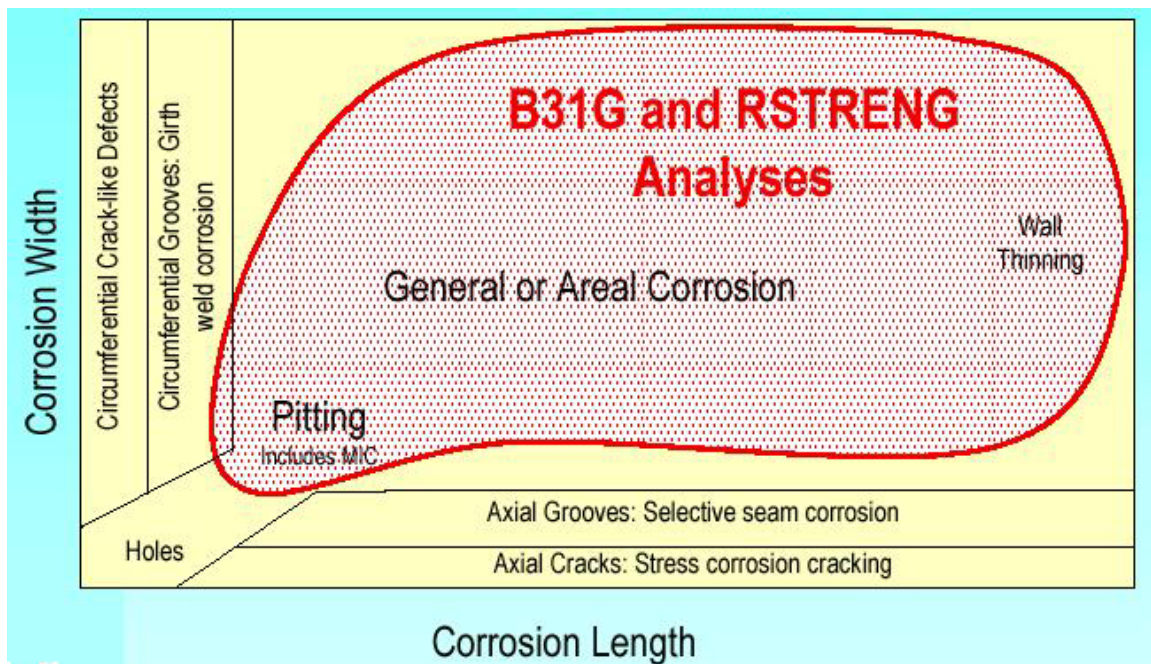


Figure 6.2 Applications Area of B31G and RSTRENG (Battelle)

6.6 API RP579

API Recommended Practice 579 (RP579), *Fitness-For-Service*, “provides guidance for conducting Fitness-For-Service (FFS) assessments using methodologies specifically prepared for equipment in the refining and petrochemical industry.” FFS assessments are “quantitative engineering assessments which are performed to demonstrate the structural integrity of an in-service component containing a flaw or damage.” API RP579 is written specifically for ASME and API codes other than B31.4 and B31.8. However, application to pressure containing equipment constructed to other codes is discussed though the referenced appendix for the primary method is still in development.

Several sections of API RP579 are applicable to assessment of flaws or damages of in-service pipelines. In particular, Sections 4, 5, and 6 cover the procedures for assessment of general and local metal loss resulting from corrosion/erosion, mechanical damage, or pitting corrosion. These assessments are geared towards rerating a line by identifying an acceptable reduced maximum allowable working pressure (MAWP) and/or coincident temperature. Application of these procedures is applicable in cases where “the original design criteria were in accordance with a recognized code or standard”.

Of particular use for review of seam welds is API RP579 Section 9, which provides guidance on assessment of crack-like flaws. This section outlines procedures for conducting Level 1, 2 and 3 assessments. Following these procedures, a Level 1 and a series of Level 2 assessments were completed to develop an acceptable flaw-length versus material-toughness relationship for a hypothetical pipeline. The intent of the exercise was to demonstrate the general method for determining the acceptable conditions for crack-like flaws in pipelines.

Most pipelines under consideration in this report were manufactured prior to 1970 (some date as far back as the 1920's) and a large majority, if not all, of the pipelines manufactured prior to 1950 were made from materials that had a low yield strength (less than 40 ksi). To best simulate these pipelines, the hypothetical pipeline analyses assumed lower strength steel. It was assumed that post weld heat treatment (PWHT) had not been performed and a uniform metal loss, to account for pipe wall reductions that have occurred over time, was included.

The case analyzed considers a crack-like flaw located within the weldment area oriented parallel to the weld seam and detected by inspection. Pipe properties used in the analyses were chosen to resemble realistic conditions of a pipeline similar to those addressed in this report. A summary of the material properties and conditions of the hypothetical pipeline is shown in Table 6.1. These values were held constant throughout the analyses.

Table 6.1 Material Properties & Conditions

Outside Diameter, OD [in]	12.75
Wall Thickness, t_w [in]	0.500
Specified Minimum Yield Strength, SMYS [ksi]	35
Ultimate Tensile Strength, σ_{uts} [ksi]	48
Post Weld Heat Treatment, PWHT	No
Crack Type	Outside Surface
Crack Depth [in]	0.08
Crack Location	Weldment
Crack Orientation	Parallel to Seam
Critical Exposure Temperature, CET [°F]	40
Reference Temperature, T_{ref} [°F]	30
Uniform Metal Loss, LOSS [in]	0.02
Future Corrosion Allowance, FCA [in]	0.0625
Maximum Allowable Operating Pressure, MAOP [psi]	1480

A Level 1 assessment follows a series of basic steps and does not take into consideration the pipeline material fracture toughness (a measure of its ability to resist failure by the onset of a crack extension to fracture). Therefore, a Level 1 assessment typically results in a conservative solution. It is also limited to the assessment of materials with SMYS lower than 40 ksi. and is intended for analysis of flaws located away from major structural discontinuities.

Level 2 assessments follow a more rigorous procedure based on more detailed material properties, including material toughness, to produce a more exact solution. Level 2 assessments also account for stress distributions near the cracked region including residual stresses (categorized as secondary stresses) from welding. If actual steel yield strengths are available for the pipeline being assessed,

the calculations for residual stresses take this into account. However, if only the minimum yield strength is available an acceptable alternate method for calculating the residual stresses is provided.

Both Level 1 and Level 2 assessments assume that the crack-like flaw is subject to loading conditions and/or an environment that will not result in crack growth and that dynamic loading effects are not significant (i.e. seismic, water hammer, surges, ...etc.).

The relationships between critical flaw length and material toughness developed by the Level 1 and Level 2 assessments conducted for the hypothetical pipeline are presented in Figure 6.3. It should be noted that in most cases a pipeline operator will not have performed the type of tests necessary to determine the fracture toughness, K_{Ic} , required to perform an assessment according to API 579. Rough correlations do exist between the CVN impact toughness upper shelf absorbed energy, which measures resistance to fracture propagation, and the static fracture initiation toughness, K_{Ic} . An understanding of the relationship between fracture initiation and fracture propagation properties in the temperature domain is also necessary to successfully use these methods.

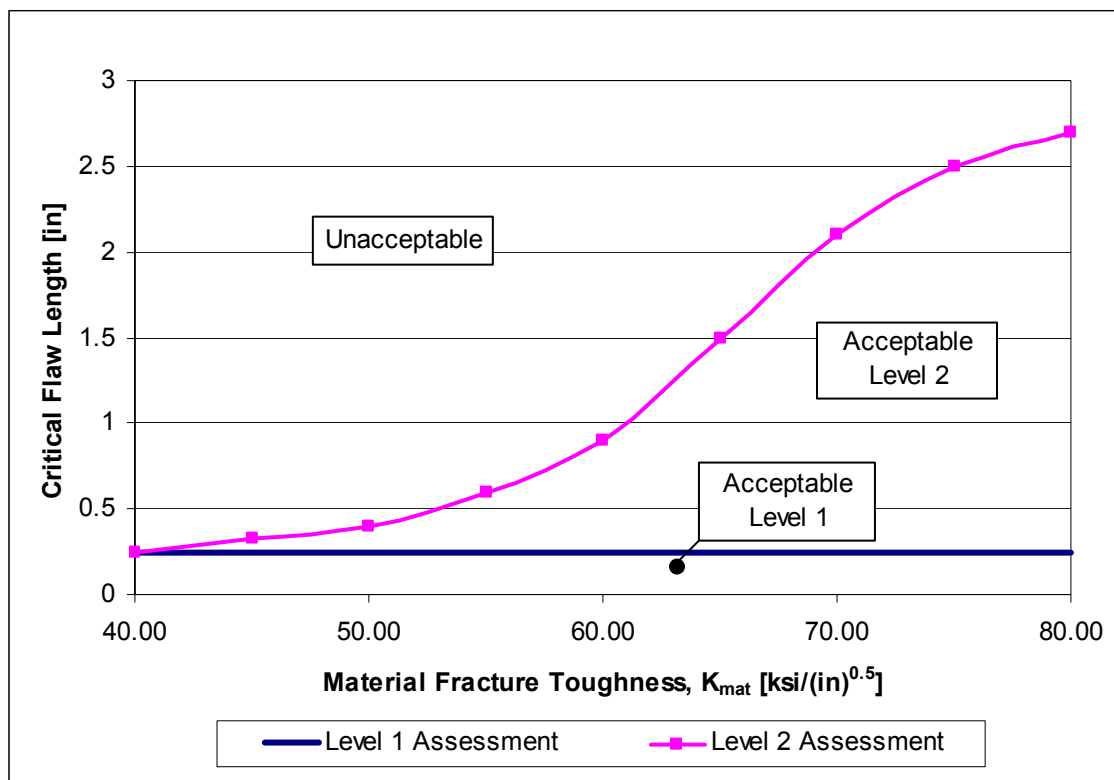


Figure 6.3 Flaw Length versus Material Toughness Relationship

Figure 6.3 clearly shows that since the Level 1 assessment does not consider material fracture toughness, it results in a conservative evaluation of critical flaw length for all cases. However, if the material fracture toughness of material being evaluated can be determined, a Level 2 assessment will potentially reduce the level on conservatism in the analysis by a significant amount.

Though a Level 1 assessment is very conservative, it does not require a significant quantity of detailed material data and can be used to quickly eliminate concerns on many flaws without requiring the rigorous collection of data that may, or may not, exist. However, due to the advent of higher SMYS materials for much of the pipe manufactured after 1950, the Level 1 procedure may not be applicable to pipelines installed more recently.

6.7 Suggested Limitations on the Evaluation of Defects Located in ERW or Lap-welded Seams

It is both necessary and desirable to have techniques for the evaluation of failure stress levels of defects in ERW and lap-welded seams. As indicated above and elsewhere in this document, appropriate equations for this purpose exist. The primary use for such techniques should be limited to predicting the need for seam-integrity assessment and the return interval for re-assessment. These techniques should not be used for evaluating the failure pressures of specific defects in or near LF-ERW, DC-ERW, EFW or furnace lap-welded pipe. It is not prudent to assess specific defects in these materials for two reasons. First and foremost, there is no proven method to determine the effective toughness of a particular piece of pipe without removing it from service. The failure pressures of defects in these materials are highly dependent on the toughness, and the toughness could lie anywhere within a wide range. While one could assume a conservative lower bound value of toughness, the size of defect that could be safely left would be so small as to make the exercise hardly worthwhile. Secondly, it is particularly difficult to determine the sizes of the types of defects involved (i.e., cracks and grooving corrosion). Therefore, it is strongly recommended that when a pipeline operator discovers and exposes a defect in one of these types of seams, the defective piece of pipe should either be removed or repaired in a manner that relieves the stress on the defect.

7 Material Toughness Evaluation

7.1 Subtask 05 – Scope

This chapter addresses Subtask 05 of the Work Scope which states:

“Evaluate the influence of material toughness on the propensity for pressure reversals and its effect on integrity of longitudinal seams with noncritical defects.

Activities:

- a) Research and explain effect of material toughness and low cycle fatigue effects
- b) Present applicable testing programs and/or field experience
- c) Relate as appropriate to Charpy/CTOD data

Deliverables:

- a) Narrative of fatigue mechanics and effect of the growth of flaws to critical size
- b) Narrative of testing/experience
- c) Narrative, quantitative to the extent possible, of the use of material data in evaluating flaw growth to critical size.
- d) Narrative guideline, with reference to industry practice, for evaluation of non-critical flaws and growth (e.g. ASME Boiler Code).”

7.2 Fatigue Mechanics

“Fatigue” is the process of initiation of a crack, propagation of the crack (i.e., enlargement of the crack), and final fracture of the crack as a result of elapsed cycles of applied stress in service. These three processes are distinct phases and although they occur sequentially, are governed by separate considerations.

7.2.1 Initiation

Initiation of fatigue occurs at nucleation sites within the material such as inclusions, pores, soft grained regions, or as they become generated through microvoid coalescence by the straining process. The presence of macroscale stress concentrators, or more accurately strain concentrators, such as grooves, notches, threads, weld toes, manufacturing flaws, or similar features, enhances this process. However, fatigue can occur eventually if stress cycles are sufficiently numerous and large in magnitude even if the material surface is apparently free of such features. (So many more cycles of stress are required in this latter scenario than would be expected in a pipeline application, that fatigue initiation in the absence of macroscopic strain concentrating features is not a scenario of interest in a pipeline context.)

The number of cycles of a given stress level required to initiate a crack in the area of stress or strain concentration is inversely proportional to the local notch acuity or notch root radius. In other words, a sharp notch will be more prone to form a fatigue crack than a blunt notch when subjected to equal

cyclical loading conditions. Similarly, the number of cycles of loading necessary to initiate a crack is inversely proportional to the magnitude of the stress variation. Consequently, a fatigue crack will initiate sooner if the stress cycles are larger, for any given notch-like geometry.

The initiation behavior of a material is described by an “S-N” curve, which is a graph of the magnitude of cyclical stress range or amplitude S plotted against the number of cycles of that stress that would cause failure N . An example is shown in Figure 7.1. Typically such curves are approximately linear when both axes are logarithmic. This curve may be interpreted to indicate that larger amplitude stress cycles result in failure in fewer cycle occurrences, while smaller stress cycles result in failure after a greater number of cycles. At a sufficiently low magnitude of stress cycle, the S-N curve may flatten out, indicating an “endurance limit”, which represents a magnitude of stress cycle below which a fatigue failure would not be expected no matter how many cycles accumulate. A basic S-N curve represents the nominally smooth un-notched condition, while more severe curves can be developed for notches having increasing local stress-concentrating effects. The S-N curves are empirically derived from large numbers of separate tests in which standard round bars of materials are cyclically loaded to specific nominal stress levels until fracture occurs. The S-N curve therefore actually encompasses all three phases of fatigue: initiation, propagation, and fracture, but since the specimens start out nominally free of defects other than a specified notch that may be present, the initiation phase is by far the largest proportion of the total test life in terms of loading cycles (e.g., 90% or more).

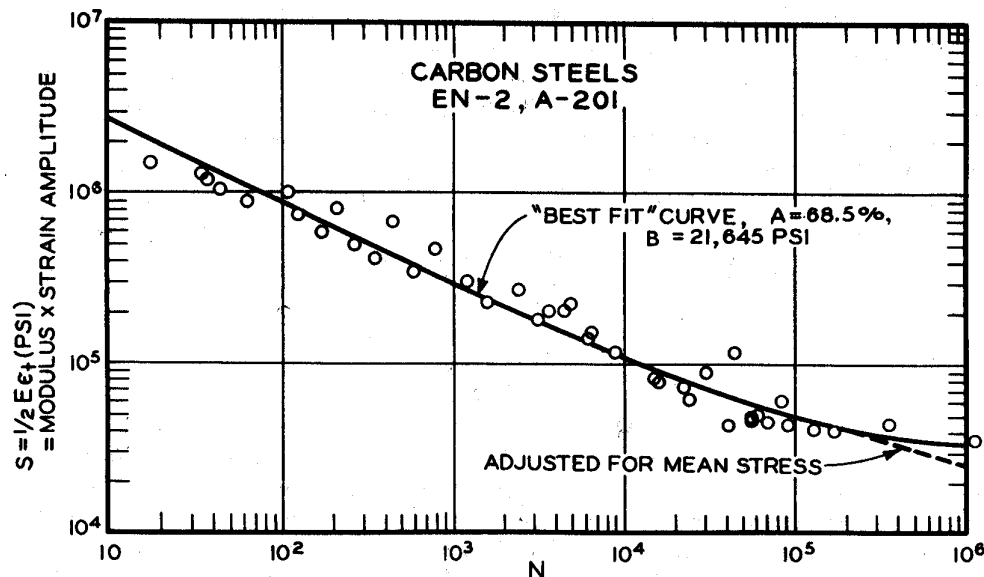


Figure 7.1 A Representative S-N Curve (ASME)

The resistance to fatigue crack initiation is generally proportional to ultimate tensile strength properties. It is enhanced by improvements in surface finish quality and by treatments that impart compressive residual surface stresses or hardened surface microstructures. If the magnitude of nominal stresses are in the elastic range and only very small potential nucleating features are present, on the order of perhaps millions of cycles of stress will be required in order to initiate a fatigue

crack. The fatigue initiation characteristics of a given material, design feature geometry, and loading level are therefore of great interest to designers of rotating machinery, vehicles, aircraft, and highway bridges because such structures rapidly accumulate large numbers of individual stress cycles. The initiation phase of fatigue is also considered in the design of process piping systems that are free to flex in response to changes in operating temperature. Here, the consideration is not that such cycles are particularly numerous but rather that the magnitude of flexural stress cycles in piping components such as elbows and tees are magnified by their geometries such that the range of stress cycle may be much larger than the yield stress. It is also important to consider that the resistance to fatigue crack initiation in steel is adversely affected by some operating environments.

In contrast, the initiation phase of fatigue is of little concern in the pressure design of pipe, because the magnitude of most hoop stress cycles is in the range where millions of cycles would be required, and the number of large-magnitude pressure stress cycles is relatively few. This is substantiated by the fact that there are no known cases of fatigue failures in pipelines due to pressure cycle effects in the absence of some sort of significant initial flaw.

7.2.2 Crack-Tip Stress Intensity

The propagation process concerns a crack that is already present, so it is necessary to consider propagation using parameters related to fracture mechanics. The crack-tip stress-intensity is an expression of the theoretical stress at the tip of a crack, derived from linear elastic fracture mechanics as:

$$K=f(\text{geometry})\times\sigma\times(a)^{1/2},$$

where

σ is a nominal applied stress,

a is the crack size, and

K is expressed in units of $\text{ksi}\cdot(\text{in})^{1/2}$ or $\text{MPa}\cdot(\text{mm})^{1/2}$.

The mathematical function of geometry produces factors that differ for certain idealized crack configurations such as a through-wall crack in a plate, a crack at one or both edges of a narrow strap, an elliptical crack embedded in a solid body, or a surface-breaking semi-elliptical shape. This last idealized configuration, Figure 7.2, is the principal one of interest in dealing with seam susceptibility issues in line pipe, since the concern is for features having configurations similar to this.

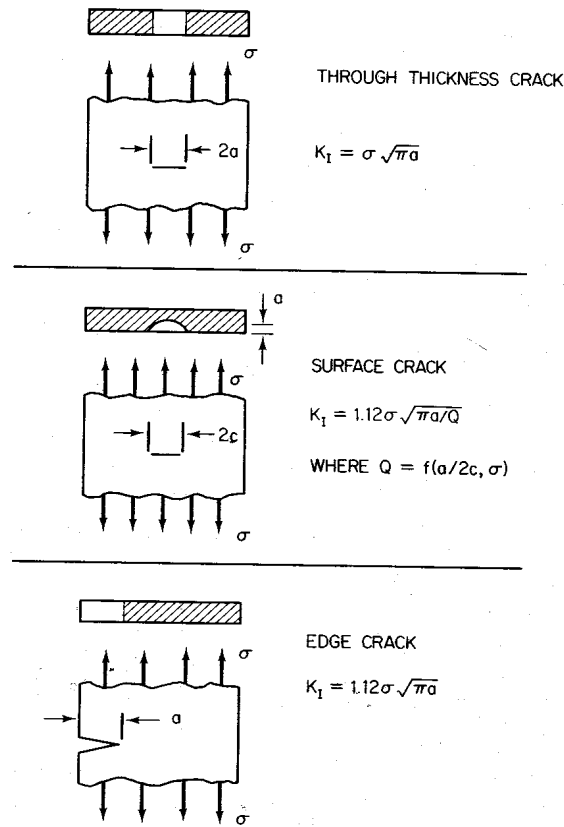


Figure 7.2 Simplified Crack Types (Barsom and Rolfe)

An expression for the crack-tip stress intensity for the semi-elliptical surface flaw is given by Raju and Newman as:

$$K = \sigma F \left(\pi \frac{d}{Q} \right)^{1/2}$$

where

$$Q = 1 + 4.595 \left(\frac{d}{L} \right)^{1.65}, \quad \frac{d}{L} \leq 0.5$$

$$F = M_1 + M_2 \left(\frac{d}{t} \right)^2 + M_3 \left(\frac{d}{t} \right)^4$$

$$M_1 = 1.13 - 0.18 \left(\frac{d}{L} \right)$$

$$M_2 = \frac{0.445}{0.1 + \frac{d}{L}} - 0.54$$

$$M_3 = 0.5 - \frac{0.5}{0.325 + \frac{d}{L}} + 14 \left(0.5 - 2 \left(\frac{d}{L} \right) \right)^{24}$$

In the above expressions, d is the depth of the crack from the pipe surface, L is the length of the crack, and t is the pipe wall thickness. Researchers have developed refinements or variations to this expression which could also be used, but the one given suffices for evaluating fatigue crack growth in a pipeline seam. If the stress fluctuates over a range $\Delta\sigma$, then the magnitude of the fluctuation in stress-intensity is

$$\Delta K = f(\text{geometry}) \times \Delta\sigma \times (a)^{1/2}.$$

7.2.3 Propagation

Propagation occurs from a flaw that either initiated due to the effects of cyclic stresses acting on a strain concentrator or that already existed when the structure entered service. This latter category is of interest to the assessment of the susceptibility of longitudinal seams in pipelines to the effects of pressure cycles because, as discussed above, fatigue failures due to pressure cycles in pipeline seams are only known to occur from some sort of initial flaw.

In every case involving fatigue in autogenous seams (e.g., ERW and EFW pipe), the initial flaws are artifacts of the manufacturing process that escaped detection by the inspection process in the pipe mill and that were also small enough to pass the hydrostatic test at the mill or in the field prior to commissioning. (Note that one type of initial flaw, the origin of which is fatigue in nature, is the “rail shipment fatigue” crack that affected a small population of large-D/t pipe manufactured using the DSAW longitudinal seam. In those cases, pipe joints at the bottom of improperly loaded rail cars developed fatigue cracks at the toes of longitudinal seam weld beads while the pipe was in transit due to the cyclical inertial stresses associated with railcar transient loadings. The fatigue-initiated cracks were small enough to pass the hydrostatic test conducted by the pipeline operator prior to commissioning the pipeline, so the pipes entered service with fatigue cracks already in place. The analysis of fatigue crack-growth life for such flaws is essentially similar to that for hook cracks in ERW seams. Also, pressure cycle fatigue propagation can occur from SCC or mechanical damage defects in the pipe body, but these are entirely separate issues from longitudinal ERW seam susceptibility.)

Propagation or growth of a fatigue crack in service is governed by the Paris Law:

$$da/dN = C [\Delta K]^n$$

where

da/dN is the increment of crack extension per load cycle,

ΔK is the magnitude of stress intensity range for a given load cycle, and

C and n are material properties.

The size of the crack, a , thus increases incrementally by da with each load cycle dN while the magnitude of the stress-intensity range, ΔK , a value that encompasses the effect of crack size, a , increases with each increment of crack growth.

The nature of the crack-growth relationship results in an exponential increase in crack growth rate and an acceleration of crack size as load cycles accumulate. The practical implication of this is that a small crack may remain small for a long time, and by the time it is detectable, either by means of in-service examination (e.g., crack detection ILI) or proof load testing (e.g., hydrostatic pressure test), the remaining safe service life could be very short, as suggested in Figure 7.3. Figure 7.3 also shows that a larger initial flaw size greatly reduces the remaining time to failure. This suggests that achieving the largest possible margin between the test pressure and the operating pressure is of value to maximizing the retest or reinspection interval.

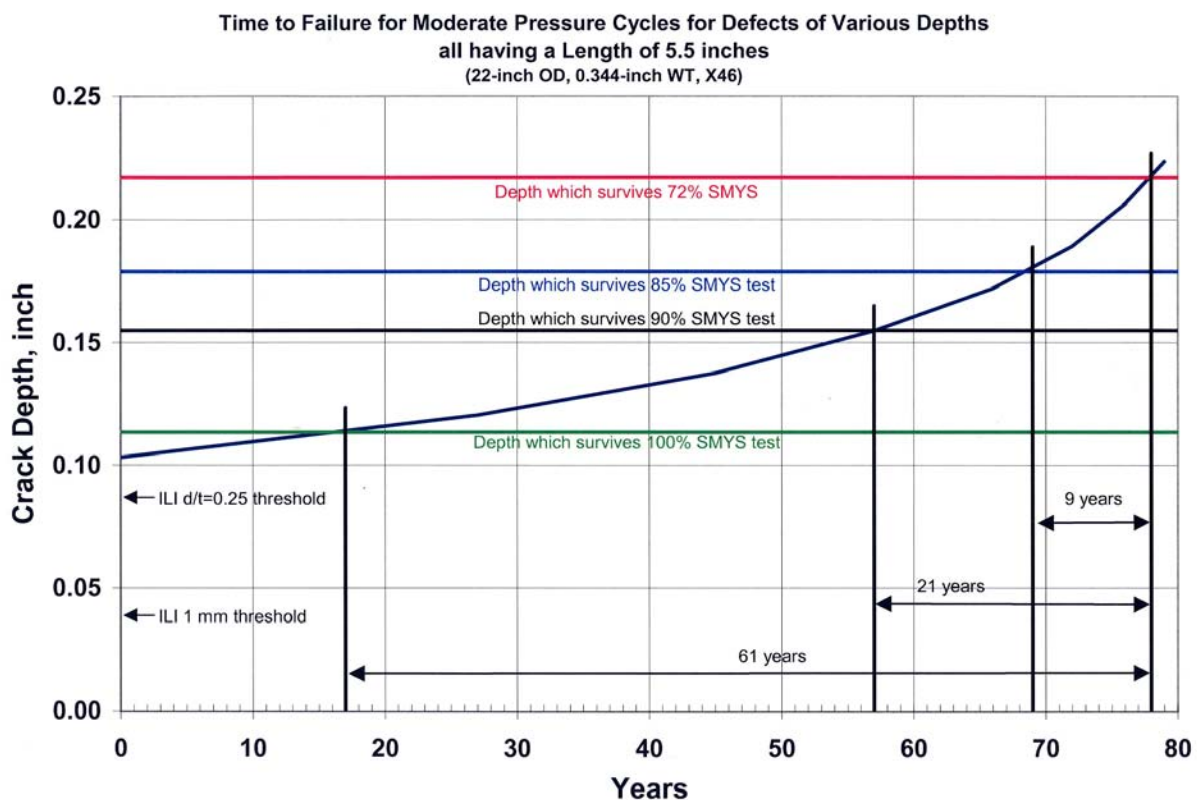


Figure 7.3 Example Crack Growth in Service

A potential value to the highest possible test pressure is the concept of “retardation”, wherein an infrequent overload cycle blunts the crack tip and introduces a large plastic zone ahead of the crack.

When the proof load is released, the residual stress field in the plastic zone is compressive, causing a delay in subsequent crack growth. While retardation is a proven phenomenon, it may not occur to a significant degree where the proof test is only 1.25 times the MOP. The effect of retardation is usually disregarded when performing incremental fatigue crack growth computations.

The values of C and n in the Paris Law vary widely. A “typical” value reported for C and n in plain carbon steel is $C=3.6 \times 10^{-10}$ and $n=3.0$ for ΔK expressed in units of $\text{ksi}(\text{in})^{1/2}$, though any given steel might exhibit very different values for the crack growth rate parameters. This “typical” relationship between da/dn and ΔK is shown in Figure 7.4. If ΔK is expressed in units of $\text{psi}(\text{in})^{1/2}$, then the value of C must be divided by $[1000]^n$ giving 3.6×10^{-19} . The value of C can vary by several orders of magnitude, while n has been observed to vary from 2 to 4, though for most pipelines n falls between 2.5 and 3. A higher C and lower n will result in a faster initial crack growth rate that does not accelerate as greatly toward failure, compared to a lower C and higher n which results in very flat initial crack growth rate and more rapid acceleration toward final failure. If only an initial and a final flaw size are known, there is no one combination of C and n that uniquely defines the crack growth curve between initial and final flaw sizes for any given operating spectrum.

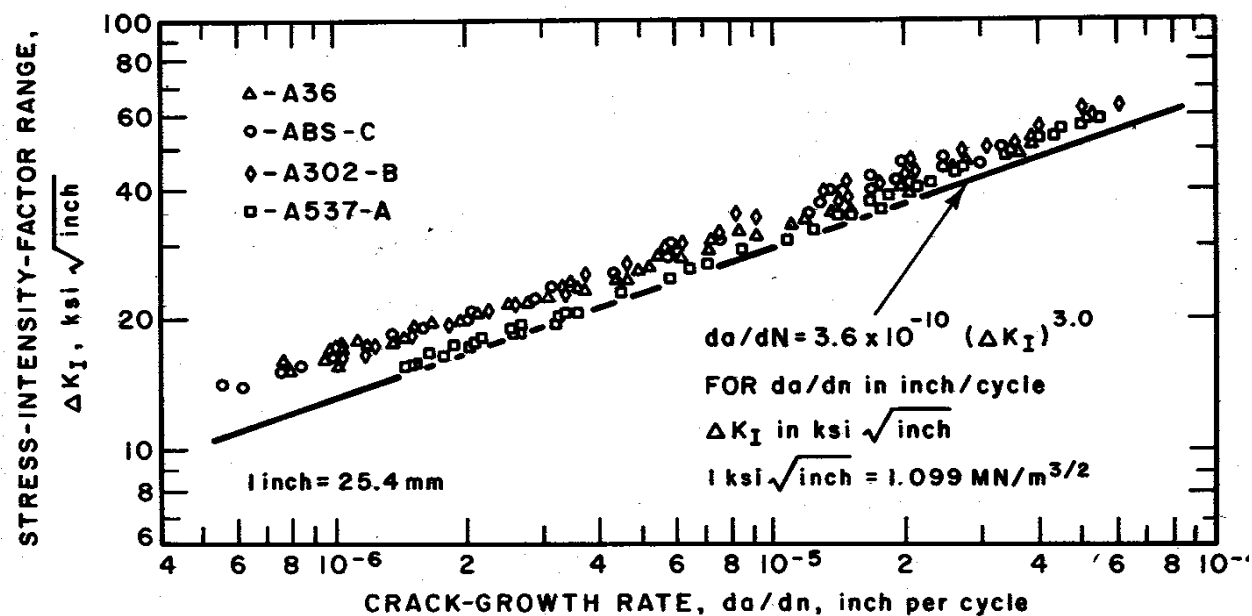


Figure 7.4 Average Crack Growth Rate for Carbon Steel (Barsom and Rolfe)

The values of C and n are influenced somewhat by load cycle frequency and stress ratio (R , the ratio of minimum to maximum stress in a cycle), and are influenced strongly by the chemistry environment that the crack tip becomes exposed to (e.g., dry versus aqueous, or the presence of oxygen, chlorides, sulfur, or hydrogen). The exposure of the fracture to environments at the soil interface, under coatings, or in the pipe interior could greatly enhance crack growth rates compared to those indicated by the “typical” coefficients, making it difficult to obtain reliable predictions of crack-growth life using those values.

7.2.4 Fracture

The final stage of fatigue crack growth occurs when the crack-growth rate accelerates under the influence of ductile tearing and the crack grows to such size as to be critical in service, meaning it could fail at the next applied load cycle. The critical flaw size depends on the nominal stress, the material strength, and the fracture toughness. The relationship between these parameters for a longitudinally oriented defect in a pressurized cylinder is expressed by the NG-18 “ln-secant” equation:

$$\frac{C_V \pi E}{4 A_c L_e \sigma_f^2} = \ln \left[\sec \left(\frac{\pi M_S \sigma_H}{2 \sigma_f} \right) \right]$$

where

E is the elastic modulus,

L_e is an effective flaw length equal to the total flaw length multiplied by $\pi/4$ for a semi-elliptical flaw shape common in fatigue,

σ_f is the flow stress typically taken as the yield strength plus 10 ksi or else as the average of yield and ultimate tensile strengths,

σ_H is nominal hoop stress due to internal pressure,

C_V is the upper shelf CVN impact toughness,

A_c is the cross-sectional area of the Charpy impact specimen. (Note that a constant for compatibility of units between C_V and A_c may be necessary.)

The term M_S is a stress magnification factor for a surface-breaking axial flaw, calculated as

$$M_S = \frac{1 - (d/t)(M_T)^{-1}}{1 - d/t}$$

where

d is flaw depth and

t is the pipe wall thickness.

The term M_T is Folias’ original bulging factor for a through-wall axial flaw, written as

$$M_T = [1 + 0.6275(z) - 0.00675(z)^2]^{1/2}, \quad z = L_e^2 / (Dt) \leq 50$$

or

$$M_T = 0.032(z) + 3.3, \quad z > 50.$$

In simplified form, this equation forms the basis for common flaw assessment methodologies such as ASME B31G and RSTRENG. The program KAPA solves a similar equation for failure pressures of irregular shaped defects including cracks. For crack-like defects the user must supply a

representative value of Charpy energy as well as the yield strength of the material and the detailed dimensions of the defect. KAPA also can be used to evaluate corrosion-caused metal loss without the need for specifying the Charpy energy because the failure pressure levels of blunt defects depend only on the tensile properties of the material.

The NG-18 equation can be understood in practical terms by a review of Figure 7.5 showing the failure pressures predicted by the NG-18 Equation for a given pipe size and material plotted as a function of flaw length and flaw depth (d/t). Several important observations can be made:

- At any given stress level, there is no single flaw size that is critical. Rather, a range of flaw sizes from short-but-deep to long-but-shallow may be equally critical at a given pressure level.
- Short-but-deep flaws tend to leak, while long-but-shallow flaws tend to rupture.
- The failure stress level decreases as the flaw becomes either deeper or longer, or both.
- The size of flaws that are critical decreases as the stress due to internal pressure increases.
- If one were to repeat the analysis considering very low toughness, all of the curves would compress toward the lower left, with the result being that only very short flaws could be tolerated even at low stress levels.

This last point illustrates the main influence of toughness levels on fatigue in a pipeline. Crack-growth rates (e.g., da/dN as a function of ΔK) are not affected by toughness. Rather toughness determines the largest flaw that could survive a hydrostatic test of the pipe (in other words, the size of the initial flaw prior to the occurrence of fatigue in service) as well as the size of flaw that fails in service. The difference between these two flaw sizes provides the margin for subcritical crack growth in service. Ironically, this difference may be less, and therefore the number of cycles to failure may be less, for a high-toughness material because the initial flaw size that survives a hydrostatic test can be much larger than would be possible in a low-toughness material.

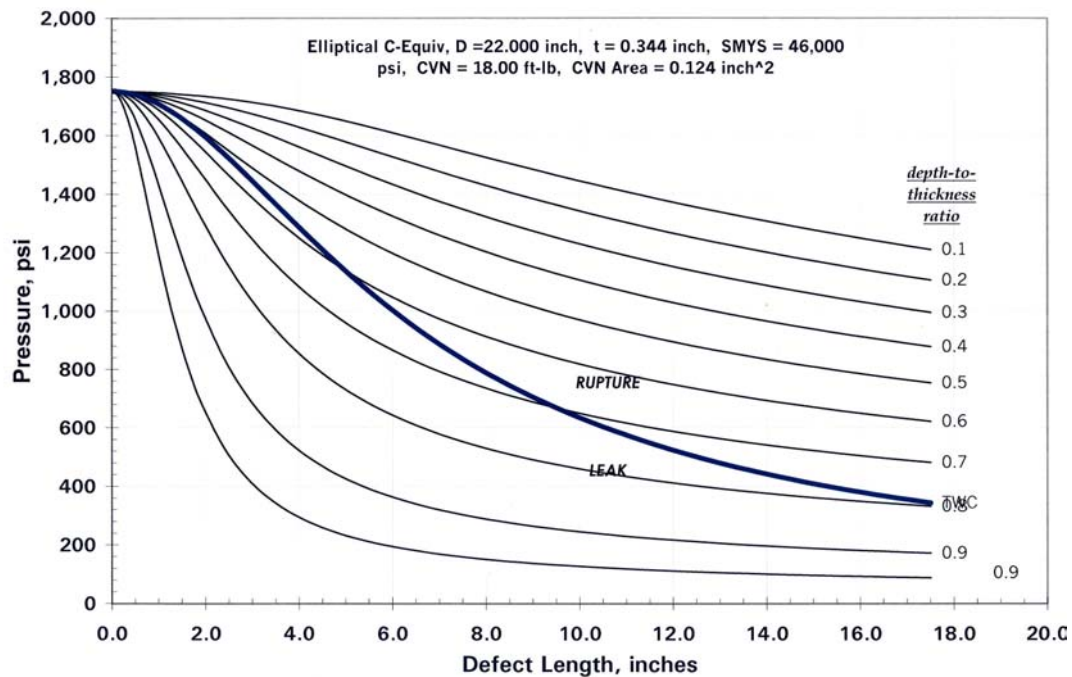


Figure 7.5 Example Relationship Between Failure Stress and Flaw Size

Some types of autogenous seams possess exceptionally low toughness (less than 1 ft-lb) on the bond line. Consequently, they are incapable of sustaining much, if any, subcritical extension of initial flaws originating at the pipe mill. And in fact, fatigue failures of bond line flaws in low-toughness seams do not occur. Bond-line flaws in low-toughness seams are susceptible to the phenomenon of “pressure reversals” wherein a defect fails at a lower pressure than a recent prior high-pressure level. These failures evidently experience an exhaustion of the limited available ductility during a high-stress event, reducing the capacity for subsequent high-stress events, in effect a form of ultra-low-cycle fatigue.

On the other hand, hook cracks, while uniquely associated with ERW or EFW seams, are not true bond-line flaws. They reside slightly off the bond line where even the HAZ material has sufficient ductility to sustain subcritical flaw growth. Hook cracks are thus prime candidates for fatigue in service if the operating pressure spectrum is conducive.

7.3 Material Testing and Experience

7.3.1 Standard Materials Tests

Standard material properties tests include yield and ultimate tensile strength, elongation, chemistry, resistance to dynamic fracture propagation as indicated by the CVN impact toughness, and resistance to static fracture initiation in welds as indicated by the CTOD test. The tests for tensile properties and notched impact toughness called for in API 5L should be carried out in accordance with ASTM A370.

The tensile and notched impact tests are carried out in pipe body material. There are two reasons why toughness tests are not performed on the ERW seam. One is that it is difficult to do reliably: the bond line is so narrow that the chances of getting the V-groove properly aligned so that the fracture initiates and propagates along it are poor. Secondly, test results from the bond line would not really matter: if the seam was normalized it would exhibit toughness on a par with the base material, and if the seam had low toughness a fracture mechanics analysis would indicate that from a practical standpoint only very small flaws could be tolerated anyway. For low-toughness seams, the only flaws that are going to grow by fatigue are hook cracks, which are off the bond line.

The CVN impact test impacts a machined bar specimen in 3-point bending with a swinging hammer having known kinetic energy at the impact point. As the specimen fractures, starting at the notch machined at a position opposite the hammer impact point, it absorbs energy and slows the hammer. The amount of energy absorbed is inferred from the angle of the hammer swing beyond the impact. The CVN test measures resistance to fracture propagation under dynamic conditions, a property important to determining the burst pressure and fracture arrest characteristics of pipe. Conducting the test on material samples at a number of different temperatures will demonstrate a transition in absorbed energy, from low values at low temperatures, to much higher values at warm temperatures as shown in Figure 7.6. The low end of the curve corresponds to brittle fracture, while the upper end of the curve corresponds to ductile fracture. Ductility is determined by measuring the proportion of the surface area that exhibits brittle or ductile shear appearance on the exposed fracture surfaces of the specimens. The fraction of shear appearance on the fracture surface undergoes a transition that parallels the trend in absorbed energy. The temperature at which the specimens exhibit 50% shear appearance defines the FATT. The temperature at which the specimens exhibit 85% SATT defines the minimum temperature at which, for all practical purposes, full upper-shelf behavior can be expected, because the additional 15% of shear fracture provides very little additional energy-absorbing capability. The FATT and SATT are independent of tensile properties or yield strength grade designation. They are a function of grain size, which is a physical characteristic that results from the rolling and heat treatment history of the steel.

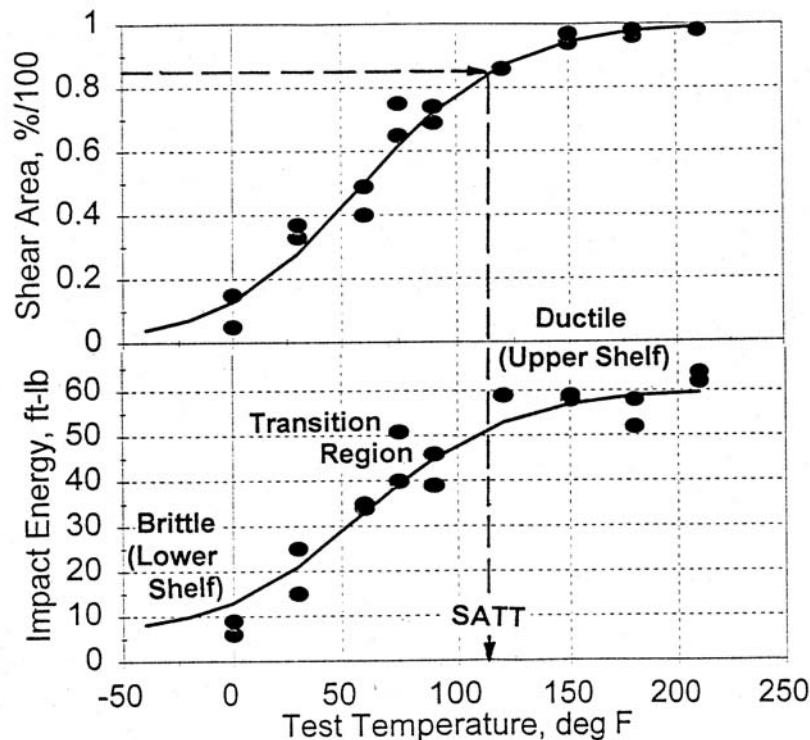


Figure 7.6 Schematic CVN Test Results

It is not uncommon for older pipe to operate at a temperature below the SATT, which means that in the event of a rupture, it is susceptible to fracture propagation in a brittle manner. Such pipe may still initiate the fracture in a ductile manner, if it operates at a temperature that is within 60°F to 100°F below the SATT. Moreover, the pipe can continue to be evaluated for corrosion using corrosion assessment methodologies that presume ductile initiation behavior, such as ASME B31G or RSTRENG. The reason for this seeming inconsistency is that the transition in ductility is affected by the strain rate. High strain rates associated with dynamic events (such as impact, or in the context of pipelines, the popping through of a surface crack to form a through-wall crack and subsequent propagation down the pipeline under the influence of line pressure) elevate the transition temperature compared to the static initiation transition, as shown in Figure 6.7.

The resistance to fracture initiation under static conditions is measured by the CTOD test. The CTOD test involves measurement of crack-mouth opening displacements versus applied load, using a specimen containing a fatigue pre-cracked notch, loaded in 3-point bending. If the CTOD test were conducted over a range of temperatures, it would exhibit a transition similar to what is observed with CVN tests, but at a temperature that is 60°F to 100°F lower. It is a much more costly test to perform than the CVN test. The CTOD test is sometimes used to measure the ductility of girth welds, because they are usually not loaded in a manner where dynamic fracture resistance is important. The fracture resistance of girth welds is outside the scope of this study.

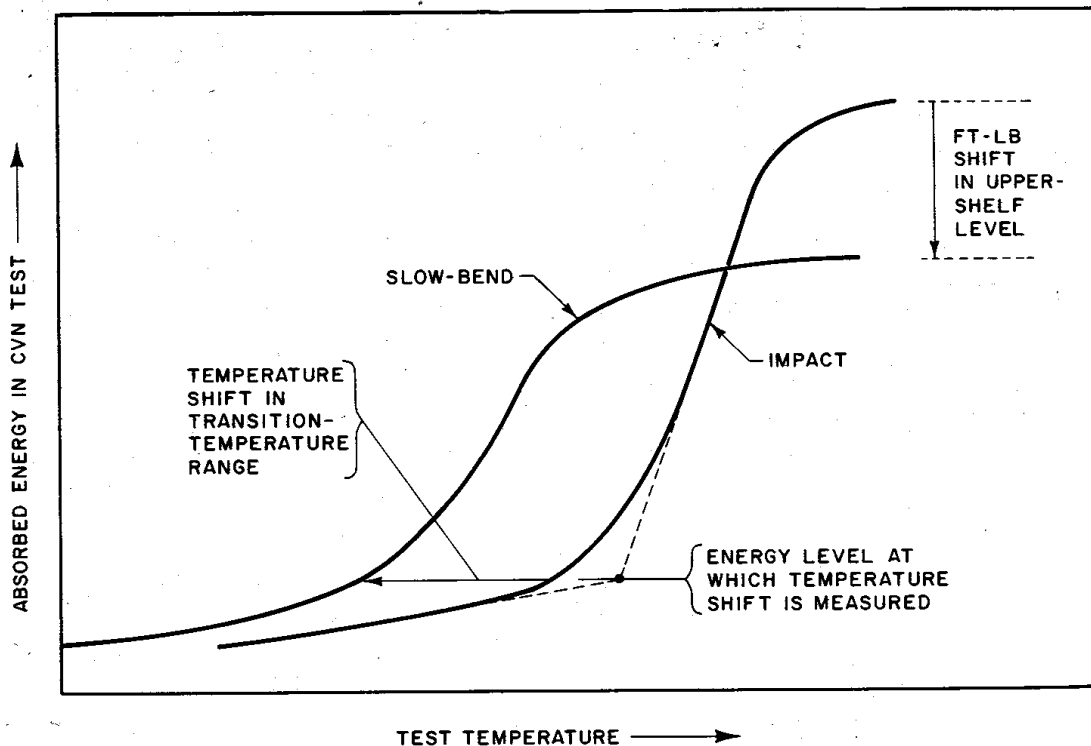


Figure 7.7 Schematic of Strain Rate Effect on Fracture Toughness Transition

7.3.2 Fatigue Properties

Tests performed on various grades of steel plate (some of which may be similar to line pipe plate in terms of chemistry and strength and therefore presumably microstructure and other properties that could affect fatigue crack-growth properties) have indicated that the resistance to fatigue initiation varies with tensile strength while fatigue crack-growth rates (C and n values) vary inversely with strength. However, pipe strength properties probably do not vary over a sufficiently wide range to exhibit significant differences in these properties from grade to grade on the basis of designated strength alone. The fatigue crack initiation and growth properties are far more strongly (and adversely) affected by the chemistry environment at the crack tip.

Crack-growth properties can be measured in the laboratory by conducting a multitude of high-precision tests. It is reasonably safe to state that up to the present, few studies have been undertaken to characterize the Paris Law crack-growth coefficients for specific line pipe steels and varieties of pipe manufacture, and those studies that have did so by backing out effective C and n values by a trial-and-error process of matching initial and final flaw sizes of actual failures using known stress histories, as opposed to specimen testing. There have probably been no studies performed characterizing how C and n are affected by environments that may be present at the ID or OD surface of a pipeline. The fact that such testing is tedious and more expensive than the standard material properties tests normally conducted in the pipe line industry, along with the lack of a

perceived need for such tests up until now, has been a barrier. Therefore, the only two practical options available right now to establishing fatigue crack-growth rate coefficients are:

- use some sort of average C and n values reported generally for ferritic-pearlitic steels, such as the value cited earlier and illustrated in Figure 7.4, and perhaps modified as reported in the literature for the adverse effects of exposure to environments, which may or may not be relevant to pipeline operating environments; or
- develop pipeline-specific effective C and n values derived by a trial-and error calibration of incremental crack-growth computations against a known service failure caused by fatigue using actual hydrostatic test and operating pressure histories.

The first option is reasonably straight-forward to apply, but the results can only be used to compare relative effects of different operating scenarios since the estimates of the service life may potentially be quite inaccurate. The second option can be quite accurate (plus or minus a factor of 2 on life) but requires performing a detailed engineering analysis using actual service history and failure data closely related to the situation of interest.

7.3.3 Lap-Welded Pipe

Lap-welded seams fail from two possible causes unique to that joint type. One is poorly-bonded seams due to oxides trapped along the bond line, and the other is embrittlement and cracking in or near the seam due “burnt metal”, a condition caused by overheating during seam formation. Failures in lap-welded seams tend to occur when the pipe is subjected to a historically high pressure level that is usually in excess of 50% of SMYS. None of the types of materials tests or flaw assessment techniques described above are useful for evaluating the susceptibility to seam related failures in lap-welded pipe.

7.4 Using Material Data for Evaluating Flaw Growth

7.4.1 Data Needs and Usage

Data required for an assessment for evaluating the susceptibility to flaw growth of ERW or EFW seam flaws includes the specified minimum yield strength, the Charpy upper shelf absorbed impact energy, the dates and pressures of previous hydrostatic tests, and representative operating pressure records. If for some reason the yield strength is not known, it should be assumed to be around 52 ksi. If the Charpy impact energy is not known, it should be assumed to be around 25 ft-lb (full size) for the base metal. Assuming lower yield strengths or lower toughness values would result in smaller estimated initial flaw sizes, which in turn would lead to longer and potentially non-conservative estimates of crack-growth times to failure.

Before crack-growth computations can be performed, the operational pressure history has to be analyzed by a rainflow cycle-counting procedure, which is a technique for decomposing a random fluctuating signal in order to characterize the quantity and magnitude of cycles. Information from prior failures, if available, should be used to determine applicable flaw lengths. If no such information is available, an assumed flaw length of $2(Dt)^{1/2}$ would be reasonable and generally in

agreement with the lengths of fatigue cracks observed in failures. The critical flaw depth corresponding to the known or assumed flaw length, at the maximum operating pressure and the most recent hydrostatic pressure test, should be determined using the NG-18 equation.

Crack-growth computations are performed using the Paris Law. In practice, the increment of crack growth is calculated for each load cycle, using the enlarged crack dimension from the previous load cycle in the ΔK relationship. It is acceptable to maintain a constant flaw length, since enlargement of the flaw along the pipe axis is usually not as significant relative to the flaw's overall severity, as enlargement through the pipe wall.

Actual pressure fluctuations in service are random and the size of the pressure cycles affects the size of incremental flaw growth, so it is important to maintain the randomness of the pressure cycle sequence, though it is acceptable to repeat the random cycle sequence as a block as many times as necessary to determine the time to failure. Because of the large amount of data processing involved with the rainflow cycle-counting analysis and incremental crack-growth computations, computer algorithms are a practical necessity to carry out the analysis in an accurate and efficient manner.

7.4.2 Example

Consider a 22-inch OD x 0.344-inch WT X46 pipeline being evaluated for susceptibility of fatigue from a hook crack. The CVN upper shelf absorbed energy is 18 ft-lb equivalent from a full-size specimen. The pipeline maximum operating pressure (MOP) is 1,035 psig, corresponding to a hoop stress equal to 72% of SMYS.

The assumed fatigue crack length is $L=2(Dt)^{1/2}=5.5$ inches. The NG-18 equation results in the relationships between flaw size and failure pressure shown in Figure 7.5. At a flaw length of 5.5 inches, a defect would become critical at the MOP at a depth of 64.5% of the wall thickness, or 0.222 inches. If the pipe were hydrostatically tested to a pressure level of 90% of SMYS, a flaw of this length would be critical at a depth of 47.1% of SMYS or 0.162 inch; if the pipe were hydrostatically tested to a pressure level of 100% of SMYS, a flaw of this length would be critical at a depth of 34.1% of SMYS or 0.117 inches.

The best means for selecting C and n values is to benchmark the values against a known incident where the initial flaw size, the final flaw size, a detailed operating pressure spectrum, and the hydrostatic test history are all known. Even so, there is no one combination of C and n that uniquely defines the crack growth curve between initial and final flaw sizes for any given operating spectrum, unless another hydrostatic pressure test or reliable crack-detection in-line inspection occurred some time later in service. The later test or ILI puts an upper bound on how large the flaw could have been at a given point in time. The test may also have left an arrest mark on the fracture surface giving an indication of the flaw size at that time, although it is usually difficult to make such correlations. If only an initial and final flaw size are known with no intermediate test or ILI, then it is not possible to define a unique C and n combination, other than by selecting a reasonable n value, perhaps based on analyses of other pipe of the same type, and changing C to match the known conditions. Considerable judgement is involved in making these choices.

Consider that for the example pipe, it was already established that $C=5.56 \times 10^{-18}$ (K in units of $\text{psi}(\text{in})^{1/2}$) and $n=2.77$ based on prior studies. Figure 7.3 shows the crack growth over time under the

influence of a particular operating pressure spectrum that happens to be moderate in terms of cycle aggressiveness. The curve shows failure at the MOP at a flaw depth of 0.222 inches, potentially as early as 9 years after a hydrostatic test to 85% of SMYS, or 21 years after a hydrostatic test to 90% of SMYS, or 61 years after a hydrostatic test to 100% of SMYS if the flaws had the maximum survivable depth at the time of the test.

Figure 7.8 shows the effect on crack growth over time, for this particular case, of more aggressive and less aggressive operating conditions. Figure 7.9 and Figure 7.10 show the effects of greater or lesser values for C with the same n value, and greater or lesser values for n with the same C value, respectively. Note that by pure coincidence, the curve shown for lower C and the same n is almost identical to the curve for the same C and lower n . This result might not necessarily occur with a different operating spectrum, however.

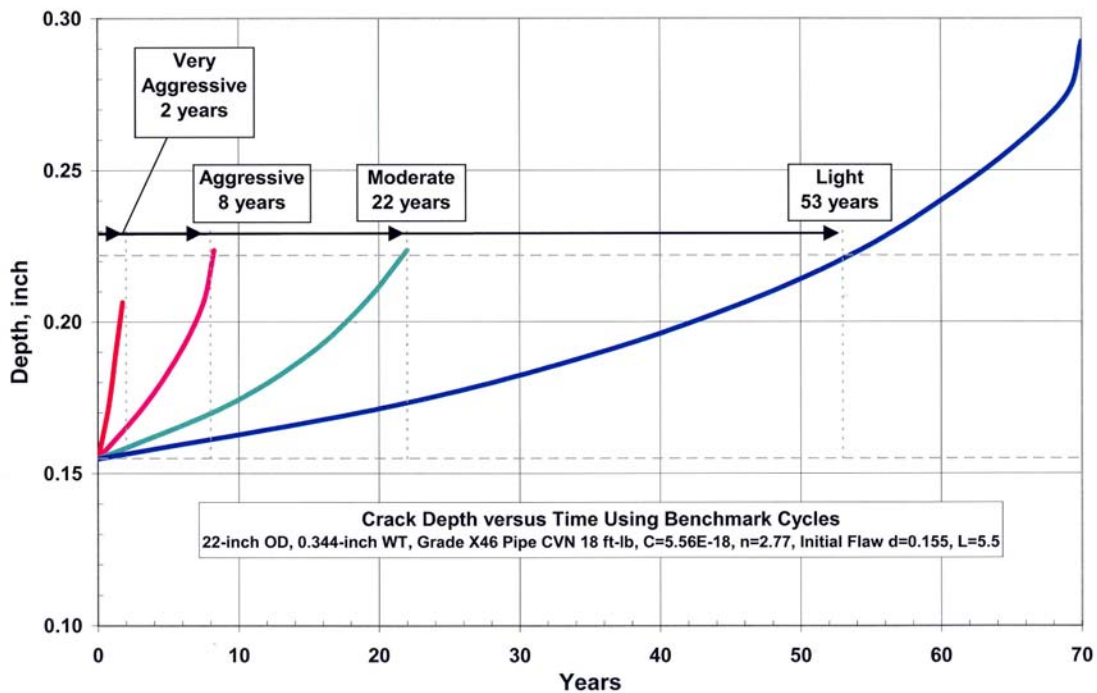


Figure 7.8 Example of the Effect of Operating Pressure Spectrum

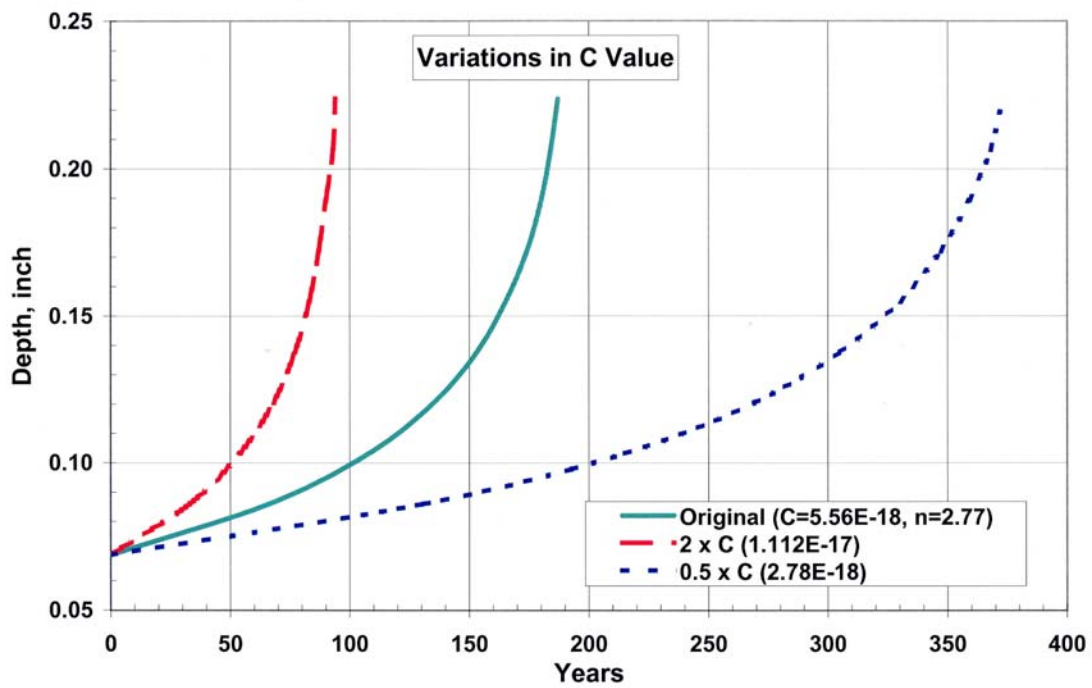


Figure 7.9 Illustration of the Effect of Variations in *C*

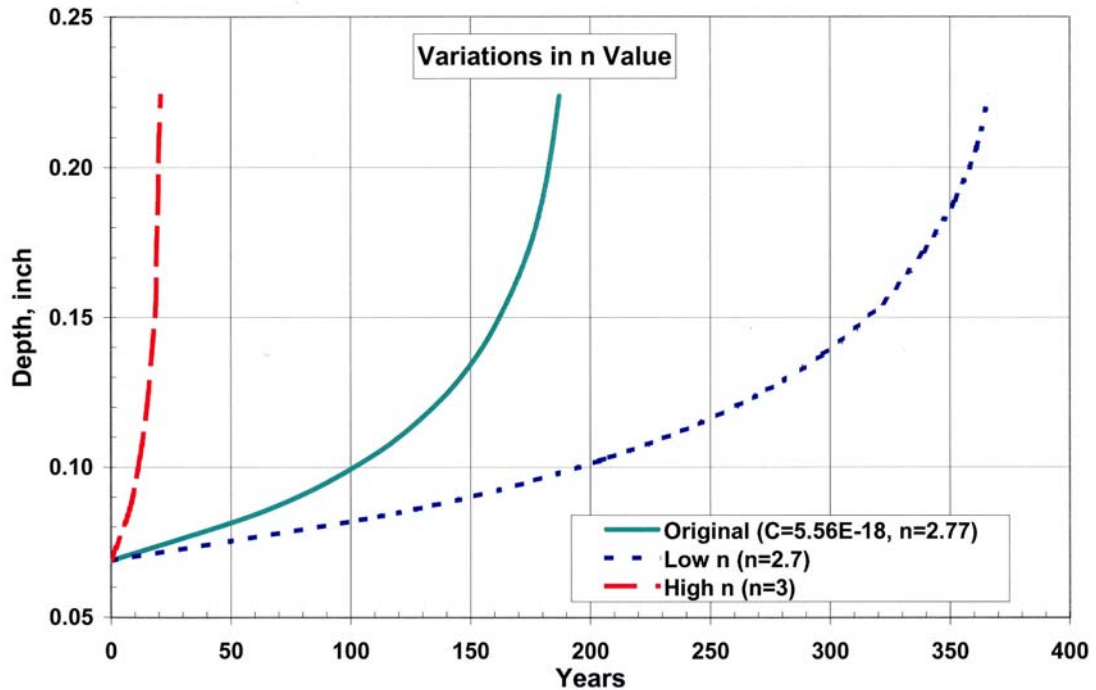


Figure 7.10 Illustration of the Effect of Variations in *n*

7.5 References

1. ASTM, “Standard Test Methods and Definitions for Mechanical Testing of Steel Products”, A 370, *Annual Book of Standards*, 2002.
2. ASTM, “Standard Practices for Cycle Counting in Fatigue Analysis”, E 1049, *Annual Book of Standards*, 2002.
3. Hertzberg, R. W., *Deformation and Fracture Mechanics of Engineering Materials*, Third Ed., J. Wiley & Sons, Inc., 1989.
4. Kiefner, J. F., Maxey, W. A., Eiber, R.J., and Duffy, A. R., “Failure Stress Levels of Flaws in Pressurized Cylinders”, Progress in Flaw Growth and Fracture Toughness Testing, STP 536, ASTM, 1973.
5. Newman, J. C., and Raju, I. S., “An Empirical Stress-Intensity Factor Equation for the Surface Crack”, *Eng. Fracture Mechanics*, v. 15, Nov. 1981.
6. Rolfe, S. T., and Barson, J. M., *Fracture and Fatigue Control in Structures*, Prentice-Hall, 1977.

8 Evaluation of Pressure Testing and ILI Combination

8.1 Subtask 04 – Scope

This chapter addresses Subtask 04 of the Work Scope which states:

“Evaluate if a combination of pressure testing and in-line inspection would provide better confidence in assessment of the ERW and lap welded pipe longitudinal seam integrity. Develop OPS acceptance criteria.

Activities:

- a) Research past experience where combination techniques were used
- b) Develop a fracture mechanics oversight of flaw size and growth for these conditions.
- c) Drawing on the oversight, qualitatively describe the flaws (size, orientation, location) which each technique detects. Describe advantages/disadvantages of each in flaw detection and growth prediction.
- d) Combine the separate evaluations to develop the additional advantages afforded by a combination of techniques. To the extent possible, describe the increase in integrity confidence.
- e) Based on flaw detection limits of ILI, describe criteria for maximum acceptable flaw. Develop a decision flowchart for integrity acceptance, alternative evaluation techniques (e.g. direct evaluation), shortening inspection intervals, or proceeding with an immediate spike test.
- f) Develop criteria/setup approach for use in establishing testing needs (i.e., pipe data, pup sample availability, etc.).

Deliverables:

- a) Narrative of past experience
- b) Narrative overview of problem from the viewpoint of fracture mechanics.
- c) Matrix comparison of separate technologies. Narrative and conclusion on the use of combination evaluation.
- d) Flow chart for combination techniques”

8.2 Overview

This subtask reviews the advantages and disadvantages of pipeline integrity evaluation by a combination of pressure testing and ILI. A discussion on the level of confidence using both pressure testing and ILI in assessing the integrity of the ERW and lap-welded pipe longitudinal seams is included. An OPS acceptance criterion is also developed.

8.3 Past Experience Using Combined Techniques

Obviously, it is possible to use both ILI and hydrostatic testing for the integrity assessment of a pipeline segment. In the case of corrosion-caused metal loss, the use of both is usually unnecessary because experience has shown that the use of ILI alone, followed up by timely responses to the findings is sufficient to assure the integrity of the pipeline. Similarly, in the case of dents, hydrostatic testing would be unlikely to provide much added value to an ILI to which the operator responds in an appropriate and timely manner. In both cases, (i.e., corrosion and dents) the use of ILI provides a much-superior approach because it locates all significant anomalies, not just the ones with failure pressures at or below the hydrostatic test pressure. The knowledge provided by the inspection allows the operator to identify the problem areas, and the sizing information provided allows the operator to schedule responses over time in a manner that provides greater overall assurance of continuing pipeline reliability than that provided by the one-time proof associated with a hydrostatic test. It should be noted, however, that one should not blindly accept any particular set of ILI results without some amount of “in-the-ditch” verification of the tool’s accuracy. This applies to the tools provided by any vendor, even those with years of experience, because the circumstances of any particular tool usage may cause unexpected variations in the reliability of the inspection.

The scope for using both ILI and hydrostatic testing would seem to be confined to cases where complete confidence in ILI has not been established. In this type of situation, the use of both techniques might be necessary to provide adequate confidence in the integrity of a particular pipeline. Moreover, the use of both might also lead to better understanding and confidence in the ILI technology at issue. In this respect, users of TFI have indicated that the tool can find longitudinal anomalies, but that sizing of the longitudinal anomalies is not accurate enough to discriminate between benign and critical defects. In this case, an operator might be prudent to use a follow-up hydrostatic test to see that no critical anomaly has escaped detection. This combined assessment activity could eventually benefit the industry by showing where the TFI technology is reliable and where it is not.

Users of transverse UT have indicated that the sizing of anomalies agrees very well with the excavated and measured defects. In this case, hydrostatic testing would seem to be an unnecessary additional cost.

8.4 Fracture Mechanics Implications for Hydrostatic Testing and In-Line Inspection

Fracture mechanics constitutes a technical discipline through which engineers attempt to understand or predict the effects that defects may have on structures or equipment. Typically, structures and equipment are designed to sustain predictable service loads throughout their useful life without failing. Also, typically, these structures or equipment are proportioned in terms of size and constructed of materials with reliable stress-carrying properties such that they will be continually able to sustain the expected service loads with a margin of safety against failure. Via fracture mechanics, engineers can, in addition, assess the maximum sizes of defects or imperfections that could exist in structures of equipment without causing their intended function to be impaired. As an adjunct to these types of assessments, the responsible engineers or designers may also apply structural-integrity-assessment techniques to assure that no defects beyond the maximum acceptable

size exist. This latter activity is precisely the intent of applying either hydrostatic testing or ILI or both to pipelines.

The essential elements of a fracture-mechanics assessment as it is applied to a pipeline situation are the level of nominal tensile stress (usually the pressure-induced hoop stress), the maximum size of a longitudinally oriented defect (usually in terms of axial length and depth penetration through-the-wall thickness of the pipe), and the inherent resistance of the pipe material to propagation of the defect either through the wall or along the axis of the pipe. The latter parameter is usually referred to as the “toughness” of the material. In terms of pipeline-integrity assessment, the role these elements may play is typically as follows. To establish the effectiveness of a hydrostatic test, the operator usually needs to compare the sizes of defects that can survive the intended test pressure level to the sizes of those that would cause a failure at the maximum operating pressure. The effectiveness of an ILI depends on being able to detect any and all defects larger than the size at which the associated failure pressure would be less than or equal to a “safe” pressure level above the maximum operating pressure. Because failure pressure is linked to defect size through toughness, the operator must have a reasonable idea of the minimum toughness level that the pipe material will exhibit. It must also be remembered that the inherent toughness of the material is a function of temperature.

To understand the impact of toughness on both hydrostatic testing and ILI, it is helpful to consider Figure 8.1 through Figure 8.5. Each is a failure-pressure-versus-flaw-size relationship for a piece of 16-inch OD, 0.25-inch-wall, API 5L Grade X52 line pipe. On each is a set of nine curves representing defects with uniform depths ranging from 10 percent to 90 percent of the wall thickness. These relationships were generated using the log-secant (NG-18 surface flaw) equation presented in Section 7 and embodied in the RECTANG.xls spreadsheet available free of charge (see www.kiefner.com). On each of the five figures, three horizontal lines appear, one at 1,938 psig (the burst pressure of a defect-free pipe), one at 1,473 psig (corresponding to 90 percent of SMYS), and one at 1,120 psig (corresponding to 72 percent of SMYS). The five figures differ from one another only with respect to the assumed toughness level of the material in each case as defined by a level of CVN energy. The levels of energy portrayed are 500 ft-lb (Figure 8.1), 25 ft-lb (Figure 8.2), 10 ft-lb (Figure 8.3), 2 ft-lb (Figure 8.4), and 0.2 ft-lb (Figure 8.5). It is obvious when one compares these relationships that the level of toughness is very significant with respect to the relationship between failure pressure and defect size.

Because toughness is obviously so important, it is also important to understand (before the impact on integrity-assessment methods is discussed) in what situations these levels of toughness are relevant. First, consider Figure 8.1 where the relationships are based on 500 ft-lb. It will be readily apparent to anyone familiar with line-pipe steels that no ordinary line pipe is capable of exhibiting 500 ft-lb absorbed energy in a CVN test. In fact, Charpy machines typically cannot break a specimen that exhibits more than 250 ft-lb. With today’s technology, it is routinely possible to obtain 100-ft-lb materials (based on full-size specimen equivalent upper-shelf energy) and with special alloys 250 ft-lb is not out of reach. But why should we even consider a 500-ft-lb material? The answer is that in the presence of blunt defects such as corrosion-caused metal loss, materials (even old ones) tend to behave as if they had that much toughness. In reality, when a blunt defect fails it does so because the ultimate tensile strength of the material is reached and not because of any crack propagation. Therefore, toughness is irrelevant, and the material behaves as if it had “optimum” toughness.

Optimum toughness is any level sufficiently high such that the onset of failure is controlled by the attaining of the ultimate tensile strength as opposed to being controlled by the resistance to crack propagation (i.e., toughness). So the purpose of the 500-ft-lb case is to show the effect that various sizes of blunt metal-loss defects can have on the pipe.

Figure 8.2 (25 ft-lb) represents the most commonly encountered scenario with respect to cracks in line-pipe materials manufactured prior to about 1980 when low-carbon thermo-mechanically treated, micro-alloyed line-pipe steels began to emerge in substantial quantities. Generally, this level of toughness is exhibited in all parts of the pipe body including the areas where hook cracks and mismatched skelp edges occur near ERW bondlines (regardless of whether they are low-frequency welded, dc welded, or flash welded). It is also common to see pipe-body materials exhibit this much toughness in static-load situations such as internal pressurization at temperatures well below the ductile-to-brittle transition temperature range. The latter (transition temperature) is determined by means of impact tests such as with CVN tests. It is well known that materials can exhibit ductile behavior at temperatures well below their “transition” temperatures as long as the effective strain rates are relatively low (as in quasi-static-loading situations). So Figure 8.2 represents a very important case with which to consider the effectiveness of hydrostatic testing and in-line inspection.

Figure 8.3 (10 ft-lb) represents a likely “worst-case” scenario for the region near but not in an ERW bondline. This might be the case if the material were extremely “dirty”, that is, if it were heavily saturated with nonmetallic inclusions. While this condition is likely to occur only rarely, it needs to be considered in the discussion of the effectiveness of the integrity-assessment methods. This level of toughness may also represent the response of ERW bondlines to grooving corrosion so it is relevant in situations where grooving corrosion could be an issue.

Figure 8.4 (2 ft-lb) and Figure 8.5 (0.2 ft-lb) represent the ranges of effective responses of the bondline regions of low-frequency-welded, dc welded, and flash-welded materials. It is obvious in both figures that these materials are extremely flaw intolerant. At first glance, this tends to be much more alarming than it actually needs to be. As it turns out, both logic and practical experience suggest that once a material such as this receives a satisfactory initial “proof” test, it cannot contain any defects of significant size. Therefore, the relatively small remaining defects pose little or no threat to the integrity of the pipeline because they are too small to become enlarged by fatigue. In fact, the author knows of no case where a small bondline flaw failed because it became enlarged by fatigue crack growth. Moreover, attempts to produce fatigue failures at such flaws within reasonable numbers of cycles have failed.

On the basis of the foregoing discussions, it is now appropriate to discuss the impact of toughness on the effectiveness of hydrostatic testing and ILI. First, consider Figure 8.1 (500 ft-lb), the situation corresponding to corrosion-caused metal loss. Almost any metal-loss tool, even a low-resolution tool, can detect metal loss that is deeper than 30 percent of the wall thickness and longer than $\frac{3}{4}$ of an inch. Thus, all anomalies lying below the $d/t = 0.3$ curve and to the right of a vertical line at 0.75 inch should be detectable. From the standpoint of a hydrostatic test to a pressure level of 1,473 psig, any corrosion with dimensions that place it below the horizontal line at 1,473 psig will be eliminated. From the standpoint of the initial safety margin demonstrated, the ILI gives assurance superior to that of the hydrostatic testing in all cases except for very short pits that fall below the length-detection threshold.

From the standpoint of reassessment interval, one can compare the results of the two types of inspection by noting that after the ILI, if all pits with depths greater than 30 percent of the wall thickness are addressed, the time to failure will be the time that it takes for the pits that are less deep than 30 percent of the wall to grow to the depth level intersected by the horizontal line at 1,170 psig (the maximum allowable operating pressure). If one assumes that defects of all lengths grow at the same rate, then for long defects (greater than 10 inches), the reassessment interval would have to be less than the time it takes for the pits to grow from 30 percent of the wall to about 50 percent of the wall. In this region of the figure, the ILI and the hydrostatic test produce equal times. However, it is clear that for shorter flaws the required time between reassessments goes up for the ILI but down for the hydrostatic test. When one considers this circumstance and the value of knowing where the non-failed corrosion exists, it is abundantly clear that ILI for corrosion-caused metal loss is far and away the better of the two methods. With the use of a reliable tool and an appropriate follow-up response by the operator to the findings, it is easy to see that ILI alone is the appropriate method for dealing with corrosion-caused metal loss. There is no added value to conducting a hydrostatic test as well. Furthermore, a hydrostatic test by itself would be a less effective means of addressing the problem (assuming that the line is piggable).

Turning to Figure 8.2, one can make a similar comparison between crack-detection tools and hydrostatic testing. In the case of crack-detection tools, the typically advertised detection threshold are (a) depths exceeding 25 percent of the wall thickness **and** lengths exceeding 2 inches, and (b) depths of 0.04 inch **and** lengths exceeding 2 inches. In the case of 0.250-inch pipe, the latter depth threshold is a d/t ratio of 0.16. Before proceeding with the discussion, it is worth noting that most fatigue cracks that have been discovered have had lengths exceeding \sqrt{Dt} where D is the diameter of the pipe and t is the wall thickness. To date only one fatigue-caused leak with a length less than \sqrt{Dt} has been recorded and its \sqrt{Dt} was only 0.83 inch. In the case of 16-inch OD, 0.250-inch wall pipe, $\sqrt{Dt} = 2$ inches, so the credible fatigue-crack threats to the pipe would likely involve defects with lengths exceeding the minimum detection threshold of the known tools. Experience has also revealed no case of a fatigue crack longer than about 8 inches. This latter circumstance is significant in terms of ILI effectiveness as discussed below.

Figure 8.2 suggests that the 25-percent depth curve crosses the 1,473-psig line somewhere between 6 and 8 inches. This suggests from the standpoint of safety margin that a reliable crack-detection tool with a 25-percent-depth threshold provides assurance levels superior to that of the 90-percent-of-SMYS test for crack lengths between 2 and about 7 inches. Similarly, a reliable crack-detection tool with a 16-percent-depth threshold provides assurance levels superior to that of the test for crack lengths of 2 to about 10 inches (covering the entire range of fatigue cracks observed to date except for one very short leak). Using reasoning similar to that discussed in conjunction with Figure 8.1, one can ascertain that the reassessment intervals using the tool will be longer than those associated with the use of hydrostatic testing. This point was demonstrated independently in Section 3. The point is that ILI **with a proven tool** is superior to hydrostatic testing from the standpoint of preventing failures from crack-propagation phenomena **as long as the material exhibits reasonable toughness**. Obviously, the lower the detection threshold, the more benefit there is to ILI. It should

also be clear that there is no added value to conducting a hydrostatic test in addition to running a **reliable** crack-detection tool.

When it comes to situations where the toughness of the material, as expressed in terms of Charpy energy, lies well below 25 ft-lb, the superiority of in-line inspection with a crack-detection tool over hydrostatic testing begins to deteriorate. Consider Figure 8.3 in light of the discussions about Figure 8.1 and Figure 8.2 presented previously. Here it becomes evident that the advantage of even the best technology begins to slip away because of the relatively low failure pressures associated with defects having dimensions right at the tool-detection thresholds. For the low-toughness bondline materials as shown in Figure 8.4 and Figure 8.5, the currently available crack-detection ILI tools would provide little if any assurance of integrity. Fortunately, as discussed previously, there is no evidence that the small bondline defects in very low-toughness bondline materials cause time-dependent integrity threats.

In summary, it appears that the use of proven ILI techniques provides a higher degree of integrity assurance than hydrostatic testing (at least to practical limits imposed by the quality of older line-pipe materials) for the most important integrity threats (i.e., corrosion-caused metal loss and crack-propagation phenomena in materials with reasonable toughness levels). In these cases, hydrostatic testing provides no added value and clearly is inferior to reliable ILI (with appropriate and timely response) used by itself. In those cases where a low or very low-toughness material is involved, however, the reverse is true. In those cases, it appears with today's tool-inspection thresholds that hydrostatic testing would give superior assurance. Also, it is noted that in these cases for reasons explained above, a one-time test would probably suffice, and that one-time test could be either the initial pre-service test or the manufacturer's hydrostatic test if that test was conducted to a sufficiently high level. It would seem then that the only reason for employing both ILI and hydrostatic test would be cases where the confidence in the ILI technology needs to be established.

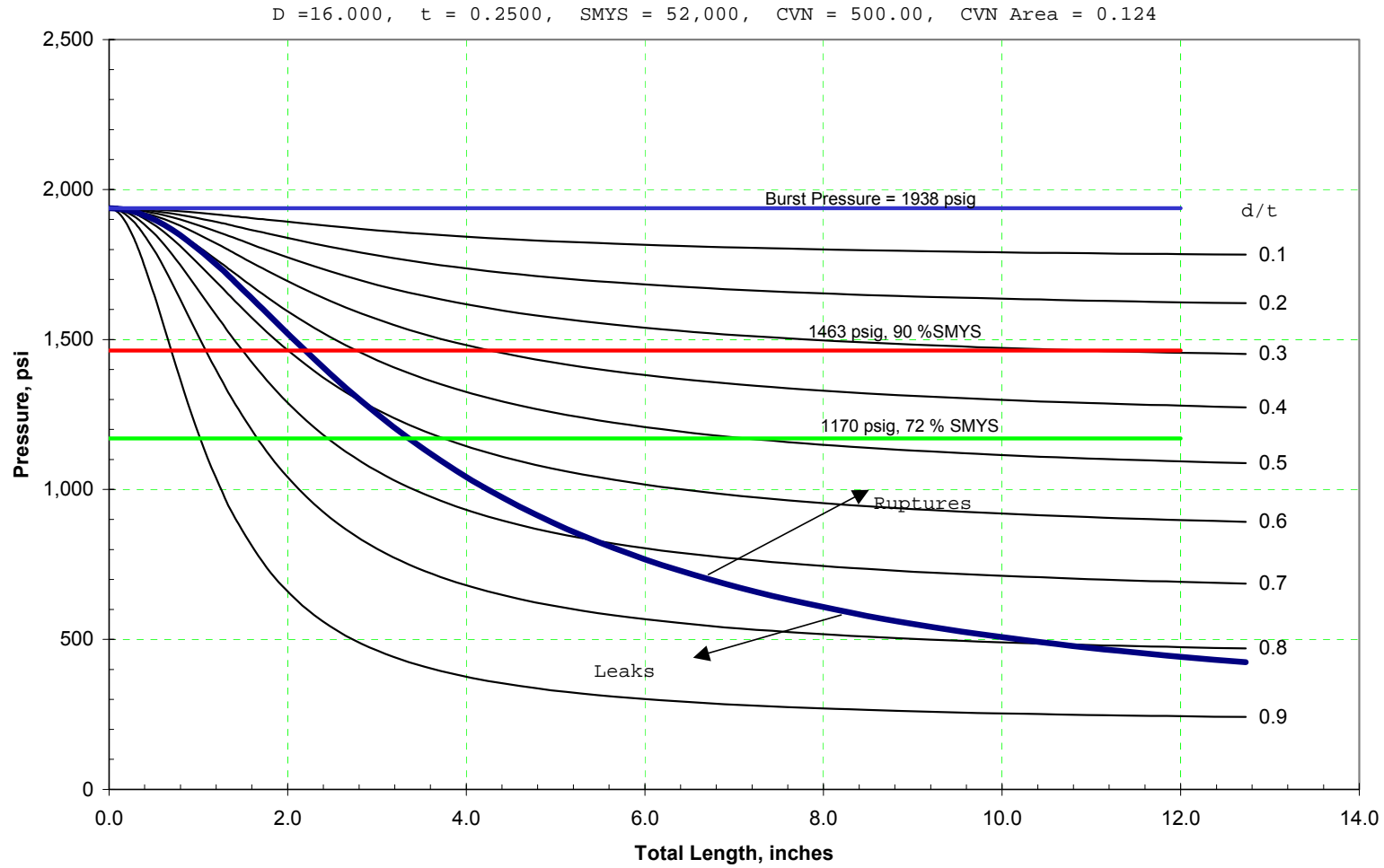


Figure 8.1 Strength-Dependent Relationship Between Failure Pressure and Flaw Size for Blunt Metal Loss in Ductile Pipe

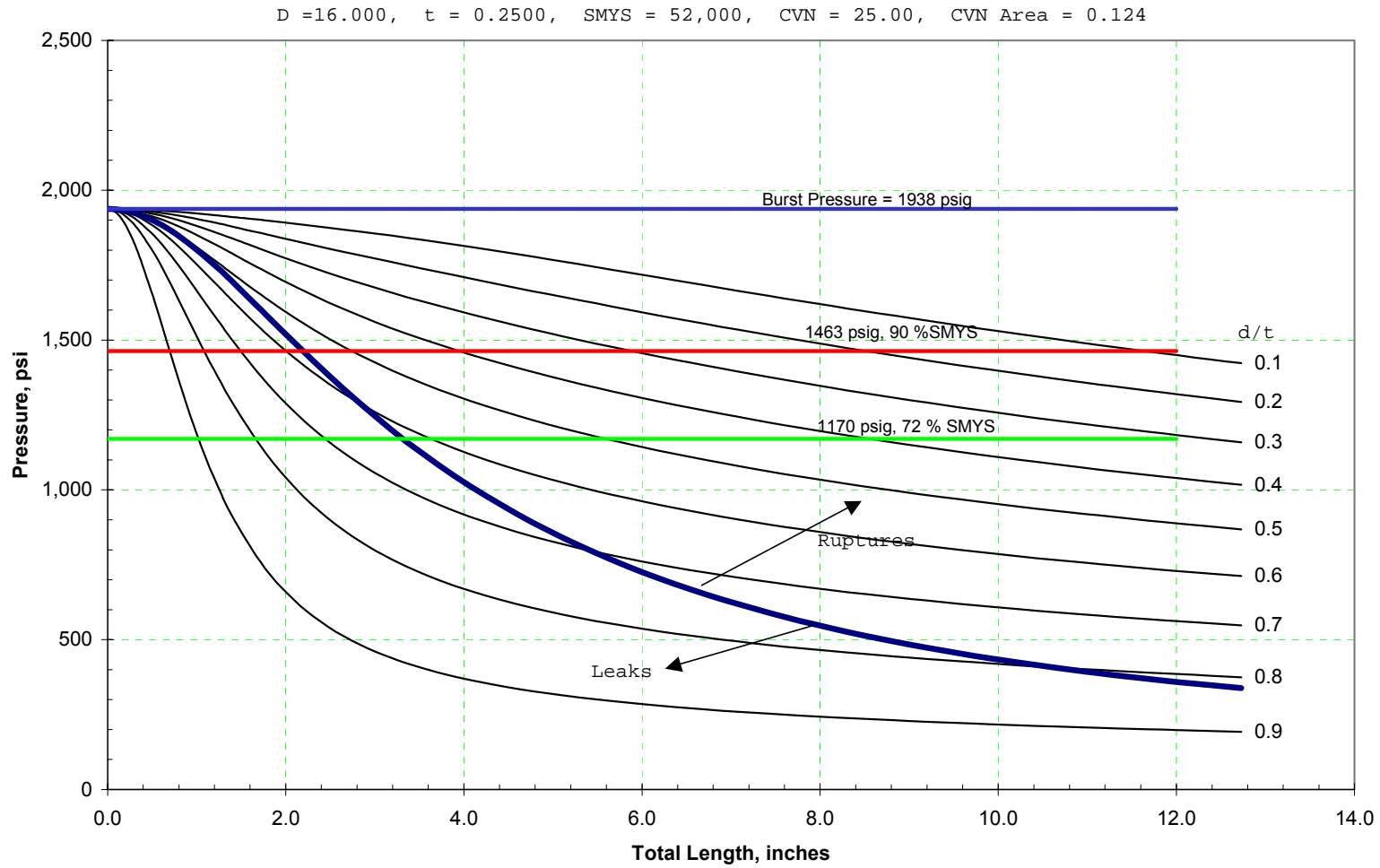


Figure 8.2 Toughness-Dependent Relationship Between Failure Pressure and Flaw Size for Cracks in Pipe Having Normal Toughness Levels (25 ft-lb)

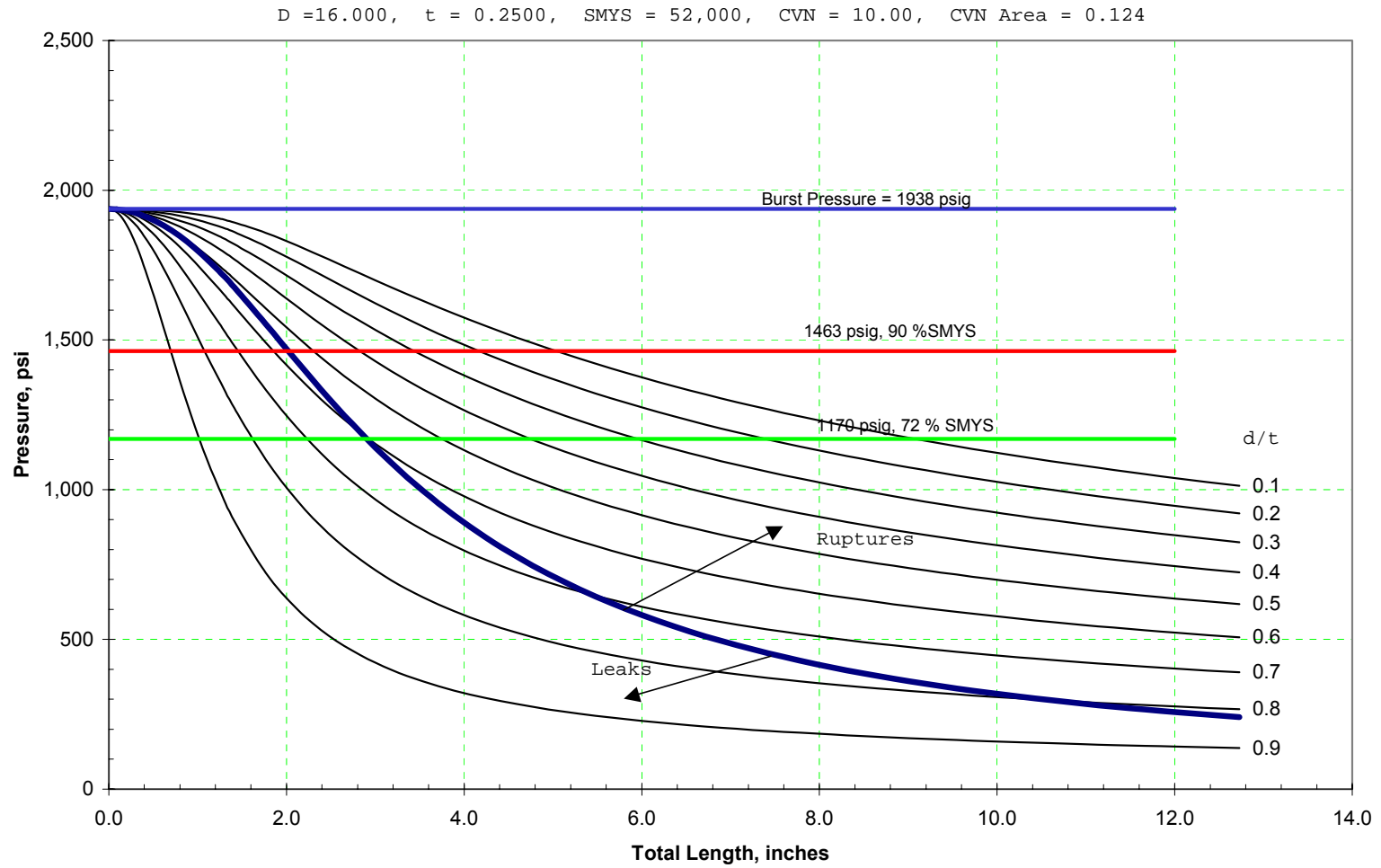


Figure 8.3 Relationship Between Failure Pressure and Flaw Size for Near-Bondline ERW Defects (10 ft-lb)

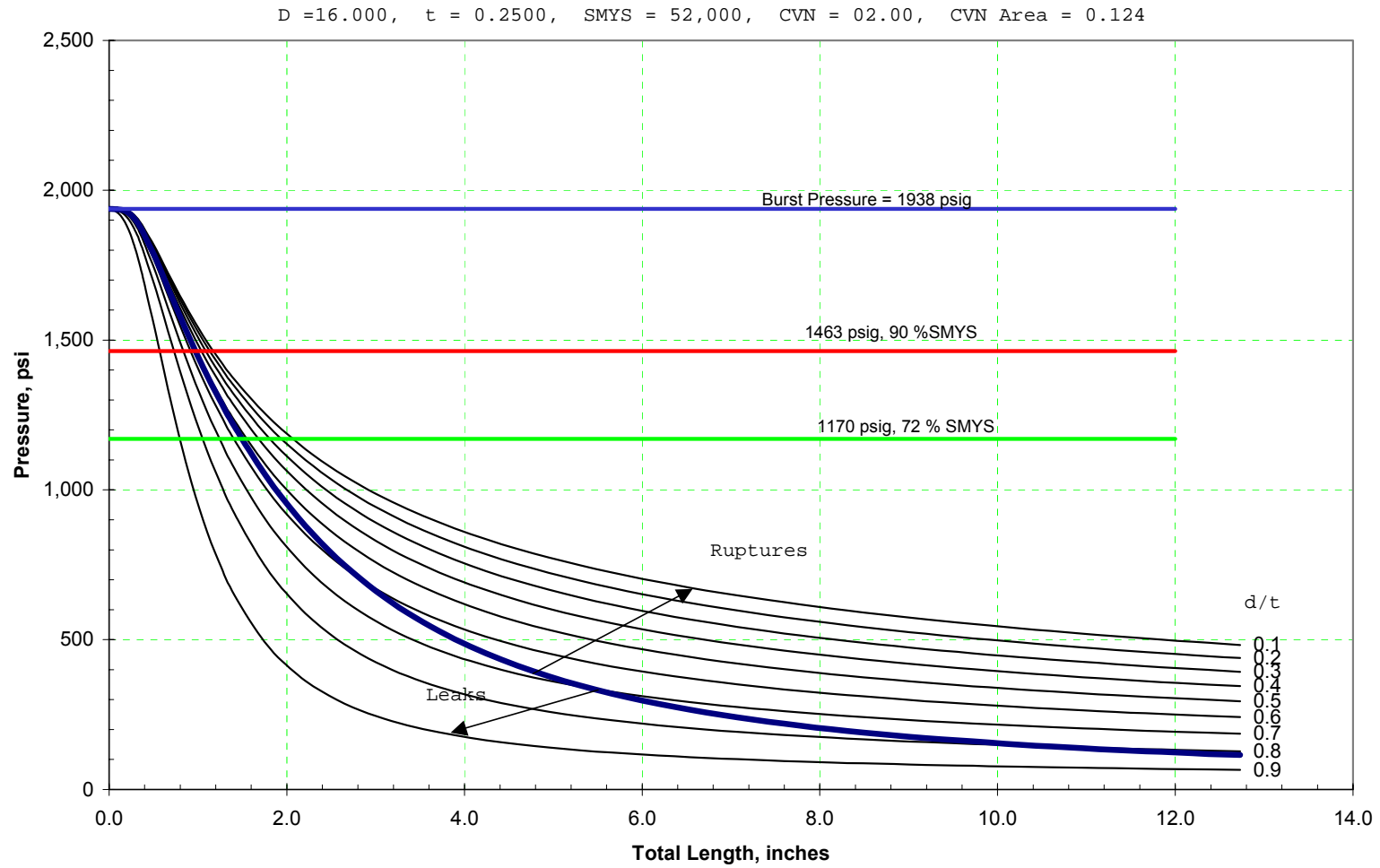


Figure 8.4 Relationship Between Failure Pressure and Flaw Size in Low Toughness Seams (2 ft-lb)

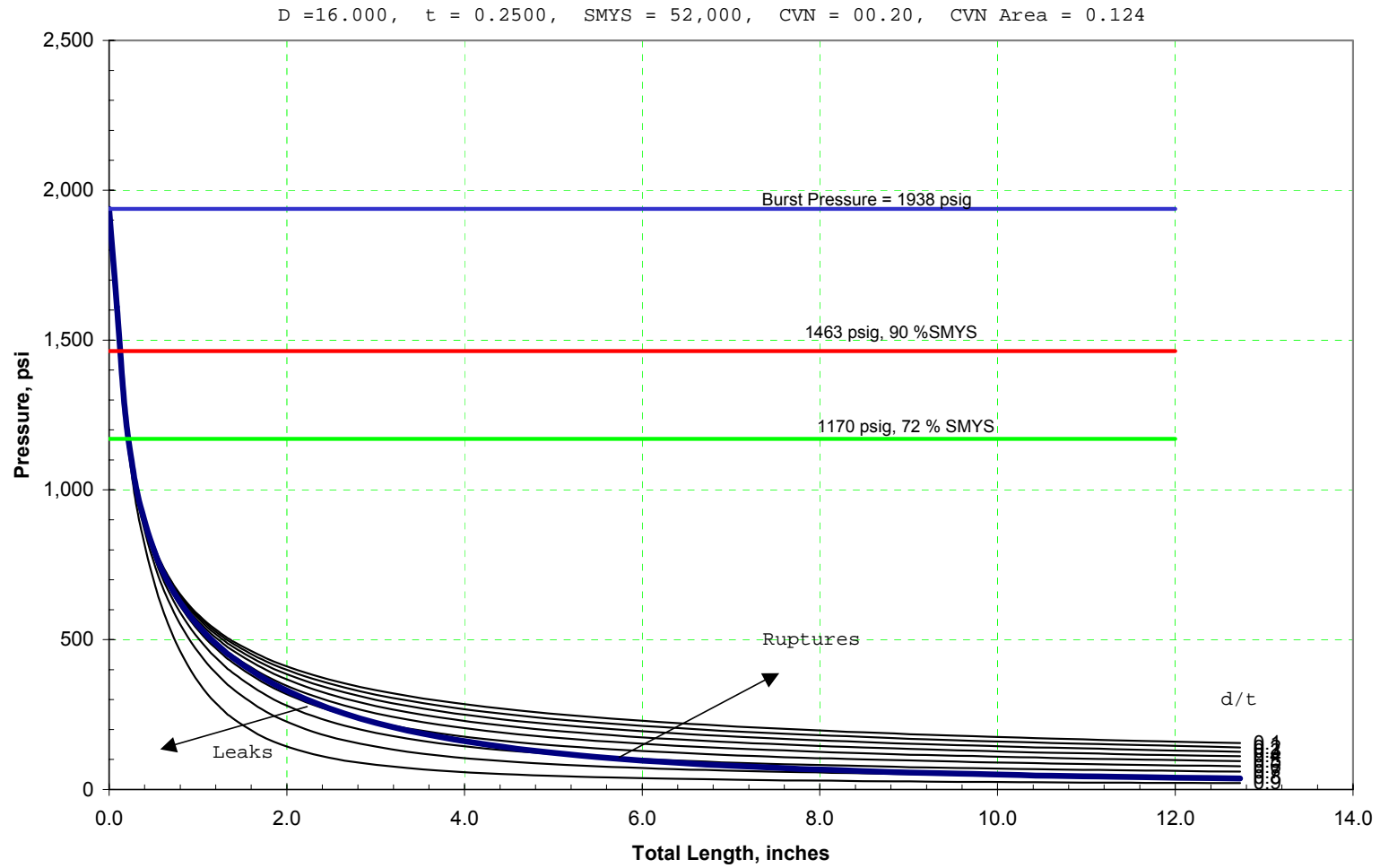


Figure 8.5 Relationship Between Failure Pressure and Flaw Size in Brittle Seams (0.2 ft-lb)

This page intentionally left blank

9 Recommendations and Suggested Guidelines

An overall process flow for the evaluation of LF-ERW, EFW and lap-welded pipe is presented in Figure 9.1. This logical step-by-step procedure provides a standardized, systematic approach to evaluation of longitudinal seam integrity.

There are three evaluation procedures presented:

- Screening Evaluation,
- Engineering Analysis, and
- NDT Evaluation.

Each of these procedures is discussed in further detail in the following sections.

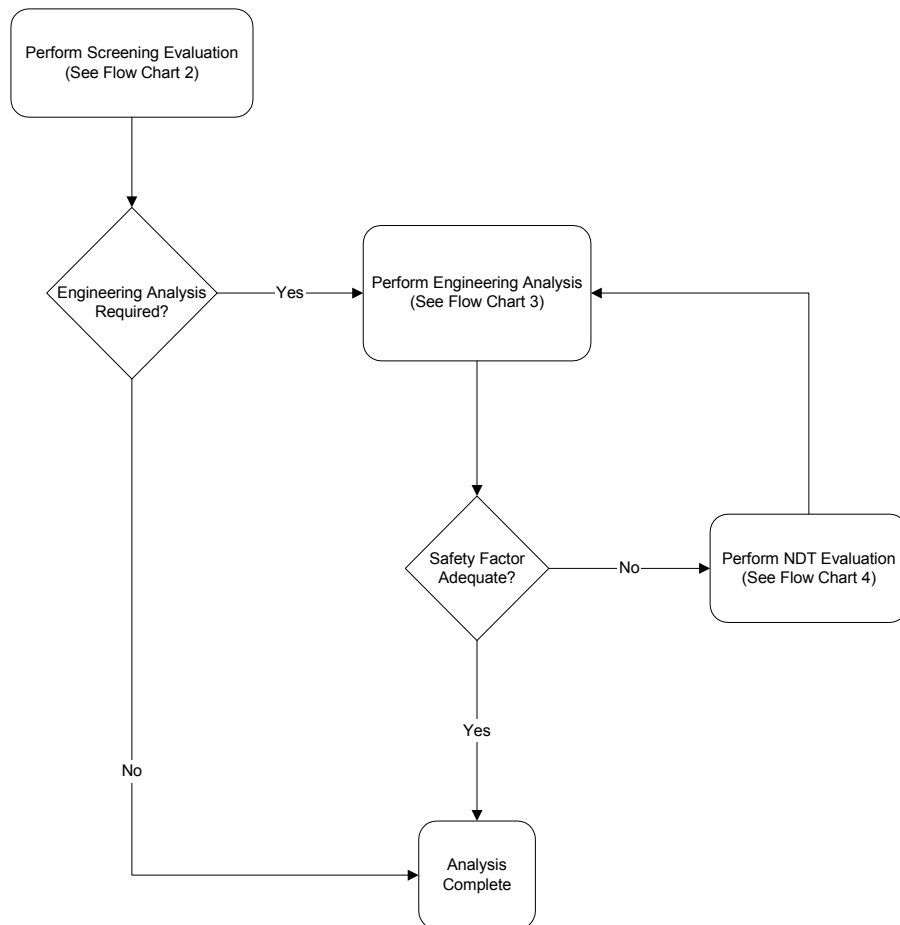


Figure 9.1 Evaluation Process (Flow Chart 1)

9.1 Screening Evaluation

The screening evaluation looks at failure history, testing history and basic stress levels within the pipe and allows, in a few limited cases, the pipe to be accepted without any further evaluations or

test. These limited cases are: LF-ERW, EFW and lap-welded pipe for which no failure history is known or suspected, has been hydrostatically tested to 1.25 of MOP and has a hoop stress at MOP less than 30% of SYMS; and LF-ERW, and EFW pipe for which no failure history is known or suspected, has been hydrostatically tested to 1.5 of MOP and has a hoop stress at MOP less than 40% of SYMS. In all other cases, the screening analysis results in the need to perform an engineering analysis.

The process flow for a screening analysis is presented in Figure 9.2.

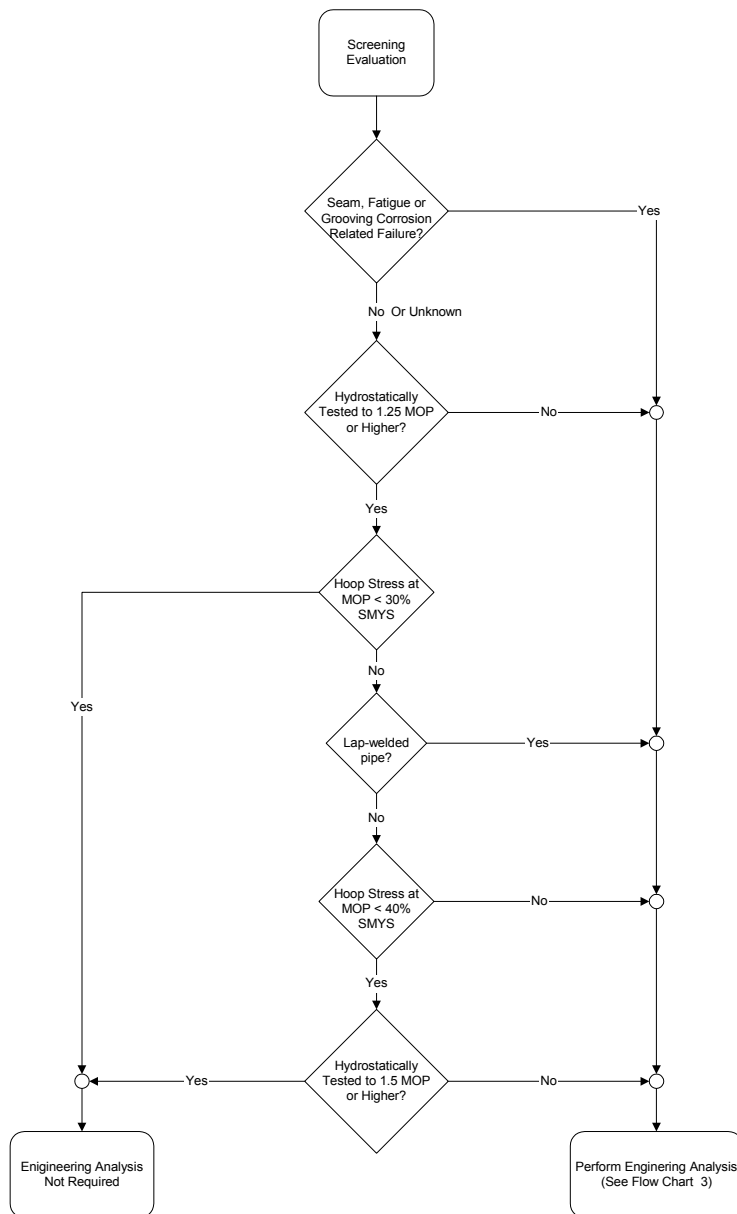


Figure 9.2 Screening Evaluation (Flow Chart 2)

9.2 *Engineering Analysis*

An engineering analysis starts with gathering detailed pipeline data, in particular, ILI and hydrostatic test data. The first step once the data has been gathered is to determine whether any ILI data is appropriate for the defect type being evaluated, in this case longitudinal seam integrity. As discussed earlier, C-UT, EMAT and TFI are currently the only methods available for accurate detection of crack-like defects, which are the types of defects commonly associated with longitudinal seam integrity for LF-ERW, EFW and lap-welded pipe. If appropriate ILI data is available, a FFS evaluation can then be conducted following procedures outlined in API RP579, or similar techniques.

If appropriate ILI data is not available, it may be possible to determine the acceptability of a pipeline given historical hydrostatic test data. By determining the maximum crack size that may have been present during the last test that would not have led to failure and postulating a crack growth rate based on fracture mechanics analysis, it is possible to determine an appropriate test interval for the pipeline. If the actual length of time since the last test is less than this calculated test interval, the analysis of the pipeline is considered complete and no further action need be taken at that time.

On the other hand, if the length of time from most recent pressure test exceeds the calculated test interval, then an NDT evaluation is required. Similarly, if the FFS analysis indicates an inadequate safety factor, then an NDT evaluation is required. In all cases, a detailed report on the engineering analysis is required.

This process is presented in Figure 9.3.

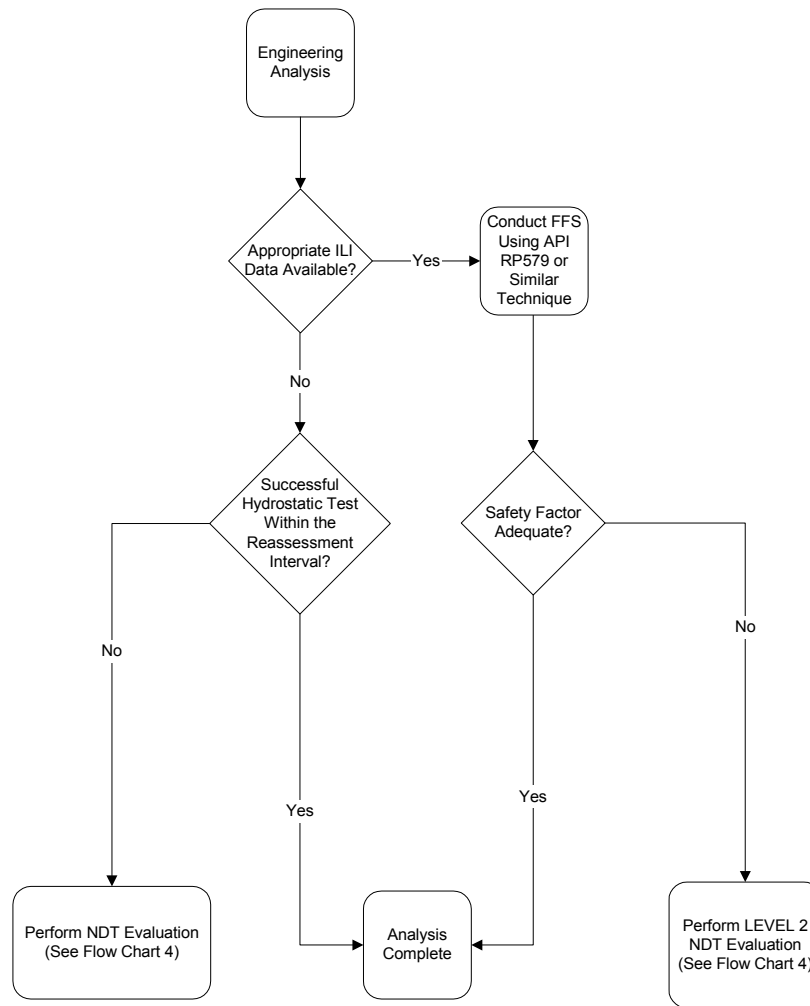


Figure 9.3 Engineering Analysis (Flow Chart 3)

9.3 NDT Evaluation

NDT evaluation is divided into two levels. Level 1 is based on ILI, while Level 2 is based on hydrostatic testing. Whether ILI, hydrostatic testing, or a combination of the two is used, after completion an engineering analysis incorporating this information is required.

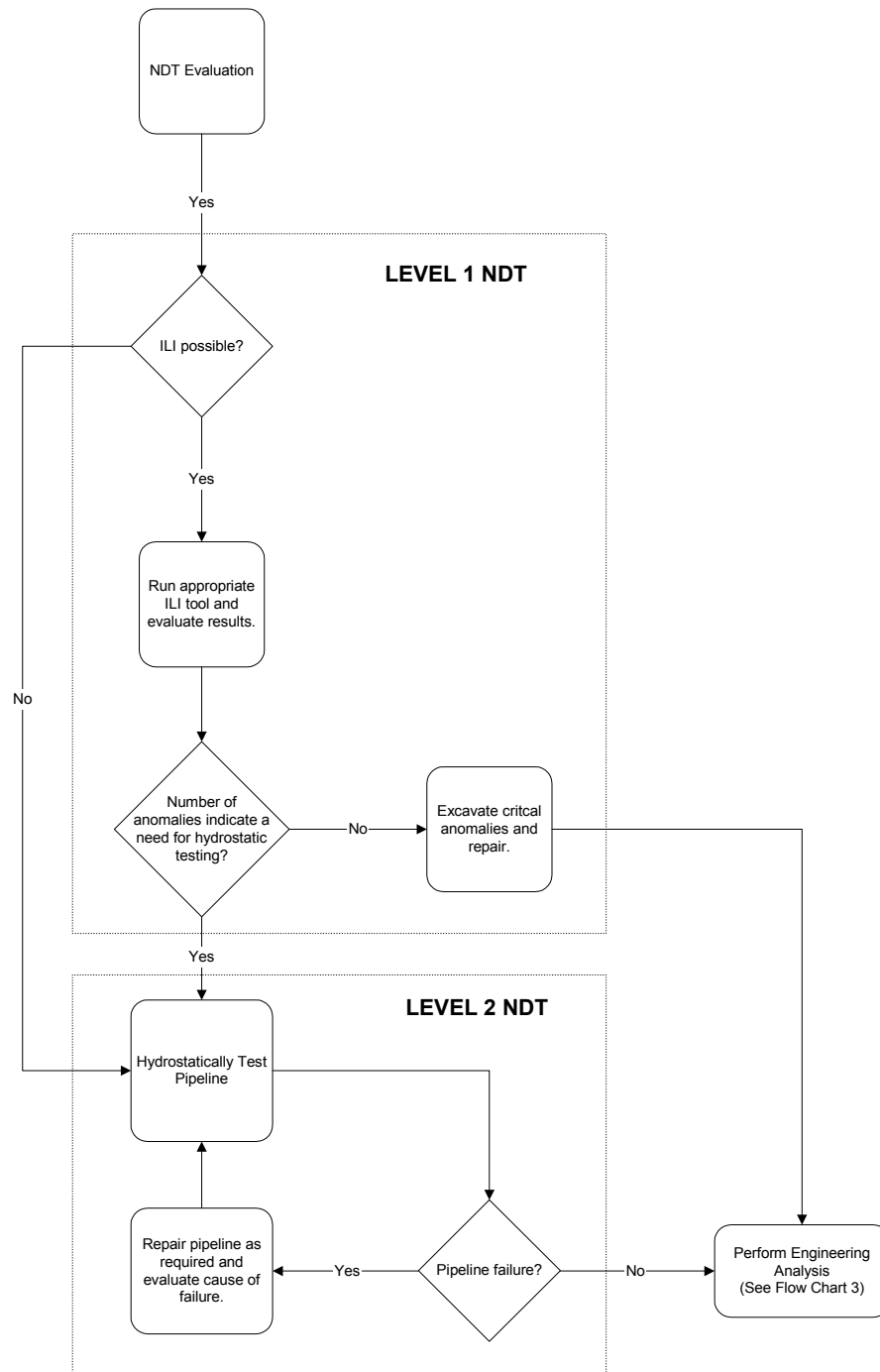


Figure 9.4 NDT Evaluation (Flow Chart 4)